INTERNATIONAL SCIENCE CONFERENCE

अंतर्राष्ट्रीय वज्ञिान सम्मेलन

EDUCATION AND PRACTICE IN THE CONTEXT OF MODERN SCIENCE

आधुनकि वज्ञिान के संदर्भ में शकि्षा और अभ्यास

दिल्ली, भारत 2025 / Delhi, India 2025

International Science Conference

EDUCATION AND PRACTICE IN THE CONTEXT OF MODERN SCIENCE

Part 2

July 16, 2025. Delhi, India

Proceedings of the International Science Conference **“EDUCATION AND PRACTICE IN THE CONTEXT OF MODERN SCIENCE”** (July 16, 2025). Delhi. India.

DOI 10.34660/conf.2025.35.97.083

Science Conference Proceedings combine materials of the conference – research papers and thesis reports of scientific workers. They examine technical, juridical and sociological aspects of research issues. Some articles deal with theoretical and methodological approaches and principles of research questions of personality professionalization.

Authors are responsible for the accuracy of cited publications, facts, figures, quotations, statistics, proper names and other information.

DOI 10.34660/conf.2025.35.97.083

CONTENTS

CHEMICAL SCIENCES

TECHNICAL SCIENCES

PHYSICAL AND MATHEMATICAL SCIENCES

DOI 10.34660/INF.2025.39.37.130

MICROBIOTA OF THE NEVA RIVER BASIN

Kletsko Lyudmila Ivanovna
Candidate of Biological Sciences, Associate Professor
S.M. Kirov Military Medical Academy,
St. Petersburg, Russia

Sboichakov Viktor Borisovich
Doctor of Medical Sciences, Full Professor
S.M. Kirov Military Medical Academy,
St. Petersburg, Russia

Abstract. *The microbiota of the Neva River water basin is considered. Neva water samples were studied to study the microbial landscape in relation to microorganisms of the Vibrionaceae family and to determine their stability in the environment. The potential possibility of using Mechnikov's vibrio as an indicator of microbiological pollution of water basins is shown.*

Keywords: *Neva, microbiota, vibrios, aeromonads, microbial pollution, Vibrio metschnikovii, Vibrio furnissii, Vibrio fluvialis.*

Rivers are the main source of drinking, domestic and recreational water use of such a megalopolis as St. Petersburg, playing an important role in the development of the epidemic process. Water enters the Neva from Ladoga and other lakes. The area of the Neva catchment basin, including the territory of Lake Ladoga, is 281 thousand square kilometers. At the same time, the river's own basin covers 5 thousand square kilometers. The river is fed mainly by the waters of Lake Ladoga, which ensures a uniform flow of water throughout the year. In addition, 26 rivers flow into the Neva. Among the main tributaries are the Mga, Tosna, Izhora, Slavyanka, Murzinka and Chernaya Rechka rivers.

Due to the low temperature of the water in the lake, its intensive mixing due to frequent waves on Ladoga, as well as the high speed of the Neva, strong aeration and unfavorable conditions for microbial contamination of the water basin are created. Passing through the silt of the lakes, the water is additionally purified. The total number of bacteria in the river from the source to St. Petersburg is from 50 to 800 CFU in 1 cm3, which meets the sanitary and hygienic requirements for

surface water sources, but already within the city limits, the water in the Neva does not meet the sanitary and epidemiological requirements [2,3].

Cholera-like vibrios are most often found in water samples. The share of non-standard microbiological samples collected from the Neva River within the city limits is usually about 80%. This indicates a possible threat of outbreaks of intestinal infections among the population of the metropolis by water. The problem of high pollution of the Neva water is primarily associated with the growth of the population due to the influx of migrants from neighboring countries with cholera problems, as well as with the ineffective purification of domestic wastewater due to the overload of the treatment facilities of St. Petersburg. In this regard, monitoring the quality of surface water sources is relevant. The aim of the work was to study Neva water samples to study the microbial landscape in relation to microorganisms of the Vibrionaceae family, which are of medical importance, and to determine their stability in the environment. Sampling was carried out once every two weeks with preliminary control of the water temperature in the Neva. The studies were conducted using classical methods in accordance with the guidelines: MUK MZ RF 4.2.2218-07 "Laboratory diagnostics of cholera" and MUK MZ RF 4.2.1793-03 "Supplement to the guidelines "Laboratory diagnostics of cholera" MUK MZ RF 4.2.1097-02. Five water samples were analyzed, from which 182 bacterial cultures were isolated, including 119 suspicious bacteria of the Vibrionaceae family. During further bacteriological examination, pathogenic bacteria of the genus Vibrio that did not belong to the V. cholerae species were identified from the 119 selected cultures: 4 strains of *V. fluvialis* (which accounted for 3.36% of the total number of suspicious cultures), 2 strains of *V. furnissii* (1.68%) and 77 strains of *V. metschnikovii* (64.71%). In addition, 36 strains of bacteria of the genus Aeromonas (30.25%) were isolated. Initially, the genus Aeromonas was attributed to the family Vibrionaceae, but later, using the molecular hybridization method, it was established that Aeromonas are not related to vibrios and were isolated in an independent family Aeromonadaceae. The following features were used to differentiate these genera: for Vibrio, the absence of the enzyme arginine dihydrolase and fermentation of sucrose, for Aeromonas, fermentation of arginine with the formation of alkaline products due to the presence of the enzyme arginine dihydrolase.

During the research, the range of water temperatures in the Neva River varied from +14ºC during the first sample collection to +3ºC during the last sample collection. When analyzing the resistance of the isolated vibrios to seasonal decreases in water temperature in the Neva, it was found that microorganisms of the genus Vibrio, species *V. metschnikovii*, had the greatest resistance to unfavorable environmental factors (water temperature). The Mechnikovsky vibrio was detected in all water samples collected throughout the entire study period. For other isolated

species (*V. furnissii, V. fluvialis*), the critical water temperatures were +12ºC, +9ºC (+/- 1 ºC), respectively, since these microorganisms were not detected in the samples at lower temperatures. In addition, we conducted additional studies to control the degree of resistance of V. metschnikovii in low temperature conditions. At a water temperature of 0ºC, two samples were taken with an interval of 10 days. 55 cultures of microorganisms were isolated and 8 were selected as suspicious for bacteria of the Vibrionaceae family. The remaining 47 cultures were represented by 30 strains of non-fermenting gram-negative bacteria, 12 strains of microorganisms of the Enterobacteriaceae family and 5 strains of gram-positive bacteria. In the course of further bacteriological examination, 3 strains of *V. metschnikovii* and 5 strains of bacteria of the genus Aeromonas were isolated from the 8 selected suspicious cultures according to the above-mentioned method. This once again confirms the high resistance of *V. metschnikovii* in unfavorable environmental conditions. Therefore, it is possible to consider this type of bacteria as an indicator of biological contamination of surface water sources with pathogenic vibrios. Vibrios have also mastered a wide range of ecosystems, including soils and the sea depths. The mechanism of change in the composition of fatty acids in vibrios and aeromonads in response to the impact of various factors (stressors) of the environment. apparently provides cells with additional opportunities to achieve high adaptive plasticity [4,5].

Mechnikovsky vibrio was discovered by Gamaleya in 1887 in Odessa during an epizootic in chickens [6]. These vibrios were isolated from intestinal contents and from blood. In morphology and biochemistry, they resemble typical cholera vibrio. The vibrio is very mobile, monotrichous, and gives a positive “cholera-rot” reaction. This test is used to distinguish cholera vibrio from other vibrios [9]. The reaction mechanism is associated with the fact that cholera vibrio reduces nitrates to nitrites, and the added sulfuric acid displaces nitrous acid from nitrite, which, when combined with indole, forms nitrosoindole, which gives the medium a red color. *V. metschnikovii* liquefies gelatin and forms colonies with a browner tint than Vibrio cholerae. Vibrio metschnikovii grows easily on common laboratory media, including TCBS agar and blood agar. Vibrio is catalase-positive, but it is the only pathogenic vibrio that is oxidase-negative. The exact differential feature was considered to be the different ratio of Vibrio metschnikovii and Vibrio cholerae to pigeons. A trace amount of Vibrio metschnikovii causes a fatal infection in pigeons, while the introduction of large amounts of *Vibrio cholerae* is harmless. The Pfeiffer phenomenon and the agglutination reaction also allow differentiation of *Vibrio cholerae and Vibrio metschnikovii*.

V. metschnikovii produces hemolysins, cytotoxins, and enterotoxins. Hemolysin causes hemolysis of red blood cells, which can lead to fluid accumulation in the intestinal lumen, resulting in diarrhea. Cytotoxin forms pores on the host cell

membrane and causes cell lysis, which promotes the survival of microorganisms at the site of infection. Enterotoxin disrupts the balance of enzyme systems, which causes the release of large amounts of fluid and electrolytes, which leads to a sharp loss of fluid.

Cytolysin (extracellular cytotoxin) *V. metschnikovii* does not have immunological cross-reactivity with hemolysins of other Vibrio species, indicating the uniqueness of this cytolysin. These bacterial strains were isolated from a fecal sample taken from a 60-year-old woman admitted to hospital with diarrhea. Cytolysin has exhibited hemolytic properties in several animal species [11]. V. metschnikovii also has a type 6 secretion system (T6SS), which allows vibrios to deliver toxic effector proteins to target cells, including other bacteria and eukaryotic cells. *V. metschnikovii*, like other vibrios, uses the T6SS to interact with the environment, including competition with other microorganisms and interactions with host cells [1,13].

In the *V. metschnikovii* genomes, 19 virulence factors associated with 161 genes have been identified, including genes encoding motility, adhesion, toxins, and secretion systems. This contributes to high levels of cytotoxicity due to the synergistic action of lateral flagella and the T6SS. The lateral flagella-associated gene flhA plays an important role in *V. metschnikovii* adhesion and colonization during the early stages of infection [7]. Vibrios metschnikovii can cause acute intestinal infections in humans, such as gastroenteritis, wound infections, and sepsis. Sources of infection include shrimp, crabs, birds, water, wastewater, and seafood. This species is a relatively new pathogen for humans. V. metschnikovii rarely causes disease in humans: only 13 cases have been reported since 1981 [8]. A patient with severe septic shock caused by V. metschnikovii has been described. Although isolation of such vibrios from human clinical samples is very rare, it still affects humans and can be fatal despite adequate treatment. This pathogen was identified in all blood samples using matrix-assisted laser desorption/ionization-time of flight mass spectrometry (99.9% probability). The result was confirmed by polymerase chain reaction and DNA analysis using the FAST MicroSeq® 500 16S rDNA Bacterial Identification Kit (Applied Biosystems). Etiotropic therapy with meropenem and piperacillin/tazobactam was carried out, since antibiotic susceptibility tests showed that this vibrio is sensitive to these antibiotics, but resistant to ampicillin [10]. According to European scientists, all isolates of Mechnikov vibrios were sensitive to ciprofloxacin, trimethoprim/sulfamethoxazole, chloramphenicol, gentamicin, imipenem, tetracycline and doxycycline. High rates of resistance to beta-lactams and streptomycin were recorded. An antibiotic resistance study identified five distinct antibiotic resistance profiles with resistance to antibacterial drugs from three classes, but no multidrug resistance was observed [12].

References

1. Zadnova, S.P. The secretion system of the sixth type of Vibrio cholerae / S.P. Zadnova, N.A. Plekhanov, T.A. Kulshan, I.G. Shvidenko, A.A. Kritsky // Problems of especially dangerous infections. – 2022. – No. 2. – P. 27–35. DOI: 10.21055/0370-1069-2022-2-27–35.

2. Kletsko, L.I. Mechnikovsky vibrio as an indicator of bacterial pollution of river water basins / L.I. Kletsko, A.M. Sokurova, E.A. Petrova // Science and education in the life of modern society: collection of scientific articles, dedicated to the memory of prof. M.V. Ivanov / ed. V.B. Sboychakov. – SPb.: Leningrad State University named after A.S. Pushkin, 2015. – Issue 2. – P. 136–138.

3. Sboychakov, VB The role of water in the transmission of infectious pathogens / VB Sboychakov, LI Kletsko // IV Luga Scientific Readings. Modern scientific knowledge: theory and practice: materials of the international scientific and practical conference, Luga, May 22, 2016. – Luga: Leningrad State University named after A.S. Pushkin, 2016. – P. 169–172. – EDN YFQHCP.

4. Shipko, ES Changes in the spectrum of fatty acids as one of the mechanisms of adaptation/persistence of microorganisms / ES Shipko, OV Duvanova // Zhurn. microbiol. – 2019. - No. 5. - P. 109-118.

5. Chatterjee, A. Effect of fatty acids and cholesterol present in bile on expression of virulence factors and motility of Vibrio cholera / A. Chatterjee, P.K. Dutta, R. Chowdhury // Infect. Immun. – 2007. – vol.75 (4). – P. 1946-1953.

6. Gamaleia, M. N. Vibrio metschnikovii (n. sp.) et ses rapports avec le microbe du choléra asiatique / M. N. Gamaleia // Annales de l'Institut Pasteur (Paris). – 1888. - vol. 2. – P. 482–488.

7. Huang, Z. Vibrio metschnikovii as an emergent pathogen: analyses of phylogeny and O-antigen and identification of possible virulence characteristics / Z. Huang, K. Yu, R. Lan, et al. // Emerg Microbes Infect. – 2023. – vol.12(2). – P.2252522. doi: 10.1080/22221751.2023.2252522/

8. Huang, Z. Vibrio metschnikovii as an emergent pathogen: analyses of phylogeny and O-antigen and identification of possible virulence characteristics / Z. Huang, K. Yu, R. Lan et al. // Emerging Microbes & Infections. – 2023. – vol. 12(2). doi.org/10.1080/22221751.2023.2252522

9. Lee, J. V. Characterization, Taxonomy, and Emended Description of Vibrio metschnikovii / J. V. Lee, T. J. Donovan, A. L. Furniss // International Journal of Systematic Bacteriology. – 1998. – vol. 28 (1). – P. 99–111. doi:10.1099/00207713-28-1-99. ISSN 0020-7713.

10.Linde, H.-J. Vibrio metschnikovii, a Rare Cause of Wound Infection / H-J. Linde, R. Kobuch, J. Sylvia et al. // Journal of Clinical Microbiology. – 2004. - vol.10. – P. 4909–4911. doi:10.1128/JCM.42.10.4909-4911.2004. ISSN 0095-1137.

11.Miyake, M. Purification of Vibrio metschnikovii cytolysin / M. Miyake, T. Honda, T. Miwatani // Infect Imun. – 1988. - vol.56 (4). - P. 954.

12.Valáriková, J. Potential pathogenicity and antibiotic resistance of aquatic Vibrio isolates from freshwater in Slovakia / J. Valáriková, J. Korcová, J. Ziburová et al. // Folia Microbiologica. – 2020. – vol.65 (3): 545–555. doi:10.1007/ s12223-019-00760-w/

13.Zheng, L. Pan-Genome Analysis of Vibrio cholerae and Vibrio metschnikovii Strains Isolated from Migratory Birds at Dali Nouer Lake in Chifeng, China / L. Zheng, L.W. Zhu, J. Jing et al. // Front Vet Sci. – 2021. – vol.6 (31). -P. 638820. doi: 10.3389/fvets.2021.638820. PMID: 34136552; PMCID: PMC8202012.

DOI 10.34660/INF.2025.21.34.131

EFFECT OF MICROORGANISMS ON SYMBIOTIC ACTIVITY OF SOYBEANS

Zubareva Kristina Yurievna
Senior research scientist, Candidate of Biological Sciences
Zotikov Vladimir Ivanovich
Corresponding Member of the Russian Academy of Sciences, Full Professor, Doctor of Agricultural Sciences
Semenov Alexey Sergeevich
Applicant for a degree
Maltsev Andrey Yuryevich
Applicant for a degree
Federal Scientific Center of Leguminous Crops, Orel, Russian Federation

Abstract. *This paper presents the results of scientific research on the influence of microorganisms on the symbiotic activity of soybean variety Lider 1. The experiments involved seed inoculation and treatment of vegetative plants in different growth and development phases of the studied variety with microorganisms. As a result, it was found that, in general, spores, living cells and biologically active metabolites of Bacillus megaterium (OPR-31), Azospirillum zeae (OPN-14), Pseudomonas aureofaciens (2391D), Montierella alpine (F-1134) had a catalytic effect on the legume-rhizobium symbiosis of soybean plants, expressed in an increase in root nodulation and functional activity of nodules compared to the variant with untreated seeds and crops.*

Keywords*: soybean, microorganisms, symbiotic nodules, biological nitrogen fixation.*

Introduction. The use of biopreparations allows the creation of biologized farming systems, including technologies for cultivating crops that directly eliminate or reduce the use of chemical pesticides, which in turn helps improve the ecology of the environment and intensify the resistance of artificial agrocenoses to biotic and abiotic stress factors [1]. An important role in the processes of biologization of the agricultural segment - plant growing is played by the introduction of scientifically based crop rotations into production, saturated with nitrogen-fix-

ing crops, which are capable of producing biological nitrogen in symbiosis with specific bacteria under optimal conditions [2]. Recently, the nitrogen-fixing crop - soybeans - has become extremely popular among agricultural producers. The sown areas of soybeans (https://rosstat.gov.ru/, accessed on 10.07.2025) are growing from year to year (Table 1) and in 2024 amounted to about 4337.0 thousand hectares in farms of all categories (share in crops 5.4%), including in the Central Federal District - 2019.7 thousand hectares and 12.8%, respectively.

Table 1

Soybean sown areas in farms of all categories, thousand hectares

	2023	**2024**	**2024 in % to 2023**	**Share in all crops, %**
Russian Federation, including:	3667,8	4337,0	118,2	5,4
Central Federal District	1547,0	2019,7	130,6	12,8
Northwestern Federal District	23,5	26,5	112,9	2,0
Southern Federal District	217,7	257,0	118,1	1,9
North Caucasian Federal District	31,7	42,2	133,2	1,0
Volga Federal District	271,0	417,7	154,1	1,7
Ural Federal District	9,1	25,1	275,9	0,5
Siberian Federal District	196,3	297,4	151,5	2,1
Far Eastern Federal District	1251,4	1371,6	91,2	58,3

An important factor, including one that influences the level of crop yield and the quality of the products obtained in biologized and organic farming systems, is the ability of agrocenoses to synthesize biological nitrogen, thereby partially providing themselves with this element during the growing season [3] and leaving available forms of nitrogen in the soil for subsequent crops in crop rotation.

Since the key to the successful implementation of the biological potential of all nitrogen-fixing crops in general, and soybeans in particular, is the creation of favorable conditions for their interaction with symbiotic nodule rhizobacteria, the selection of production tools that intensify legume-rhizobial symbiosis is of particular relevance [4, 5].

The aim of the research was to study the effect of various biopreparations on the symbiotic activity of early ripening soybean varieties of the Lider 1 variety in specific soil and climatic conditions.

Materials and research methods. The studies were conducted in the Laboratory of Vegetation and Production Process Management of Agricultural Crops of the Federal Scientific Center for Grain Legumes and Cereal Crops in 2022-2024. The soil of the experimental plot is dark gray forest medium loamy. The object of the research was an early soybean variety with a tendency to mid-early Lider

1 of the determinate type of growth and development (in the State Register of the Russian Federation since 2019), zoned for the 5th region (selection of AST LLC). Plants were grown on plots of 10 m2, fourfold repetition. The placement method of the experimental plots is randomized. Predecessor - fallow. Sowing method - wide-row. Seeding rate - 600 thousand viable seeds. The studies were carried out according to the following scheme: 1. Control (without the use of biological products); 2. Pre-sowing treatment; 3. Pre-sowing treatment + 1 foliar dressing in the phase of 1-3 trifoliate leaves; 4. Pre-sowing treatment + 2 foliar dressings in the phase of 1-3 trifoliate leaves and budding. The tank mixture for pre-sowing dressing and foliar treatments contains spores, live cells and biologically active metabolites of *Bacillus megaterium* (OPR-31), *Azospirillum zeae* (OPN-14), *Pseudomonas aureofaciens* (2391D), *Montierella alpine* (F-1134). The consumption rate of the working solution for pre-sowing seed treatment is 10 l/t, for foliar dressing of vegetative soybean plants - 200 l/ha.

Nitrogenase activity of symbiotic co-specific nitrogen-fixing bacteria was determined by the "acetylene" method. Results of the research. As a result of the constant presence of nitrogen-fixing crops, including soybeans, in the crop rotation of the experimental plot, a fairly numerous stable population of nitrogen-fixing bacteria was formed in the soil, the fact of which is confirmed by the presence of nodules on the roots of soybean plants in the control and experimental variants. Additional introduction of microbiological preparations in the tank mixture in the pre-sowing treatment of seeds and in foliar feeding affected the activation of soil microflora, namely the aboriginal race of co-specific symbiotic nitrogen-fixing bacteria found in the soil (since seed inoculation with Bradyrhizobium japonicum was not carried out before sowing) (table, figure).

Table

Symbiotic indicators of plants in the flowering phase of the soybean variety Lider 1 under the influence of microbiological preparations (2024)

Options	Values
Number of tubers, pcs/plant	
Untreated seeds and plants (control)	19
Pre-sowing seed treatment	27,8
Pre-sowing seed treatment +1 foliar fertilization	31,5
Pre-sowing seed treatment +2 foliar fertilizations	30,5
Average by experiment	27,2
HCP_{05}	9,4
Weight of tubers, g/plant	
Untreated seeds and plants (control)	0,07
Pre-sowing seed treatment	0,11

Pre-sowing seed treatment+1 foliar application	0,11
Pre-sowing seed treatment+2 foliar application	0,18
Average by experiment	0,12
HCP_{05}	0,08
Nitrogenase activity, µg N2/ml/h/1 plant	
Untreated seeds and plants (control)	1,21
Pre-sowing seed treatment	1,68
Pre-sowing seed treatment+1 foliar application	1,92
Pre-sowing seed treatment+2 foliar application	1,84
Average by experiment	1,66
HCP_{05}	0,18

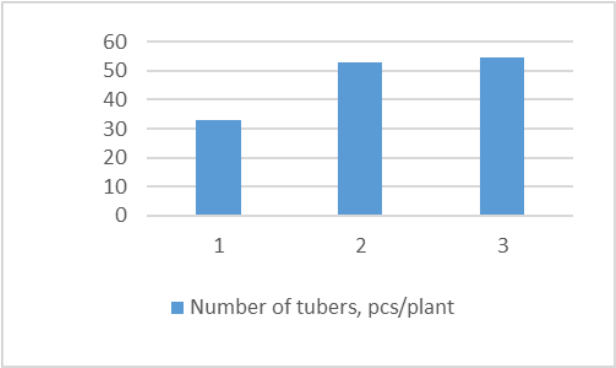

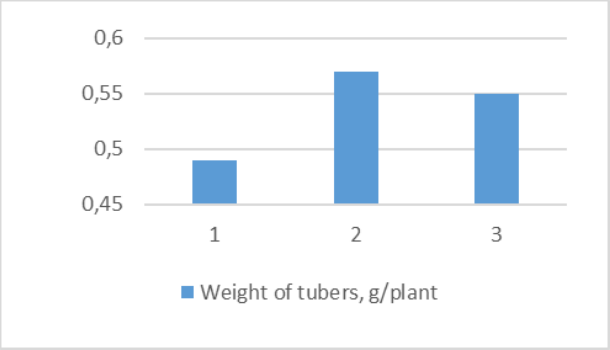

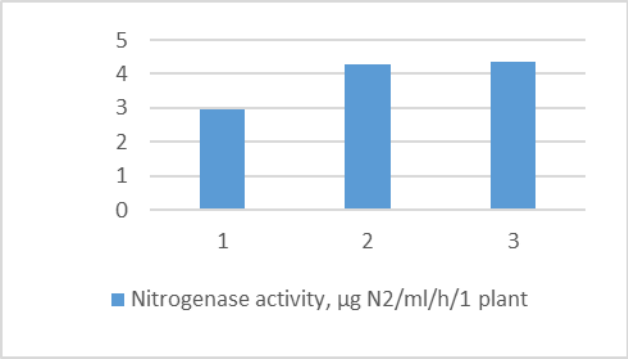

Figure. *Symbiotic indices of plants during the flowering period in the soybean variety Lider 1 depending on the use of microbiological preparations (on average for 2022-2024): 1 - control, 2 - pre-sowing treatment + 1 foliar fertilizing, 3 - pre-sowing treatment + 2 foliar fertilizing*

It should be noted that the complex of microorganisms used in pre-sowing seed treatment and in foliar fertilizing had a positive effect on the symbiotic nitrogen-fixing capacity of the root system of soybean plants. Symbiotic indices in the experimental variants with the use of foliar fertilizing on average over 3 years of research on the Lider 1 variety increased in comparison with the control: the number of symbiotic nitrogen-fixing nodules on the roots of soybean plants by 20.45 pieces or by 61.6%; fresh weight of nodules by 0.32 g or by 65.3%; nitrogenase activity of nodules by 1.37 µg N2/ml/h/1 plant or by 46.11% (Figure).

Conclusion. It can be unequivocally stated that microorganisms Bacillus megaterium OPP-31, Azospirillum zeae OPN-14, Pseudomonas aureofaciens 2391D, Montierella alpine F-1134 create a consortium with Bradyrhizobium japonicum, living in the soil (in this case), and have a beneficial effect on the activity of the latter in soybean crops.

References

1. Zotikov, V. I. Use of microbiological preparations in the cultivation of promising soybean varieties in the conditions of the Oryol region / V. I. Zotikov, K. Yu. Zubareva // Russian agricultural science. - 2024. - No. 4. - P. 14-19. – DOI 10.31857/S2500262724040034. – EDN FLNHPD.

2. Golovina, EV Exogenous regulation of symbiotic activity of new soybean varieties under the conditions of the Central Chernozem Region / EV Golovina, OV Leukhina // Grain legumes and cereal crops. – 2024. – No. 2(50). – P. 30-39. – DOI 10.24412/2309-348X-2024-2-30-39. – EDN TFPDDX.

3. Vasilchikov, AG Search for highly effective inoculants for promising soybean varieties / AG Vasilchikov, AS Akulov // Grain legumes and cereal crops. – 2019. – No. 4(32). – P. 66-71. – DOI 10.24411/2309-348X-2019-11134. – EDN LFNHLJ.

4. Zotikov, V. I. Diversification of agricultural practices that have a minimal impact on the environment / V. I. Zotikov, K. Yu. Zubareva // Current scientific developments for the crop production industry: Proceedings of international scientific and practical conferences, Orel, June 29 – July 03, 2023. – Orel: Printing Company "Kartush", LLC, 2023. – P. 40-49. – EDN GICXFX.

5. Golovina, E. V. Exogenous regulation of symbiotic activity of new soybean varieties under the conditions of the Central Chernozem Region / E. V. Golovina, O. V. Leukhina // Grain legumes and cereal crops. – 2024. – No. 2 (50). – P. 30-39. – DOI 10.24412/2309-348X-2024-2-30-39. – EDN TFPDDX.

DOI 10.34660/INF.2025.42.21.132

THE USE OF MICROORGANISMS IN THE PRODUCTION OF FERMENTED MILK PRODUCTS

Sboychakov Dmitry Viktorovich
Biotechnologist
Luga Dairy Plant, Luga, Russia

Reshetnikova Olga Vasilyevna
Candidate of Biological Sciences, Associate Professor
Leningrad State University named after A.S. Pushkin (Luga branch), Luga, Russia

Sboichakov Viktor Borisovich
Doctor of Medical Sciences, Full Professor
Leningrad State University named after A.S. Pushkin (Luga branch), Luga, Russia

Abstract. *The technology of production of fermented milk products is considered. Their role in healthy human nutrition is shown. Microorganisms of starter flora are considered. Biotechnological methods of production of fermented milk products are reflected. Emphasis is placed on the determination of the main allergens in milk by the enzyme immunoassay method. The advantage of the reservoir method of production over the thermostatic method is shown.*

Keywords: *fermented milk products, milk, fermentation, lactic acid microorganisms.*

Fermented milk products are dairy or composite dairy products obtained by fermentation of milk or dairy products, into which live starter microorganisms are introduced, leading to a decrease in pH and coagulation of protein. To obtain these vital products, it is necessary to induce the process of milk fermentation with the formation of lactic acid (lactate) using lactic acid bacteria [1,6]. By the nature of fermentation, a distinction is made between products with lactic acid homofermentative fermentation (ryazhenka, varenets, sour milk, yogurt, etc.) and products with mixed heterofermentative fermentation, when, along with lactic acid, alcohol, carbon dioxide and volatile acids are formed from lactose (kefir, ayran, kumiss, etc.). In the production of fermented milk products, lactobacilli (Lactobacillus delbrueckii subsp. bulgaricus, L. acidophilus, L. amylovorus, L. casei) are in

first place as “starters”. The lactobacilli currently used have a rapid biomass gain during cultivation, high biochemical and antagonistic activity and a shortened lag phase during milk fermentation. The strains do not have hemolytic, proteolytic, lecithinase, hyaluronidase, antilysozyme, DNA and RNA activity; they ferment glucose, galactose, sucrose, salicin, trehalose, maltose, celobiose, lactose, urea, and slowly ferment rhamnose, xylose, and D-arabinose [8].

In second place are bifidobacteria (Bifidobacterium adolescentis, B. animalis, B. bifidum, B. infantis, B. lactis), as well as mesophilic lactic acid streptococci (Streptococcus salivarius ssp. thermophilus, Lactococcus lactis ssp. cremoris, L. lactis ssp. lactis biovar diacetylactis) and a number of other bacteria. In the dairy industry, mesophilic streptococci Streptococcus salivarius ssp. thermophilus, Lactococcus lactis ssp. cremoris belong to the homofermentative group and decompose milk sugar to lactic acid. In some cases, they form small amounts of volatile fatty acids and acetone; they are active acid formers, the optimal temperature for their growth is 25°C - 30°C. Mesophilic heterofermentative streptococci (S. paracitrovorus, S. diacetilactis, S. acetoinicus, S. citrovorus) form lactic acid during the decomposition of lactose and diacetyl during the decomposition of citric acid. During this period, their growth temperature is 30°C, and for S. citrovorus and S. paracitrovorus - 21-25°C [7]. Thermophilic streptococcus is a mesophilic lactic acid streptococcus, represented by one species S. thermophilus, the optimal growth temperature is 40-45 °C □3□. Fermented milk products have an antagonistic effect on pathogenic bacteria (Salmonella spp., Shigella spp., Brucella spp.). Previously, this was associated with the acidic environment of the product, caused by the synthesis of lactic acid during fermentation. Later, bactericins produced by starter microorganisms were discovered. The latter also have an immunomodulatory effect [10].

Particular importance when selecting microorganism cultures for probiotic fermented milk products is given to such a property as resistance to antibiotics. Representatives of the genus Bifidobacterium are characterized by natural resistance to a number of antibiotic drugs. The combined use of antibiotics and antibiotic-resistant microorganisms contributes to the effective restoration of human microbiota [5]. The ability of individual strains of bifidobacteria to produce gamma-aminobutyric acid (GABA) and have a psychotropic effect allows them to be classified as psychobiotics [2].

Fermented milk products have a reduced lactose content, since it serves as a substrate for lactic acid fermentation processes, so these products can be consumed by people with lactase deficiency, as well as in hypoxic conditions [1,11]. Food allergies often develop when drinking milk. The main proteins of cow’s milk (beta-lactoglobulin, alpha-lactalbumin, bovine serum albumin (BSA), etc.) can cause allergic reactions [9]. Currently, enzyme-linked immunosorbent assay

(ELISA) is successfully used as a screening test [4]. Test systems have been developed to detect beta-lactoglobulin, alpha-lactalbumin and BSA in dairy products that have undergone all stages of technological processing [3,7]. There are two methods for producing fermented milk products: reservoir and thermostatic. In thermostatic - fermented milk is poured into small containers and fermented at optimal temperatures in a thermostatic chamber. After the clot is formed, the product is cooled to +2-6°C. This method is energy-intensive, requires large production areas and there is a risk of releasing a non-standard product in individual packages. In tank production, the entire technological process takes place in tanks, which reduces production areas, labor costs and energy resources, allowing you to get a product of stable quality.

In general, the tank process for the production of fermented milk products can be represented as a sequence of the following technological stages: raw material acceptance - cleaning - homogenization - pasteurization - cooling - fermentation - mixing - fermentation - mixing - ripening - bottling, packaging and labeling.

The most important role in ensuring the quality and safety of finished dairy products belongs to the quality of the original raw milk. Milk purification for the purpose of removing mechanical impurities is carried out on milk separators with periodic manual or centrifugal sediment discharge. Homogenization of the mixture is carried out to prevent fat settling. Homogenizers are designed to crush and evenly distribute fat globules. Plate or tubular coolers are used to cool milk. Such equipment prevents the active growth of psychrophilic bacteria by quickly cooling fresh milk from 35°C to 4–6°C. Intermediate storage should not exceed 24 hours. Plate coolers are a set of plates made of food-grade stainless steel and rubber sealing gaskets. In tubular coolers, pipes become the cooling element. Plate coolers allow the milk flow to be divided into the thinnest layers, evenly alternating with layers of coolant or heat carrier. Heat exchange in such systems is carried out at high speed, while the heat exchanger itself is small in size, but highly efficient. This is the main advantage of plate units. Tubular units heat the product using steam or electric heaters. All tubular units consist of heat exchangers, which include tubes for cooling or heating the product. To achieve a certain temperature, you can connect or disconnect some cylinders. Thus, some cylinders can be used to lower the temperature, and others - for pasteurization. Pasteurization of the mixture is carried out in plate pasteurization and cooling units to destroy pathogenic microbiota, destroy enzymes, impart flavor to the product and extend shelf life. The pasteurization temperature should not exceed 99 ° C. During this heat treatment, the process of complexation between casein and whey proteins occurs. Varenets is subjected to heat treatment for up to 1 hour during production, ryazhenka - 3-5 hours. This process is called languishing. It is carried out in capacitive pasteurizers. Tanks for processing raw materials must be equipped with

a jacket for supplying ice water, hot water and steam. After pasteurization, the container must be immediately cooled with ice water only.

The fermentation modes are selected depending on the composition of the starter used. If a starter of thermophilic bacteria is used, the milk is cooled to +40–45°C, mesophilic – to +30–35°C, kefir – to +18–20°C. The starter corresponding to the type of product being manufactured is added to the raw material cooled to the required temperature. As a result, the products acquire a pronounced light cream color, characteristic taste and aroma (the formation of melanoidins, carbonyl and other intermediate compounds occurs). Then the substrate is cooled in order to create conditions for the development of the starter microbiota in universal tanks. The starter is introduced into the tank in order to direct the microbiological processes at a temperature of 38–42°C. The starter is prepared in accordance with the technological instructions and fed into the tank. As a result of the vital activity of microorganisms, a deep breakdown of lactose, lipids and milk proteins occurs. The mixture is fermented in tanks for fermented milk drinks, equipped with special mixers that ensure uniform and thorough mixing of the mixture with the starter. Fermentation is carried out in order to increase acidity and form a dense clot in the tank at a temperature of 38–42°C for 4–5 hours, until a clot forms.

Then the finished product is fed to a packaging machine for packaging in order to give the product a marketable appearance, protect it from environmental influences and facilitate transportation.

References

1. Gavrilina, A.D. Fermented milk products as a component of functional nutrition / A.D. Gavrilina, I.R. Shelaginova, Z.S. Zobkova // Dairy industry. – 2019. – No. 2. – P. 44.

2. Danilenko, V. N. Bifidobacterium adolescentis 150 and Bifidobacterium angulatum GT 102 strains synthesizing gamma-aminobutyric acid / V. N. Danilenko, O. V. Averina, M. S. Dyachkova // Patent No. 2614110 Russian Federation, IPC C12N 1/20, C12P 7/52, C12R 1/01. publ. 22.03.2017.

3. Zvereva, E. A. Enzyme-linked immunosorbent assay of milk proteins as biomarkers in monitoring the composition of dairy and meat products / E. A. Zvereva, N. I. Smirnova, O. D. Gendrikson et al. // Actual biotechnology. – 2021. – No. 1 (35). – P. 111.

4. Panin, A.L. Options for performing enzyme immunoassay / A.L. Panin, S.G. Fedorova, D.V. Sboychakov // Science and education in the life of modern society: collection. scientific articles dedicated to the memory of prof. M.V. Ivanova / rep. ed. V.B. Sboychakov. – SPb.: Leningrad State University named after. A.S. Pushkina, 2015. – pp. 115–122.

5. Rozhkova, I.V. Probiotic potential of Bifidobacterium adolescentis MS-42 / I.V. Rozhkova, A.V. Begunova // Dairy industry. – 2021. – No. 3. – P. 34-37. – DOI 10.31515/1019-8946-2021-03-34-36.

6. Sboychakov, D. V. Actual problems of production of fermented milk drinks / D. V. Sboychakov // X Anniversary Luga Scientific Readings. Modern scientific knowledge: theory and practice: Proceedings of the international scientific conference, St. Petersburg, May 23, 2022. – St. Petersburg: Leningrad State University named after A.S. Pushkin, 2022. – P. 375-379. – EDN NKXSEC.

7. Tabyldieva, A. G. Biotechnology of production of fermented milk products in a private enterprise / A. G. Tabyldieva, T. Smailova, A. B. Sultangazieva // Bulletin of the Kyrgyz National Agrarian University named after K.I. Skryabin. – 2023. – No. 3(66). – pp. 98-104. – EDN XZCOEM.

8. Tarabukina, N.P. A new strain of Lactobacillus delbrueckii subsp. bulgaricus K 1903 / N. P. Tarabukina, M. P. Neustroev, N. A. Oboeva, S. I. Parnikova // Veterinary and feeding. – 2023. – No. 3. – P. 73-76. – DOI 10.30917/ATT-VK-1814-9588-2023-3-19.

9. Bartuzi, Z. The contribution of the analysis of molecular allergens in the diagnosis of Allergy to milk / Z. Bartuzi, R. Cocco, A. Muraro, W. Nowak // Curr. Allergy Asthma Rep. – 2017. – Vol. 17 (24). – P. 46–52.

10. Meyer, A.L. Probiotic, as well as conventional yogurt, can enhance the stimulated production of proinflammatory cytokines / A.L. Meyer, I. Elmadfa, I. Herlacek // J. Human Nutr. and Diet. – 2007. – Vol. 20 (6). – P. 590–598.

11. Song, K. Lactobacillus delbrueckii subsp. bulgaricus Alleviates Acute Injury in Hypoxic Mice / K. Song, H. Ling, L. Wang [et al.] // Nutrients. – 2024. – Vol. 16, No. 10. – P. 1465. – DOI 10.3390/nu16101465. – EDN XCSMZW.

DOI 10.34660/INF.2025.17.60.133

THE INFLUENCE OF ARTIFICIAL VENTILATION ON THE CORRELATIONS OF LABORATORY BIOCHEMICAL PARAMETERS AND HEMODYNAMIC PARAMETERS IN ACUTE CEREBRAL INSUFFICIENCY AT THE AGE OF 3.1-7 YEARS

Muhitdinova Hura Nuritdinovna
Doctor of Medical Sciences, Full Professor
Center for the Development of Professional Qualifications of Medical Workers

Rahimova Suraye Rusmetovna
Deputy Chief Physician
Republican Scientific Center for Emergency Medical Care

Myrzayeva Adiba Damirovna
Head of Department
Republican Scientific Center for Emergency Medical Care

Abstract. *During the first week of intensive care in the compensated stage of ARF, minor ACI against the background of spontaneous breathing, an increase in the activity of the proliferative phase of the SVR was noted. The identified correlations of the functional activity of lymphocytes were practically absent in children of group 2. In conditions of initially more pronounced ARF, ACI in children of group 2, more active intensive complex therapy with mechanical ventilation revealed an increase in the effectiveness of corrective effects of traditional intensive care, optimizing the outcome of treatment of children of group 2 aged 3.1 to 7 years.*

Keywords: *artificial ventilation of the lungs, laboratory and biochemical parameters, hemodynamics, acute cerebral insufficiency.*

Relevance. Acute cerebral failure is a life-threatening condition accompanied by “neurogenic” multiple organ failure, the development of which aggravates the course of the disease and increases the risks of an unfavorable outcome. It has been proven that intracranial hypertension leads to a violation of neurohumoral regulatory processes and vegetative functions, as well as to a breakdown of compensatory mechanisms. “Neurogenic” organ dysfunction requires clinicians to

conduct basic monitoring of vital parameters, a set of measures for the prevention and treatment of neurogenic complications.

Organ damage develops as a result of a mediator storm against the background of severe cerebral damage by an acute systemic inflammatory response (ASIR) and is nonspecific for ACI. Activation of the sympathoadrenal system reduces intestinal blood flow and leads to intestinal ischemia, which primarily damages the most metabolically active intestinal epithelium with its necrosis. Acute cerebral injury, accompanied by the picture of ACI, often leads to neurogenic activation of the sympathetic system and the development of a catecholamine storm. Excessive cerebral activation of the sympathoadrenal system contributes to the contraction of the spleen, which has predominantly sympathetic innervation, which is accompanied by the release of neutrophils and an increase in the concentration of serum proinflammatory cytokines. Subsequently, after 3-5 days, the phase of activation of the immune system is transformed into the stage of immunodepression, characterized by the synthesis of anti-inflammatory cytokines and a decrease in the number of leukocytes. There is an assumption that immunodepression can play an important role in reducing the severity of neuroinflammation, damage to the blood-brain hormone and secondary cerebral injury. At the same time, the immunodepression phase can play an unfavorable role in the development of purulent-septic complications that aggravate the course of ACI. The brain and spinal cord have the largest reserves of platelet activating factor, and in case of hypoxic, ischemic, or traumatic brain damage, its concentration increases 20-fold. Both hypercoagulation and hypocoagulation are factors of secondary cerebral damage that enhance the primary one [1-8]. Due to the insufficient data on the study of ACI in children, we attempted to somewhat expand our understanding of the effect of complex intensive care, including artificial ventilation, on the formation of compensatory connections in children aged 3.1-7 years.

Objective of the work. To study the effect of artificial ventilation on the correlations of clinical and biochemical parameters and hemodynamics in ACI at the age of 3.1-7 years.

Material and methods of research. The results of continuous prolonged monitoring with hourly recording of hemodynamic parameters, myocardial oxygen demand (MOD), body temperature, respiration, as well as laboratory and biochemical parameters of blood tests were studied in children admitted to the ICU of the RRCEM in a serious condition caused by pneumonia complicated by acute respiratory and cerebral insufficiency at the age of 3.1 to 7 years. Intensive care was carried out in accordance with the recommendations in thematic clinical protocols. In group 1, 7 children were studied who had no indications for mechanical respiratory support upon admission to the clinic and throughout intensive care. Almost all patients in group 2 (9 children) were transferred to mechanical

ventilation from the moment of admission to the clinic according to indications. The research data were processed by the method of variation statistics using the Excel program by calculating arithmetic means (M) and errors of means (m). To assess the reliability of differences between two values, the parametric Student criterion (t) was used. The critical significance level was taken to be 0.05. The relationship between the dynamics of the studied indicators was determined using the pair correlation method.

Results and discussion. As shown in Table 1, the red blood cell counts in children of group 1 during spontaneous breathing did not differ from physiological parameters, a tendency to an increase in the average number of blood leukocytes to 10.4±1.5 10^9/l, a tendency to an increase in the number of metamyelocytes 3.7±1.6%, monocytes 4.2±1.5% were noted. In the first week of complex intensive care with the use of artificial ventilation, in contrast to the parameters of group 1, a tendency to a decrease in blood hemoglobin was revealed, in the absence of significant differences in other blood components despite more severe ACI, ACI. In the subsequent second week of intensive care, no noticeable changes in the parameters of the general analysis of peripheral blood were observed, the parameters corresponded to the data of the first week of observation of the acute period of SVR in children of group 2.

Table 1.

Composition of peripheral blood

Blood parameters	1 group	2 group 7 days	2 group 14 days
Erythrocytes x10^12/l	3,7±0,2	3,3±0,5	3,4±0,4
Hemoglobin, %	114,9±4,9	93,8±14,1	97,0±11,8
GMT,%	35,0±1,0	32,8±1,9	33,1±2,0
Thrombocytes, thousand/mcl 10^9/l	221,6±16,1	204,7±8,4	210,8±10,6
Leukocytes, 10^9/l	10,4±1,5	9,7±1,8	9,6±1,4
Metamyeloc,%	3,7±1,6	2,0±0,1	2,0±0,1
Palanuclear,%	4,5±1,5	3,5±2,0	3,2±2,1
Segmented,%	63,0±11,4	70,0±7,9	70,9±6,0
Eosinophils,%	1,0±0,0	2,1±0,6	1,9±0,7
Lymphocytes,%	28,8±14,4	22,0±7,9	21,0±6,1
Monocytes,%	4,2±1,5	5,0±1,8	5,3±1,7
ESR, mm/hour	8,6±1,0	10,5±4,2	9,8±3,3

Table 2.

Blood biochemistry indicators

Blood parameters	1 group	2 group 7 days	2 group 14 days
Glucose, mol/l	6,1±0,7	5,2±0,2	4,8±0,5

Total protein, g/l	66,8±6,3	60,5±6,8	62,1±5,1
Albumin, g/l	24,4±12,7	33,0±6,4	32,3±5,2
Blood urea, mol/l	3,9±2,6	5,5±1,0	5,6±1,4
Creatinine, mol/l	0,3±0,1	0,05±0,01	0,05±0,01
Blood diastase, mol/l	39,0±1,8	78,0±35,2	68,6±26,7
Plasma potassium, mol/l	4,2±0,1	3,7±0,2	3,7±0,3
Plasma sodium, mol/l	132,0±5,0	141,3±2,4	140,0±2,8
Plasma calcium, mol/l	2,3±0,2	2,2±0,3	1,6±0,6
ALT, u/l	51,5±17,0	28,0±6,8	31,3±8,8
AST.u/l	59,9±14,1	47,2±10,6	45,9±10,1
PI,%	94,8±0,05	95,2±14,5	95,2±14,5

The initial biochemical blood composition in group 1 was characterized by a tendency to hypoalbuminemia (24.4±12.7 g/l, treatment was carried out without albumin transfusion), an increase in ALT (51.5±17.0 u/l), AST (59.9±14.1 u/l). While in a more severe condition in group 2 in the first two weeks of complex intensive therapy, more active corrective therapy, including albumin transfusion, contributed to maintaining total protein and blood albumin at a physiological level (32.3±5.2 g/l), ALT and AST within normal values (Table 2). The fluid balance corresponded to physiological needs according to the age and weight of children in both groups. No more than 16% in group 1 and 20% in group 2 were administered intravenously, which contributed to the preventive exclusion of the likelihood of prerenal ARF. Thus, diuresis in group 1 was 1.8 ml/kg per hour, in group 2 – on average 2 ml/kg per hour.

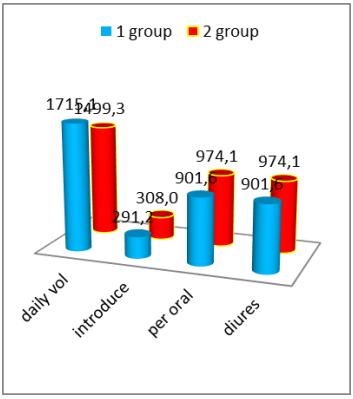

Figure 1. *Water balance in ml/day.*

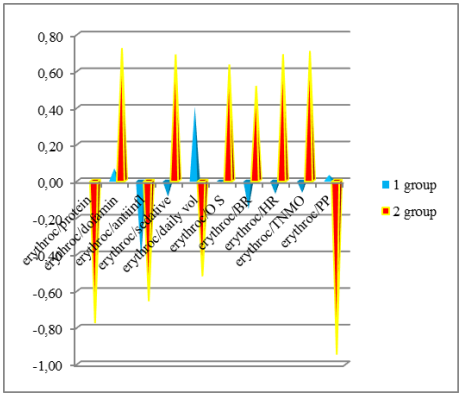

Figure 2. *Correlation relationships of red blood cells*

In the absence of significant changes in the content of red blood cells in the blood in group 2, a negative correlation with albumin transfusion was found, that is, the correction of hypoalbuminemia was accompanied by a tendency to decrease red blood cells in the blood (Fig. 2). The introduction of dopamine and sedative therapy to children in group 2 contributed to an increase in the number of red blood cells (0.72; 0.69; respectively) within the physiologically acceptable values. Accordingly, the increase in the number of red blood cells revealed a positive trend towards an increase in the oxygen saturation index, RR, HR, and PMC (0.63; 0.52; 0.69; 0.71, respectively). The detected inverse correlation between erythrocytes and cardiac output (-0.95) indicated a high risk of decreasing cardiac output (an indirect indicator of cardiac output) (-0.95) with an increase in the number of red blood cells by more than 3.4±0.4 x10^12/l.

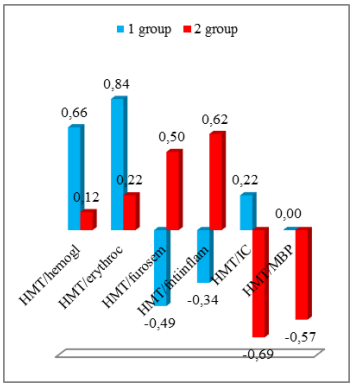

Figure 3. *Correlation relationships of GMT.*

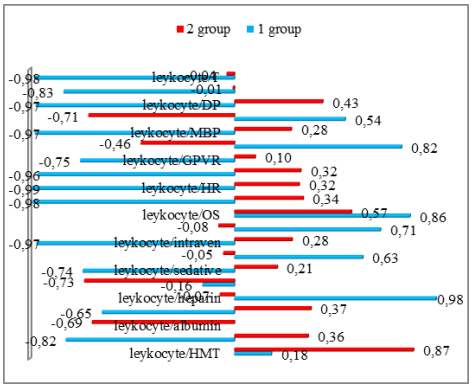

Figure 4. *Correlation relationships of leukocytes.*

The physiological direct relationship between the GMT, hemoglobin (0.66), and the number of erythrocytes (0.84) indicators in group 1 was completely leveled out in the more severe condition of children in group 2, amounting to 0.12; 0.22, respectively, against the background of the absence of significant differences in the average levels of the studied indicators. That is, the SVR with the development of more severe ACI and ARF and more radical intensive therapy disrupted the functional correlation relationships that have a compensatory value between the indicators of the number of erythrocytes in the peripheral blood, GMT and hemoglobin (Fig. 3). In group 1, in the acute period of SVR, diuretic therapy was accompanied by a decrease in the number of leukocytes in the blood (-0.82), the same direction of the effect of furosemide was revealed with respect to the parameters of sedatives (-0.74), parenteral infusion therapy (-0.97), respiratory

rate (-0.98), heart rate (-0.99), PMC (-0.96), total peripheral vascular resistance (-0.75), mean arterial pressure (-0.97), diastolic arterial pressure (-0.97), systolic arterial pressure (-0.83) and body temperature (-0.98) in group 1 of children with spontaneous breathing (Fig. 4). While in group 2 these correlations almost completely disappeared due to more intensive complex therapy with artificial ventilation. Apparently, more extensive stress-limiting therapy with complete leveling of the brain's control function due to cerebral hypoxia complicated by acute cerebral insufficiency and severe acute renal failure almost completely suppresses the protective compensatory mechanisms of a balanced state of homeostasis, which functioned quite actively in mild forms of acute cerebral insufficiency with minor impairment of consciousness. Under these conditions, the protective compensatory mechanisms operating in a moderate mode due to limited individual reserve capabilities, a more significant energy-deficient state, being insufficient, do not provide the necessary intensity for life-support of the functions of organs and systems in the process of adaptation of the body to severe acute cerebral insufficiency, acute renal failure, ultimately leading to the development of polyneuropathy. Excessive protective activity of compensatory mechanisms in children is manifested primarily by clinical signs of acute cerebral insufficiency, acute renal failure, disturbances in hemodynamic parameters, requiring urgent radical measures, including artificial ventilation, administration of vasopressors, etc.

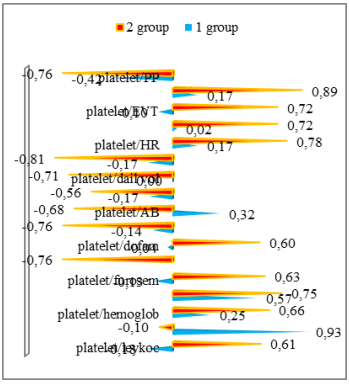

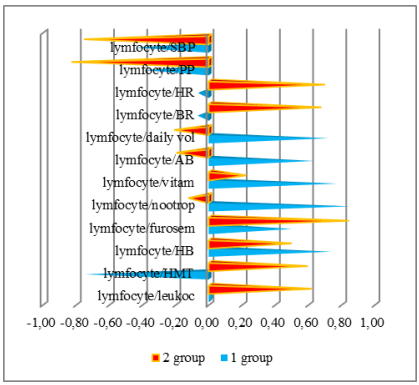

Figure 5. *Correlation relationships of platelets.*

Figure 6. *Correlation relationships of lymphocytes.*

Direct correlation relationship of the number of platelets with the GMT index (0.93), as well as with the number of erythrocytes (0.57) in group 1 at a level of 221.6 ± 16.1 corresponded to the growth of the red part of the blood due to hemoconcentration caused by dehydration (Fig. 5). In group 2, the revealed direct cor-

relation relationships of platelets with leukocytes (0.61), hemoglobin level (0.66), erythrocytes (0.75) confirmed the growth of the tendency to hemoconcentration (Fig. 5).

In group 2, against the background of more significant stress-protective drug therapy, external respiration prosthetics, signs of stress autonomic response (0.72), increased heart rate (0.78), increased myocardial oxygen demand (0.89) appeared. Albumin transfusion contributed to the tendency to decrease the platelet count (-0.76) within 210.8±10.6 10^9/l. The antiplatelet effect of platelets was promoted by the introduction of heparin (-0.76), antibacterial therapy (-0.68), anti-inflammatory (-0.56), an increase in the daily volume of fluid administration (-0.71), and an increase in the excretory activity of the kidneys (-0.81). Thus, in the conditions of initially more pronounced ARF, ACI in children of group 2, the more active intensive complex therapy with artificial ventilation revealed an increase in the effectiveness of the corrective effects of traditional intensive care, optimizing the outcome of treatment of children of group 2. The growth of GMT caused a decrease in the number of lymphocytes (-0.75), but at the same time a direct connection was noted between the increase in the number of lymphocytes due to the growth of hemoglobin (0.73), nootropic (0.85), metabolite (0.77), antibacterial (0.63) activity, an increase in the daily volume of water (0.71) in group 1. That is, an increase in the activity of the proliferative phase of the SVR was noted during the first week of intensive therapy at the compensated stage of ARF, insignificant ARF against the background of spontaneous breathing (Fig. 6). It should be noted that the identified correlations of the functional activity of lymphocytes practically disappeared in children of group 2.

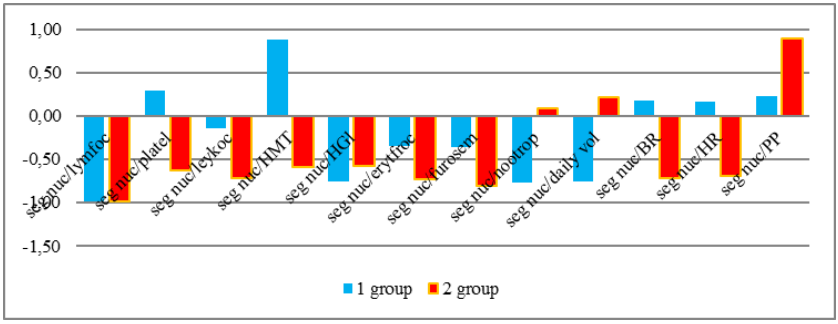

Figure 7. *Correlation links of segmented nuclei.*

Segmented nuclei are mature forms of leukocytes, which play a key role spend in the blood for only about two hours, then are distributed among the tissues in both groups were normally in a physiological inverse correlation with the number

of lymphocytes, amounting to in group 1 (-0.98), in group 2 (-0.99). The differences were manifested in a positive relationship with GMT (0.89), a negative correlation with the level of hemoglobin (-0.75), nootropics (-0.77), daily volume of administered fluid (-0.75) in group 1, which were absent in group 2 (Fig. 7).

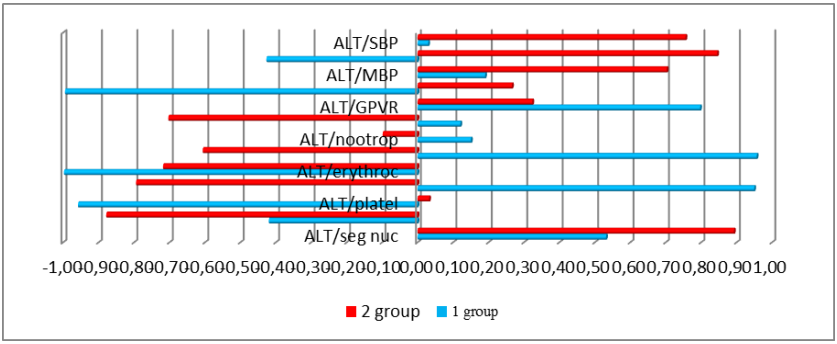

Figure 8. *Correlation links of ALT.*

The growth of alanine aminotransferase (ALT) indicates damage to hepatocytes, the higher the value, the more pronounced the necrosis of ALT-rich hepatocytes, indicates a cytolytic syndrome, characterizing severe intoxication, toxic effect of hepatotropic substances. In group 1, a tendency towards an increase in ALT was revealed (51.5±17.0 u/l). With moderate cytolytic syndrome, an inverse relationship was revealed with the number of platelets (-0.96), erythrocytes (-0.91), and SV (-0.99). But the direct correlation of ALT and GMT (0.95), with the activity of diuretic therapy with furosemide (0.96), OPSS (0.88), and the inverse with SV (-0.99) characterized thrombolytic, hemolytic activity in conditions of blood hemoconcentration with a simultaneous increase in the tone of peripheral vessels and a negative effect on cardiac output. Thus, in group 1, an increase in ALT contributed to thrombolytic activity in conditions of a tendency to develop a hypodynamic type of hemodynamics, an early sign of acute heart failure in conditions of intensive conservative (without mechanical ventilation) therapy of moderate ARF and ACF. Transfer to mechanical ventilation of children in a more severe condition did not significantly affect the number of erythrocytes (-0.72), noticeably increasing the hemolytic effect, which is confirmed by the appearance of an inverse relationship with GMT (-0.79). The increase in ALT was accompanied by a decrease in oxygen saturation (-0.7), an increase in mean arterial pressure (0.7), an increase in systolic blood pressure (0.76) and pulsed blood pressure (0.85) (Fig. 8).

Conclusion. During the first week of intensive care in the compensated stage of ARF, slight acute cerebral insufficiency against the background of spontaneous breathing, an increase in the activity of the proliferative phase of the respiratory tract was noted. The identified correlations of the functional activity of lymphocytes were practically absent in children of group 2. In conditions of initially more pronounced ARF, acute cerebral insufficiency in children of group 2, the more active intensive complex therapy with artificial ventilation revealed an increase in the effectiveness of the corrective effects of traditional intensive care, optimizing the outcome of treatment of children of group 2.

References

1. Aleksandrovich Yu.S., Pshenisnov K.V. General recommendations for the diagnosis and treatment of acute cerebral insufficiency in the neonatal period. In the book: Emergency neurology of newborns and young children. St. Petersburg: SpetsLit, 2017. Pp. 11-57.

2. Belkin A.A., Zislin B.D., Avramchenko A.A., Alasheev A.M., Selsky D.V., Gromov V.S., Domansky D.S., Inyushkin S.N., Pochepko D.V., Rudnik E.I., Soldatov A.S. Acute cerebral insufficiency syndrome as a concept of neuroreanimatology. Anesthesiology and reanimatology. 2008;2:4-8.

3. Gromov V.S., Levit A.L., Belkin A.A., Shilko Yu.V., Prazdnichkova E.V. Cerebrocardial manifestations in acute cerebral failure of various origins: differential diagnostics and treatment tactics. Blood circulation pathology and cardiac surgery. 2014;18(3):48-52. http://doi.org/ 10.21688/1681-34722014-3-48-52

4. Zadvornov A.A., Grigoriev E.V. Extracerebral manifestations of acute cerebral failure in critically ill patients. Fundamental and clinical medicine. 2022;7(3):64-73. https://doi.org/10.23946/2500-0764-2022-7-3-64-73

5. Rachfalska N, Putowski Z, Krzych tJ. Distant Organ Damage in Acute Brain Injury. Brain Sci. 2020;10(12):1019. http://doi.org/ 10.3390/ brainsci10121019

6. Battaglini D, Robba C, Lopes da Silva A, Dos Santos Samary C, Leme Silva P, Dal Pizzol F, Pelosi P, Rocco PRM. Brain-heart interaction after acute ischemic stroke. Crit Care. 2020;24(1):163. http://doi.org/ 10.1186/s13054-020-02885-8

7. Amin HZ, Amin LZ, Pradipta A. Takotsubo Cardiomyopathy: A Brief Review. J Med Life. 2020;13(1):3-7. http://doi.org/ 10.25122/jml-2018-0067

8. Towner JE, Rahmani R, Zammit CG, Khan IR, Paul DA, Bhalla T, Roberts DE. Mechanical ventilation in aneurysmal subarachnoid hemorrhage: systematic review and recommendations. Crit Care. 2020;24(1):575. http://doi.org/ 10.1186/s13054-020-03269-8

DOI 10.34660/INF.2025.92.38.134

FORMATION OF HYGIENIC SKILLS IN SCHOOL-AGE CHILDREN IN TERMS OF PREVENTION OF CONTAGIOUS SKIN DISEASES

Efanova Elena Nikolaevna
Candidate of Medical Sciences, Associate Professor
Surgut State University, Surgut, Russia

Annotation. *Prevention of contagious skin diseases, including among the child population, does not lose relevance at the present time. The prevalence of contagious skin diseases depends on the formation of hygienic skills of the population and its sanitary and hygienic literacy. In the presented work, in addition to highlighting the significance of the study, an analysis of the survey of school-age children on personal hygiene was carried out. The aim of the study was to determine the level of formation of hygiene skills in children of primary and secondary school age in the city of Surgut (on the example of a secondary school). As a research method, a group questionnaire was used in a distributing way. The questionnaire included closed, semi-closed and open questions. It is shown that a significant part of schoolchildren do not attach importance to some aspects of personal hygiene, thereby underestimating the increase in the likelihood of infection with various infectious dermatoses (pyodermatitis, scabies, lice, ringworm, viral skin diseases, etc.). Conclusions are drawn about the need to strengthen the work on hygienic education and upbringing of schoolchildren, as well as their parents. Propaganda of medical and hygienic knowledge among the population contributes to the reduction of morbidity and mortality, helps to bring up a healthy, physically strong generation.*

Keywords: *school-age children, hygiene skills, contagious skin diseases, skin, questioning.*

Introduction

Hygienic education is a set of educational, upbringing, propaganda and promotional activities aimed at creating a healthy lifestyle, preventing diseases, maintaining and strengthening health, increasing the working capacity of people, prolonging their active life [1].

Hygiene education and upbringing is based on the concept of healthy lifestyle formation, the main tasks are formulated: reduction of smoking prevalence; im-

proving the quality of nutrition; increased physical activity; mitigating the impact of damaging psychosocial factors and improving the quality of life; reduced alcohol consumption; prevention of drug use; observance by the population of measures of personal and public hygiene [1, 2].

The formation of hygiene skills is aimed at improving the health of the population and is inextricably linked with the education of a culture of behavior.

Education in children the skills of personal and public hygiene plays an important role in protecting their health, promotes proper behavior in everyday life, in public places. Not only their health, but also the health of other children and adults depends on the knowledge and implementation by children of the necessary hygienic rules and norms of behavior [2, 3].

Failure to comply with hygiene requirements and standards can contribute to the penetration of pathogens into the human body and the development of infectious diseases, including skin lesions (pyodermatitis, scabies, lice, dermatomycosis, viral lesions, and others) [1, 3].

Many underestimate the importance of the skin, considering it just a shell of a person, but it performs a number of irreplaceable functions in the body. First of all, the skin is a barrier to the penetration into the body of both pathogens and a large number of substances harmful to humans. The colonization resistance of the skin is such that most microorganisms, in the absence of microtraumas, are unable to overcome this barrier. The only exceptions are Staphylococcus aureus and Propionibacterium acne. The protective function of the skin in children is imperfect due to the fact that the stratum corneum of the epidermis is thin, and its keratinization and connection with the dermis are insufficient. Insufficiency of local immunity is also associated with underdevelopment of the glands, dry skin, a reaction close to neutral [3, 4, 5].

In the issue of the spread of infectious skin diseases, social reasons are of particular importance: often the population has a low level of education about the disease. Propaganda of medical and hygienic knowledge among the population contributes to the reduction of morbidity and mortality, helps to bring up a healthy, physically strong generation [6].

Purpose: to determine the level of formation of hygiene skills in children of primary and secondary school age in the city of Surgut (on the example of a secondary school).

Materials and methods: the method of group questioning was used in a distributing way. The questionnaire included closed, semi-closed and open questions.

Results: The survey involved 127 children in the age range from 7 to 14 years; of them 60 boys and 67 girls. Most of the respondents have satisfactory living conditions: 86 people live in a separate apartment or house, 11 people in a rented apartment, 3 people in a hostel, 28 people chose the answer “other” (with relatives, etc.).

The majority of respondents are aware of the need to observe elementary rules of personal hygiene as a preventive measure for contagious skin diseases. 62 girls and 53 boys wash their hands before eating, 13 children do not wash their hands. 63 girls and 53 boys wash their hands after going to the toilet, 11 children do not wash their hands.

To the question "Do you wash your hands after playing with animals?" 84 children answered "yes" (of which 53 were girls), "no" - 43 people.

To the question "If you have animals, do you take them to bed?" 56 children answered in the affirmative (of which 21 were boys, 35 were girls), and 71 people answered in the negative (of which 40 were boys and 31 were girls) (figure 1).

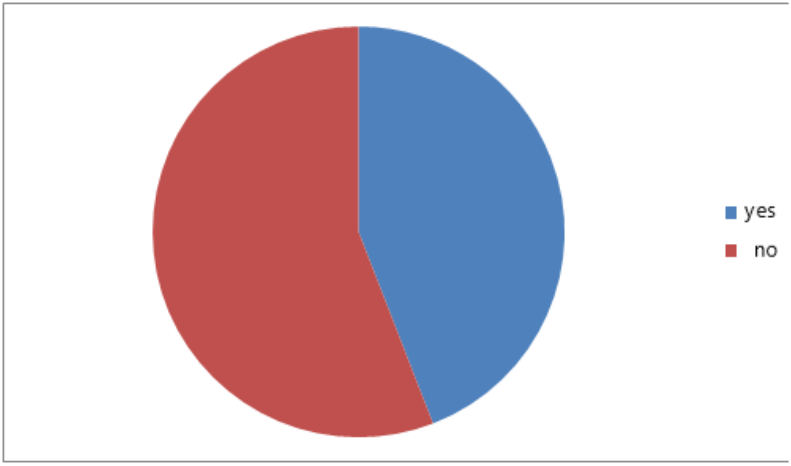

Figure 1. *Do you have animals; do you take them to bed?*

30 children answered "yes" to the question "Do you pet homeless animals?" (of which 15 were boys, 15 were girls), 97 people answered "no" (of which 45 were boys, 52 were girls).

It was found that the majority of children wash their hands before eating and after going to the toilet. However, it is sad that 43 out of 127 people did not wash their hands after contact with animals, and 56 children took animals to bed. Undoubtedly, this category of respondents is at risk for infection with ringworm (microsporia and trichophytosis).

To the question "How often do you wash your face?" 22 children answered "only in the morning", 5 - "only in the evening", 58 - "in the morning and in the evening", 23 (and only girls) - "several times a day". Hygiene of the face area 1 time per day is clearly insufficient; the accumulation of microorganisms and dead

scales of the stratum corneum of the epidermis contribute to the development of pustular skin diseases. The other extreme - washing several times a day - also negatively affects the condition of the skin due to a violation of the water-lipid mantle.

Regarding the use of face skin care products (tonic, milk for washing, face cream) when washing, disappointing results were obtained: 45 people answered in the affirmative, 82 answered negatively (the proportion of boys and girls is comparable). It can be concluded that there is a lack of awareness among children about facial skin care.

Only 30 children wash their feet before going to bed (of which 15 are boys, 45 are girls), 97 people do not wash their feet (of which 45 are boys, 52 are girls). In this group, the risk of fungal and viral lesions of the feet is increased.

On questions of body hygiene, the following data were obtained. 67 people wash their bodies every day (of which 40 are girls and 27 boys) and 46 of them with a washcloth, 28 people once a week, 32 people 2 times a week.

After taking a shower, do you use skin care products (body milk, body lotion, body oil, body cream)? 44 children (of which 10 are boys, 34 are girls), do not use - 83 people (of which 59 are boys, 24 are girls).

Regarding hair hygiene, it was found that 31 children (7 girls and 24 boys) wash their hair daily, 52 children wash their hair once a week, 40 children wash their hair 2 times a week, 4 children wash their hair once a month (3 boys and 1 girl, respectively) (figure 2).

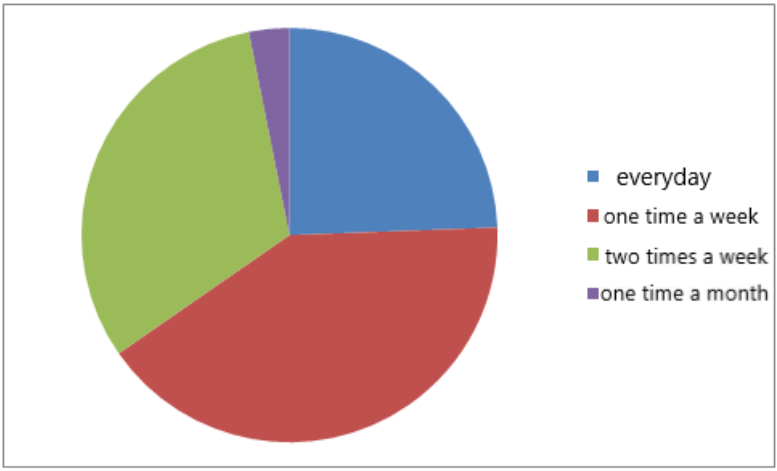

Figure 2. *How often do you wash your hair?*

According to the results of the survey, insufficient knowledge of children in matters of body and hair hygiene was revealed (% wash the body once a week and fall into the risk group for pustular skin diseases).

To the question "How often do you cut your nails?" 84 respondents answered once a week, 25 people - twice a month, 18 children - once a month.

Change socks daily 45 children (boys 14, girls 31), 1 time in 2 days 70 children, 2 times a week 12 children.

To the question "Do you use someone else's comb?" - "yes" was answered by 45 people (approximately equal number of boys and girls), "no" - 82 children.

To the question "Do you walk barefoot?" answers were received: 6 children do not walk (5 boys, 1 girl), the rest walk barefoot (several options are allowed) (at home - 97 people, on the grass - 26, on the sand on the beach - 63 people). There is no doubt that when walking barefoot, the risk of infection with dermatomycetes increases. When visiting swimming pools, baths, saunas, 120 children use individual shoes (an approximately equal number of boys and girls), "no" - 7 people. "Do you use someone else's shoes in everyday life (parents, siblings, friends, at a party, etc.)?" - "yes, always" answered 3 children, "yes, sometimes" - 27 children, "no" - 97 people.

To the question "Do you use someone else's toothbrush?" - "yes, always" answered 3 children, "yes, sometimes" - 2 children, "no" - 122 people.

To the question "Do you try on and wear other people's hats, clothes, shoes?" 34 people answered in the affirmative, 93 children answered in the negative.

44 children use other people's headphones, 83 children do not. 114 children know that they need to have their own towel, 13 children do not know.

To the question "What do you do when you get scratches, abrasions, wounds?" data were obtained: "I seek medical help" - 51 people, "I treat abrasions and scratches on my own" - 45 children, "I do nothing, it will heal itself" - 20 children, another - 11 respondents (I seek help from parents, teachers, etc.).

Conclusions

Summarizing the above, we can conclude that a significant part of school-age children are not sufficiently knowledgeable in matters of personal hygiene, and constitute a risk group for the development of contagious skin diseases, primarily dermatomycosis and pyodermatitis. It is necessary to strengthen the work on hygienic education and upbringing of schoolchildren, as well as their parents, because basic personal hygiene skills are taught in the family.

Literature

1. Andreev, E.E., Kataeva, V.A., Glinevo, V.M., Kozhevnikova, N.G. Hygiene and Human Ecology. Moscow: Publishing House of MIA, 2014. 600 pp.

2. Aleshchenko, S.N., Drobot, E.V. Prevention of Disease: textbook. Publisher : Academy of Natural Sciences, 2015.

3. Andreeva, E.P., Moisya, M.K. Peculiarities of Formation of Hygienic Habits for Children of Preschool Age // Young Scientist. 2016, № 9.3, pp. 1–2.

4. Kuchma, V.R. Hygiene of Children and Adolescents. Moscow: GEOTAR-Media, 2013. 528 pp.

5. Lukushkina, E.F., Abelyevich, M.M., Baskakova, E.Yu. Modern Approaches to Prevention and Treatment of Skin Diseases in Children // Russian Medical Journal, 2014, № 21, p. 1502.

6. Magometova, I.V., Moisya, M.K. Diagnostics of Interaction Between Teachers and Parents in the Process of Physical Upbringing of Senior Preschoolers // The days of science SPF SGU: proceedings of 11-th all-Russian scientific.-pract. Conf. undergraduate and graduate students — Sochi: RIC FGBOU VPO. - Saratov state University, pp. 95–97.

DOI 10.34660/INF.2025.55.52.135

SPORTS INJURIES OF FIGURE SKATERS

Karavanova Julia Artemovna
Student
Bashkir State Medical University, Ufa, Russia

Faizova Diana Eduardovna
Student
Bashkir State Medical University, Ufa, Russia

Scientific supervisor - **Gilmutdinova Lyra Talgatovna**
MD, Professor
Bashkir State Medical University, Ufa, Russia

Scientific supervisor - **Faizova Elvira Railevna**
PhD, Associate Professor
Bashkir State Medical University, Ufa, Russia

Abstract. *Figure skating is one of the most beloved and graceful sports. Performing complex elements and movements requires athletes to develop physical qualities associated with a high risk of injury and significant physical stress on the body. The authors explore the specific features of injuries in figure skating and the possibility of continuing a sports career.*

Keywords: *figure skating, sports injuries.*

The relevance of the topic. Figure skating is a spectacular, beautiful, and dangerous sport. Figure skaters' injuries are associated with falls and excessive impact. Every athlete has experienced injuries in their career that have forced them to pause or stop their training process [1].

The purpose of this work is to analyze the scientific and methodological literature on the specific features of injuries in figure skating.

Materials and methods. The analysis of scientific literature on sports medicine and Internet resources about the life of famous figure skaters was carried out, statistical studies of injuries in figure skating were studied.

Results and discussion. Knowledge of sports terminology allows a figure skater to understand the coach and perform an element correctly. Lack of understanding of the technique of performing an element can lead to injury of the athlete [2]. Элементы фигурного катания требуют точного их выполнения.

Если фигурист не освоит технику выполнения прыжка и не подготовится к правильному приземлению, то может получить травму в виде растяжения или разрыва связок. Skater slang has keywords, such as the jumps “axel”, “toeloop”, “flip”, “lutz”, “salchow” and “rittberger”. “Dupel” is a simplified version of a double axel, and “trixel” is a triple. When performing a quad (a 4-turn jump), skaters must remember to use the correct rotation technique to avoid knee injuries. Mistakes such as incorrect edges or under-rotations can lead to back injuries. In a cascade, jumps are performed in a row, and each subsequent jump is performed using the speed from the previous one [3]. If a figure skater does not take into account all the details of the “cascade” of jumps and performs them incorrectly, they risk injuring their meniscus. Rotations are performed on one or two legs. It is important to properly “interact” with the ice to avoid injuries to the wrists or head due to insufficient control over movements. Skaters are more likely to experience injuries to the ankle (27.7%) and knee (18.6%), as well as to the lumbar spine (15.4%). Head injuries are less common (9.8%), with half of them occurring in pair skating, about 29% in ice dancing, and up to 21% in single skating. The frequency of injuries among athletes is higher when mastering new elements during training [5,6]. The figure skater’s costume at competitions does not provide for the presence of protective equipment, so falls, which are not uncommon in figure skating, significantly increase the risk of injuries. The most traumatic type of figure skating is pair sports skating. Female partners are more prone to injuries, as they are thrown and lifted by a stronger partner [4]. After severe impacts on the ice during falls from high supports and throws, concussions are more common (up to 33% of total injuries).

There have been numerous injuries among pairs skaters and ice dancers. In January 1996, Russian figure skater Elena Berezhnaya suffered a serious head injury during a training session. During a spin, her partner Oleg Shlyakhov accidentally hit her in the temple with his skate. The figure skater’s temporal bone was punctured, and the fragments damaged the brain’s membrane. Due to the damage to her speech center, Elena was unable to speak. **The athlete underwent two complex neurosurgical operations, after which she had to relearn how to walk and talk. Three months after the injury, the athlete recovered and returned to competition.** Later, Elena won the championship title with Anton Sikharulidze. In 1998, the pair won silver medals at the Nagano Olympics (her speech was still impaired at the time), became two-time European champions (1998, 2001), two-time World champions (1998, 1999), and Olympic champions in Salt Lake City in 2002. At the 2005 Grand Prix in America, Russian figure skater Tatiana Totmianina fell from a support and lost consciousness. Her partner, Maxim Marin, failed to catch her. Tatiana was diagnosed with a concussion. At the Olympic Games in Turin, Chinese figure skater Dan Zhang fell from a quadruple throw, hit the side

of the ice rink hard, and could not overcome the pain for ten minutes. The athlete recovered and completed the program with her partner, winning the Olympic silver medal. Her compatriot Wenjing Sui fell from a support during training in the spring of 2016, temporarily losing sight in one eye and injuring her ligaments. She required surgery and ten months of rehabilitation. For a while, the Chinese woman used a wheelchair, and then she relearned how to walk. At the 2018 World Championships, Sui and Han won gold, and at the 2022 Beijing Olympics, they became Olympic champions in pair skating.

Single skaters' injuries are not uncommon in figure skating. Alexei Yagudin, the 2002 Olympic champion from Russia, has experienced pain in his right leg since childhood. In October 2002, he was diagnosed with congenital hip dysplasia. Due to constant heavy loads, the joint was constantly injured, leading to the development of aseptic necrosis. *The hip joint was almost completely destroyed. In the summer of 2003, Alexei underwent his first surgery to remove fragments of damaged cartilage. There was a temporary relief, but a few months later, the disease returned. In 2003, Yagudin retired from competitive skating.* The second operation, hip replacement, was performed in the summer of 2007. Alexey got back on his feet 12 hours after the surgery, and 2 weeks later shocked the doctors by running a 10-kilometer cross-country race. *One and a half months later, Yagudin began rehearsals for the Ice Age project, and 90 days after the surgery, on October 6, 2007, he performed a triple toe loop [6].* In early October 2021, it was reported that Alexandra Trusova had injured her leg, but she participated in the Skate America 2021 Grand Prix (late October 2021), where she won first place and set a new personal record in the short program. Later, it was revealed that it was a stress fracture of the metatarsal bone in her foot. The injury halted Sasha's preparations for the Olympic Games. The discomfort in her leg still bothers her. According to statistics, the fifth, the smallest of the metatarsal bones, experiences the maximum load, and its fracture occurs in 90% of cases. There are two types of fractures: traumatic and fatigue fractures. In a traumatic fracture, an excessive force is applied to the bone, which it is not designed to withstand. In a fatigue fracture, frequent overexertion disrupts the bone's nutrition, making it more fragile and prone to breaking even under normal stress. Such fractures disrupt microcirculation in the tissues and cause nerve necrosis, so the pain syndrome is less pronounced. Evgeniya Medvedeva had a similar injury in the fall of 2017. Shortly before the Olympics, she was diagnosed with a stress fracture (a crack in the fifth metatarsal bone). Evgeniya flew to Germany for treatment, where she was advised to reduce her activities and prescribed vitamins. A short time later, Medvedeva performed at the Grand Prix stage in Japan, after which the figure skater was put in a cast. Usually, stress fractures take 6–8 weeks to recover. When using a plaster cast or a special fixing boot, rehabilitation can be reduced to a

month, but Medvedeva needed about two. In January 2018, Evgenia competed at the European Championships in Moscow and placed second. Anna Shcherbakova in the middle of July 2017 at training camps in Novogorsk performed a triple Rittberger - triple toe loop cascade. After two jumps, the athlete decided to take a risk and attach another unplanned Rittberger as a third jump. Anna struggled to get into the ice and fell. She broke her tibia and spent six weeks in a cast. She recovered in about six months and won the Russian Cup Final a month later. In the 2018–2019 season, she made her debut in the Junior Grand Prix series and won stages in Slovakia and Canada. In February 2022, Anna became an Olympic champion. In August 2022, the athlete suffered a knee injury and underwent surgery for a torn posterior horn of the meniscus.

Athletes face various injuries, but proper treatment and rehabilitation tactics help them return to sports. Athletes spend a lot of money on rehabilitation (Alliluyev I. G., 2001; Schmidt I. R., 1998–2001; Vein A. M., 1997, 2001; Belova A. N., 2000). According to the Federal Scientific and Clinical Center of the Federal Medical and Biological Agency of Russia, a comprehensive professional approach significantly reduces the recovery time for injured athletes. The main rehabilitation cycle includes massage courses, gymnastics, and light stretching. Later, the loads can be increased, but it is recommended to do this gradually. It is better to miss one competitive season than to aggravate the situation and be banned from participating in professional competitions. To prevent injuries in figure skating, stretching and warming up the muscles before training is used. It is important to learn how to fall properly. To do this, you should group yourself by touching the platform with the outer surface of your thigh.

Conclusion.

1. Figure skating is a complex-coordination sport that requires good coordination, balance, and a sense of time and space, and proper technique can reduce the risk of injury.
2. Qualified medical care and timely rehabilitation allow to overcome the consequences of multiple injuries suffered by figure skaters.
3. Some figure skaters manage to achieve outstanding results after injuries, while others leave the sport forever, but they do not stop being great athletes.

Literature

1. Bumar skova, N. N. Traumatism in figure skating /N. N. Bumar skova, V. A. Nikishkin //Scientific notes of the University named after P. F. Lesgaft. – 2020. – No. 2 (180). – Pp. 63–68.

2. Selected Issues of Therapeutic Physical Culture and Sports Medicine / L. T. Gilmutdinova, A. Yu. Tikhomirov, N. S. Kutliakhmetov [et al.]. – Ufa: Pereplet, 2009. – 196 p.

3. Merkulova, M. V. The main causes of injuries in figure skating /M. V. Merkulova, T. Ya. Magun, E. V. Chaplygina //The current state and trends in the development of physical culture and sports: Collection of scientific articles based on the results of the international scientific and practical conference, Belgorod, November 26, 2021 – Belgorod: ID "Belgorod" NIU "BelSU", 2021. – P. 753–756.

4. Traumatic injuries. Overtraining. Recovery in figure skating: A textbook for students of higher educational institutions of physical education studying in bachelor's programs / I. O. Cherepanova, K. S. Dunaev, A. S. Solntseva [et al.]; Ministry of Sports of the Russian Federation, Moscow State Academy of Physical Education. – Malakhovka: Moscow State Academy of Physical Education, 2020. – 168 p.

5. Physical Rehabilitation in Traumatology and Orthopedics / L. T. Gilmutdinova, E. R. Faizova, B. R. Gilmutdinov [et al.]. – Ufa: Bashkir State Medical University, 2023. – 263 p.

6. Yagudin A., Prauz L. HAPROLOM. - M.: Gorodets Publishing House, 2008. - 272 p.

DOI 10.34660/INF.2025.13.15.136

MEDICAL REHABILITATION IN INDIA

Ramegowda Juwatedj Doddighatta
Student
Bashkir State Medical University, Ufa, Russia
Faizova Diana Eduardovna
Student
Bashkir State Medical University, Ufa, Russia
Scientific supervisor - **Gilmutdinova Lyra Talgatovna**
MD, Professor
Bashkir State Medical University, Ufa, Russia
Scientific supervisor - **Faizova Elvira Railevna**
PhD, Associate Professor
Bashkir State Medical University, Ufa, Russia

Abstract. *In May 2023, the World Health Organization Assembly adopted a resolution recognizing rehabilitation as a public health priority. In recent decades, there has been an increase in the share of rehabilitation technologies in global medical practice. India is actively involved in global health trends. The authors of the article studied and analyzed the system of organization of medical rehabilitation in India.*

Keywords: *medical rehabilitation, Rehabilitation Council.*

The relevance of the topic. The centuries-old history of Indian medicine combines national characteristics with the experience of other countries. There are specific features and problems: large populations, remote villages and overpopulated cities, castes, prejudices, and religious prohibitions. The country's leadership cares about the health of over a billion of its citizens. The organization of medical rehabilitation is an important task of modern healthcare in India.

The purpose of the work is to analyze the main aspects of medical rehabilitation in India.

Materials and methods. The analysis of modern scientific literature and Internet resources on the organization of medical rehabilitation in India is carried out.

Results and discussion. Medical rehabilitation is a branch of healthcare in India. The Indian state supports a unique system of traditional treatment methods

and modern medical approaches. To understand the organization of rehabilitation in the country, an excursion into the history of medicine is necessary. India's healthcare system has its roots in national traditional medicine and "colonial healthcare" during the reign of the British Crown. The mix of Western (colonial) and Eastern (traditional) medicine creates a balance between tradition and innovation [3,7]. Historically, the people of India did not trust "Western" doctors and did not want to be treated with their methods. In 1976, the Ministry of Health incorporated two Departments: Health and Family; Ayurveda, Yoga, and Naturopathy. In 2022 The World Health Organization has decided to establish a Global Center for Traditional Medicine in India. Modern India actively cooperates with international health organizations [4,8].

Today, the population of India is being treated by doctors with a Western approach and by specialists in traditional medicine. India's healthcare is funded from the state budget according to five-year plans. A significant proportion of medical institutions, 80%, are in the private sector. According to the program of support for the poor, certain categories of citizens of the country can receive a subsidy ($7200 per year) to pay for treatment in private clinics, insurance from employers and regional subsidies [Dikikh A. A., 2018, Fedonnikov A. S., 2023, Kumar M. Sh., 2024, Sorokina E. V., 2024]. Digitalization of India's healthcare is currently in its infancy. Electronic medical records will be launched in 2021. Basic medical education in India can be obtained in 5.5 years. The next stage is specialization in the hospital for two or three years [7,8].

The Rehabilitation Council of India (RCI) was established in 1986. In September 1992, Parliament passed the law on the RCI, and on June 22, 1993, it became a government agency. The Rehabilitation Council of India (RSIN) is the highest government body [3,4]. The Rehabilitation Council of India registers rehabilitation specialists in its central registry and regulates their training programs. Persons who have received the RCI certificate have the right to engage in vocational rehabilitation in any region of India. Only specialists or rehabilitation staff with a recognized rehabilitation certificate can be entered in the Central Register of Rehabilitation Specialists. The authority of the RCI includes the regulation and monitoring of services for people with disabilities. "In India, disability is assessed in five categories: vision, speech, hearing, musculoskeletal system and mental activity ..." [Thomas 2005]. The law provides penalties for unqualified professionals who provide services to people with disabilities. The mission of the RCI organization is "to provide high-quality services to people with disabilities that meet the best international standards."

In 2000, RCI included people with disabilities caused by mental illness. The Law consists of three chapters. Chapter I, The Preliminary Chapter, contains information on the name, definitions, etc. Chapter II, The Rehabilitation Council of

India, reflects the composition, terms of office of officials, data on executive committees, vacancies, and dissolution of the council. Chapter III "Functions of the Council" informs about the functions of the Council, recognition of qualifications, examination centers, professional registration, professional conduct, etc.

Modern clinics in India offer comprehensive rehabilitation programs tailored to the needs of each patient. An integrated approach to recovery with continuous care promotes recovery from traumatic injuries, diseases, and surgical interventions. In addition to inpatient rehabilitation, there is also outpatient rehabilitation (day hospital). Indian rehabilitation centers offer various recovery programs. The main areas of rehabilitation in India are cardiorehabilitation, neurorehabilitation, orthopedic, postoperative, sports, pediatric, gynecological and oncological rehabilitation. Thousands of patients receive rehabilitation services in India every year after strokes, traumatic brain, spinal cord, orthopedic, sports injuries, as well as other conditions requiring restorative treatment [6,9].

The rehabilitation team consists of rehabilitation physiotherapists, nurses, speech therapists, and other rehabilitation specialists. There are eight licensed groups of specialists: audiologists and speech therapists, clinical psychologists, hearing aid and earplug specialists, rehabilitation engineers and technical specialists, special teachers for the education and training of people with disabilities, professional consultants, specialists in employment and vocational guidance for people with disabilities, multidisciplinary rehabilitation specialists, technical specialists and other categories of professions. In recent years, the list has been supplemented by rehabilitation psychologists.

Indian rehabilitation specialists are characterized by high professionalism and a desire for innovation. According to international experts, India's medical innovation activities are rated as one of the most progressive in global healthcare (for creativity and efficiency) [2]. India has achieved significant success in medical rehabilitation due to the combination of the features of Indian traditional medicine and its modern achievements. Indian rehabilitation specialists have unique robotic and computer simulators, installations for early verticalization of bedridden patients, interactive tools using virtual and augmented reality technologies, etc.

In modern India, technological innovations are harmoniously combined with traditional Ayurvedic methods. This makes it possible to achieve high results of medical rehabilitation in India, regardless of the severity, nature and degree of neglect of the disease [5]. After comprehensive rehabilitation, up to 90% of patients in Indian rehabilitation centers are able to return to normal life and get back to work.

Conclusion.

1. India is building a modern medical rehabilitation system in the unique conditions of a mix of Western colonial and Eastern traditional medicine.

2. The Rehabilitation Council of India is the key body overseeing rehabilitation centers and licensed rehabilitation education across the country.

3. Medical rehabilitation in India is developing ahead of scientific and practical activities in the field of medical innovation.

Literature

1. Dikikh A. A. India's national health policy from the beginning of independence in 1947 to the present // Health issues. — 2018–No. 1 — pp. 6-13.

2. Dukkipati U. The Indian approach to global innovations in healthcare at the national level // Bulletin of International Organizations. — 2011–№ 3 (34). — pp. 96-104.

3. Sorokina, E. V. Financing and organization of medical care in the BRICS countries (Russia and India): comparative legal analysis / E. V. Sorokina, M. E. Pakhunov // Education and Law. – 2024. – No. 4. – pp. 48-53.

4. Kharitonova, V. I. Transformation of traditional Oriental medicine in the modern world / V. I. Kharitonova // Bulletin of Anthropology. – 2024. – No. 4. – pp. 356-372.

5. Chandiramani N. M. Medical tourism: consequences for India // Bulletin of the O.E. Kutafin University (MGUA). - 2022–No. 1 — pp. 30-38.

6. Shreya, D. Features of rehabilitation of COVID-19 patients in Russia and India / D. Shreya, S. Nikita, A. G. Kononova // Youth and medical science: Abstracts of the VIII All-Russian Interuniversity Scientific and Practical Conference of Young Scientists with International Participation, Tver, November 26, 2020. Tver: State Budgetary Educational Institution of Higher Professional Education Tver State Medical Academy of the Ministry of Health of the Russian Federation, 2021, pp. 41-42.

7. Aditya, R. Current state of health care in India / R. Aditya // Policy, Economy and Innovations. – 2023. – No. 3(50).

8. Anushka, A. Modernization of health care systems in India and U.S / A. Anushka // Policy, Economy and Innovations. – 2024. – No. 2(55).

9. Rehabilitation of patients with corona virus infection in India / 9. L. T. Gilmutdinova, E. R. Faizova, B. R. Gilmutdinov [eta.] // Fundamental Science and technology - promising developments: Proceedings of the XXX Scientific and Practical International Conference, Bangalore, India, April 17-18, 2023. – Bangalore, India: Pothi.com , 2023. – pp. 16-21.

DOI 10.34660/INF.2025.19.63.137

MONITORING AND CORRECTION OF SYSTEMIC HEMODYNAMICS INDICATORS IN SOLVING STRATEGIC PUBLIC HEALTH PROBLEMS

Seliverstov Konstantin Olegovich
Junior Research Fellow
National Research Institute of Public Health named after N.A. Semashko,
Moscow, Russian Federation

Yakushin Mikhail Alexandrovich
Doctor of Medical Sciences, Associate Professor, Chief Researcher, Head of Department
National Research Institute of Public Health named after N.A. Semashko,
Moscow, Russian Federation

Kudrin Alexey Pavlovich
Junior Research Fellow
National Research Institute of Public Health named after N.A. Semashko,
Moscow, Russian Federation

Annotation. *A new paradigm for managing arterial hypertension has been proposed, based on personalized correction of systemic hemodynamics and polymodal therapy for metabolic syndrome. The selection of antihypertensive drugs is suggested to be aligned with the influence of medications on the individual systemic hemodynamic profile. An expert system has been developed, enabling automated telemetric matching of a patient's unique combination of systemic hemodynamic parameters with specific antihypertensive drugs. The clinical efficacy of the proposed method has been proven.*

Keywords: *arterial hypertension, systemic hemodynamics, expert system, volumetric compression oscillometry.*

The dizziness of the successes of the global medical community in the treatment of arterial hypertension (AH) weakly correlates with the real state of affairs: regardless of the region, level of prosperity and degree of development of the

healthcare system, only a third (~35%) of patients achieve target blood pressure (BP) values [1]. And this is despite the fact that the disease affects almost half of the world's population, including children [2] and is the direct cause of 45% of fatal outcomes from coronary heart disease and 51% from stroke [3]. Two-thirds of losses in this "duel" is a significant blow to public health!

In each new edition of the recommendations of the European Society of Cardiology and the European Society of Hypertension (hereinafter the Recommendations), the issues of hypertension management are worked out more and more clearly. The 2018 Recommendations more carefully place emphasis on comorbid diseases and concomitant clinical conditions; special attention is paid to the treatment of patients in older age groups. The Recommendations are gradually acquiring an algorithmic form that is closest to the needs of a practicing physician. However, even the developers of the document themselves complain about the insufficient effectiveness of the proposed measures. In their opinion, the main reasons for this phenomenon are:

- Medical inertia (insufficient strengthening of therapy, especially monotherapy);
- Low patient compliance with treatment (especially when several drugs are prescribed in separate tablets).

It is argued that if doctors made maximum efforts, showed initiative and made patients follow the instructions exactly, the problem would be solved. The strategists do not see any other obstacles (for example, the lack of effectiveness of the approaches they have developed) to the total cure of hypertension. In their defense, they cite the following arguments: "Blood pressure control can be achieved in most patients participating in clinical trials, and of these patients, only 5-10% demonstrate resistance to the chosen therapy regimen, which indicates that the ineffectiveness of drug therapy is not the source of the problem" [1]. However, these arguments are more like shifting the problem from the sick head to the healthy one.

Of course, some medical inertia does exist and it must be fought. However, as practice shows, when a doctor is given a truly effective technology, neither he nor the patient needs to be pushed in the applied use of this method. This happened, for example, with infectious diseases. Antibiotics appeared - and the incidence curve quickly went down. The same is true for antitumor drugs, drugs that change the course of multiple sclerosis.

In our opinion, the main reason for the unacceptably low effectiveness of hypertension treatment is associated not so much with the insufficient activity of doctors and patients, but with a systemic error in the strategy for choosing antihypertensive therapy!

According to the Guidelines, after deciding on the need for drug therapy, the physician is offered a choice of five main classes of antihypertensive drugs

(AHD): angiotensin receptor blockers (ARBs), angiotensin-converting enzyme inhibitors (ACEIs), calcium channel blockers (CCBs), thiazide diuretics (TDs), and beta-blockers (BBs). Since the overall effect on cardiovascular risks and mortality is approximately the same with treatment with all five classes of drugs (as proven by numerous randomized clinical trials and meta-studies) [1], the physician is advised to focus on contraindications and priorities of the therapeutic effect of drugs on individual nosological entities. In this case, attention is paid primarily to diseases associated with hypertension. The priorities of choice are the ability to restore impaired function (for example, ACE inhibitors and ARBs have proven efficacy in reversing left ventricular hypertrophy), preventive effect (for example, CCBs have a greater effect in preventing strokes, and TDs in preventing heart failure), slowing the progression of a particular disease (for example, the inhibitory effect of CCBs on the progression of coronary atherosclerosis), or the beneficial effect of drugs on comorbid organs and systems (for example, improvement of insulin metabolism against the background of ARBs).

With regard to combination therapy, it has now been proven that all five main classes of drugs can be combined with each other, with the exception of ACE inhibitors and ARBs. In this case, combination therapy is constructed as the arithmetic sum of the effects of the set of prescribed drugs.

At first glance, the logic of choosing an anticoagulant drug is impeccable: determine the patient's concomitant disease (associated clinical condition - ACC, affected organ - target of anticoagulant drug - AOD) and prescribe the most appropriate drug that has an evidence base of effectiveness for this disease. If there are several diseases, select the appropriate combination of drugs, each of which will contribute to recovery [4].

In fact, such an approach is only valid for the late (II or III) stage of the disease, which is characterized by the involvement of the POM in the pathological process and the addition of ACS. It is no coincidence that the 2018 Recommendations prescribe starting antihypertensive therapy immediately with a combination of two drugs. One drug is already considered an ineffective measure, which actually indicates the failure of the conceptual approach to treating the initial stage of the disease.

At the first stage of AG, comorbid diseases, ACS and POM are absent; therefore, it is not possible to rely on them when choosing an AG; the first few years from the onset of the disease are a blank spot in the Recommendations; personal criteria for choosing drugs are simply absent from them. The doctor is offered to be guided by impersonal circumstances, to prescribe any drug, as long as it has no contraindications.

Systemic arterial pressure (SAP) is directly dependent on the listed SBP indicators and is calculated using the formula:

SBP = HR x SV x OPSS,

where HR is the heart rate; SV is the stroke volume; TPR is the total vascular resistance.

Different people have different ratios of HR, SV and OPSS. Without knowing the initial profile of the values of these indicators, it is impossible to predict the hemodynamic, and therefore the clinical effect of any antihypertensive drug. The effect of antihypertensive drug on the SGD can acquire a polar direction, which makes it irrational, and in some cases, dangerous to prescribe antihypertensive drug without taking into account the personal SGD profile.

OPSS could only be done using the Swan-Gatz method, based oncatheterization of the pulmonary (!) artery. The technique is complex and fraught with numerous (including fatal) complications, which negates its practical significance, especially for mass use.

The domestic device KAP CG osm - "GLOBUS" (Manufacturer OOO Globus; registration certificate dated 15.12.2017 No. RZN2017/6582 - hereinafter referred to as the Device), based on the non-invasive method of volumetric compression oscillometry, developed for the needs of Soviet space medicine, allows for the automated determination of the level of heart rate, SV and OPSS, as well as 20 more indicators of the SVD.

Data on the influence of individual AGP on the SGR allow assigning each of them a corresponding combination of numbers (Code); the first component of the Code displays the influence of AGP on HR (1 - decreases, 2 - does not affect, 3 - increases the value); the second component of the Code displays the influence of AGP on TPR (1 - decreases, 2 - does not affect, 3 - increases the value, 4 - increases in the first month, decreases after a month and further); the third component of the Code displays the influence of AGP on SV (1 - decreases, 2 - does not affect, 3 - increases the value) (Table 1).

Table 1

The influence of AG on the profile of the SHD

AGP Group	**AGP**	**Impact of AGP on SGS (Code)**
Calcium antagonists	Nitrendipine	312
	Nifedipine	313
	Diltiazem	112
	Amlodipine	212
ACE inhibitors	Perindopril, enalapril	213
	Zofenopril, captopril, quinopril, lisinopril, ramipril, fosinopril	212

Beta-blockers	Betaxolol	111
	Nebivolol	112
	Atenolol, bisoprolool, metoprolol	141
Angiotensin receptor blockers	Losartan	113
	Valsartan, candesartan, eprosartan, irbesartan, telmisartan	212
Selective imidazoline receptor agonists	Moxonidine	212
Diuretics	Dichlorothiazide, indapamide	212

The method of choosing pharmacotherapy for hypertension that we propose is based on establishing a correspondence between the personal profile of the SHR, which is determined by the level of HR, TPVR and SV of the patient, and the effect of the antihypertensive drug on the SHR, i.e., its Code. The drug of choice is a medicine that has a normalizing effect on the changed (increased or decreased) indicators of HR, SV and TPVR and does not affect the SHR indicators that are within the normal range.

By correlating the influence of the AGP on the indicators of the SRS (Code), it is possible to determine in a ranked form the compliance of the AGP with each SRS profile (Table 2).

Table 2

Correspondence between the profile of the CHG and the AGP

Profile No. SGG	Ranked list of AGPs
1	111, 141,112, 212
2	112, 111, 141, 212, 113
3	113, 112, 213, 212
4	111, 141, 212, 112
5	112, 141, 111, 212, 113, 213
6	113, 112, 213, 212
7	141, 111, 212
8	112, 141,212,113, 213
9	113, 112, 213, 212
10	111, 212, 112
11	212, 112, 111, 141, 213
12	213, 113, 212, 112
13	111, 212, 112
14	212, 112, 111, 141, 213, 312
15	213, 113, 112, 212
16	141, 212, 112

17	212, 141, 112, 213
18	213, 113, 112, 212
19	212, 312
20	312, 212, 213
21	313, 213, 312, 212
22	312, 212
23	312, 212, 213
24	313, 213, 312, 212
25	312, 312, 212
26	312, 212, 213
27	313, 312, 213, 212

If at the time of treatment, the patient is not taking antihypertensive drugs, diagnostics and subsequent treatment are carried out according to the following algorithm.

P. 1 The Device is used to measure blood pressure, heart rate, total peripheral vascular resistance and stroke volume.

If elevated blood pressure is detected, to exclude "White Coat" hypertension, repeated measurements of the SBP indicators are taken twice with an interval of 5 minutes. If the value of systolic blood pressure, diastolic blood pressure during repeated measurement changes by more than 5%, the study is continued with an interval of 5 minutes until the indicated indicators stabilize.

If normal blood pressure values are established, drug treatment is not prescribed.

With an increase in systolic BP and/or diastolic BP, the patient's HR, TPR, and SV profile correlates with one of the SHD profiles (Table 2). If, according to current medical recommendations (currently - European recommendations, 2018), the patient is indicated for monotherapy from the ranked list of antihypertensive drugs, the first drug in line for this SHD profile is prescribed (Table 2).

P. 2 During the next 2 weeks, the SRS indicators are measured daily, and the trends of the personal SRS profile are determined. In case of positive dynamics of blood pressure (normalization trend, trend towards normalization of SRS indicators), treatment is continued in the established regimen until its complete normalization. In the absence of a normalization trend after 5 days from the start of treatment or if a negative trend is detected (i.e. if deviations of SRS indicators from the norm worsen), the dose of the drug is gradually increased every 1-2 days within the limits and proportions established for this AGP until blood pressure is normalized.

P.3 If there is no effect after 2 weeks from the start of treatment, the antihistamine is replaced with the next one in the ranked list (Table 2) and the SGS is

monitored and the drug dose is selected in a similar sequence. If there is no effect or insufficient effect, the drugs of the ranked list of antihistamines are successively replaced (Table 2).

P. 4 If there is no effect after 2 weeks from the appointment of the last antihistamine from the list of ranked antihistamines, a combination treatment is prescribed taking into account their compatibility: antihistamine No. 1 + antihistamine No. 2 (Table 2) and in a similar sequence, the blood pressure is monitored and the dose of the drug is selected.

P. 5 If there is no effect after 2 weeks from the prescription of the combination of AGP No. 1 + AGP No. 2, a combination of AGP No. 1 + AGP No. 3 is prescribed (if No. 4, 5, etc. of the ranked list are ineffective).

P. 6 If the patient is prescribed combination therapy in accordance with current medical recommendations, a combination of drugs is prescribed: AGP No. 1 + AGP No. 2 from the ranked list.

Over the next 2 weeks, the SRS parameters are measured daily, and the trends of the personal SRS profile are determined. In case of positive dynamics of BP (normalization trend, trend towards normalization of SRS parameters), treatment is continued as per the established regimen until it is completely normalized. If there is no normalization trend after 5 days from the start of treatment or a negative trend is detected (i.e., if deviations of SRS parameters from the norm worsen), the dose of the first-line drug is gradually increased every 1-2 days within the limits and proportions established for this AGP until BP is normalized. If there is no effect or the effect is insufficient, the dose of AGP№1 of the second line is increased.

P. 7 If there is no effect after 2 weeks from the start of treatment, antihypertensive drug No. 2 from the ranked list is replaced with antihypertensive drug No. 3 (if No. 4, 5, etc. from the ranked list are ineffective) until blood pressure is completely normalized.

Based on the proposed algorithm, we have developed an expert system “Monitoring and correction of SRS indicators” (Expert system), which allows, based on the SRS personal profile, to automatically select the most effective AGP.

The experience of testing the proposed approach shows its absolute effectiveness.

The study involved 272 patients over 60 years of age suffering from hypertension, including 167 (61.4%) women and 105 (48.6%) men. The average age in the female group was 77.2 years, in the male group – 71.5 years. Depending on the stage of the disease, which was determined in the established manner based on risk factors, degree of blood pressure, damage to target organs, the presence or absence of associated clinical conditions, the patients were combined into 3 groups. The first group included 13 patients (7 women and 6 men) with stage I of the disease,

the second – 114 (67 f; 47 m) patients with stage II hypertension; the third – 145 (93 f; 52 m) patients with stage III hypertension.

Results:

In group I, the deviation in mean blood pressure was +9.6±2.3%; in group II +17.3±3.7%; in group III +33±4.3%.

The greatest range of SV values was observed in group I: SV - from -37% to +67%; HR - from 47 to 133 beats per minute; TPR - from -23% to + 55%; in group II, SV values were in a narrower range: SV - from -42% to +52%; HR - from 56 to 112 beats per minute; TPR - from -19% to + 44%; in group III: SV - from -35% to +33%; HR - from 45 to 98 beats per minute; TPR - from -6% to + 69%. The most frequent ratio of SV values in group I was decreased SV, normal HR, and increased TPR; in group II - normal SV, normal HR, and increased TPR; in group III – increased SV, normal heart rate and increased total peripheral vascular resistance.

During the treatment, the duration of which was 4 weeks, the target value of mean BP of 90-95 mm Hg was achieved in all patients of group 1 without exception, without changing medications. In group 2, mean BP decreased by 15.1%, reaching the target value in 104 patients (91.2%); three patients had to change one medication due to low treatment efficacy; in group 3, mean BP decreased by 21.7%, reaching the target value in 133 patients (91.7%); 17 patients needed to adjust drug therapy.

Thus, the choice of treatment for hypertension based on the analysis of the personal profile of the SGS is a highly effective therapeutic method. This approach does not exclude, but only complements the Recommendations established by professional communities. The remote format of the diagnostics and treatment facilitates the patient's contact with the doctor and is fully consistent with the conceptual position of the strategy of actions in the interests of senior citizens of the Russian Federation, approved by the Decree of the Government of the Russian Federation of 05.02.2016 No. 164-r, on the need to expand the range of medical services at home.

Taking into account the personal profile of the SHD when choosing rational therapy allows to reduce to zero possible errors associated with the variability of the hemodynamic effect of AG. Remote monitoring of reference indicators of the SHD (HR, OPSS, SV) makes it possible to titrate the doses of AG and consolidate the achieved results. We believe that the widespread use of the method of remote monitoring and correction of the SHD in the treatment of hypertension will significantly reduce the cardiovascular risks associated with the development of POM, ACS, their severe, including fatal complications, and the overall negative impact of hypertension on public health.

References

1. 2018 EOC/EOAH Guidelines for the treatment of patients with arterial hypertension.

2. Pereira M, Lunet N, Azevedo A, Barros H. Differences in prevalence, awareness, treatmen and control of hypertension between developing and developed countries. J Hypertens 2009; 27:963–975.

3. Antonovich M.N. Hypertensive and discirculatory encephalopathy: diagnostics and treatment // Healthcare (Minsk) 2012. No. 12. P. 38-45.

4. Yakushin M.A., Dasayeva L.A., Matyukhina E.B. Algorithm of drug treatment of arterial hypertension in elderly and senile age. - Advances in Gerontology, 2011, Vol.24, No.4, pp. 674-680.

DOI 10.34660/INF.2025.72.23.138

RESULT OF LASER THERMOTHERAPY IN THE TREATMENT OF SPINAL TUMOR

Turanov Semen Alexandrovich
Postgraduate student
Russian Scientific Research Institute for Neurosurgery prof. A.L. Polenov - branch of the V.A. Almazov National Medical Research Center
ORCID ID: 0000-0003-3464-9265

Ivanenko Andrei Valentinovich
Doctor of Medical Sciences, Associate Professor
Russian Scientific Research Institute for Neurosurgery prof. A.L. Polenov - branch of the V.A. Almazov National Medical Research Center
ORCID ID: 0000-0002-9712-4661,

Kudziev Andrey Valerievich
Doctor-Neurosurgeon
Russian Scientific Research Institute for Neurosurgery prof. A.L. Polenov - branch of the V.A. Almazov National Medical Research Center
ORCID ID: 0000-0002-9712-4661

Abstract. *According to autopsy data, metastasis to the spine occurs in more than 70% of cancer patients. Treatment of patients with this pathology is mainly palliative. The practice of spinal oncology is becoming more variable as innovations in surgical technology appear, which can reduce the volume of intervention with maximum preservation of the quality of life. One of such treatment methods is laser interstitial thermotherapy.*

Objective: *to analyze the effect of laser interstitial thermotherapy in patients with space-occupying lesions of the spine on the preservation of functional activity, neurological status and quality of life.*

Materials and methods: *the study included 60 middle-aged patients with a space-occupying lesion of the spine. Two groups of 30 people were formed. Patients of the study group were operated using the LAHTA-MILON semiconductor laser. The surgical intervention was performed in 2 stages: Stage 1 - transcutaneous*

intracapsular exposure to paravertebral tumor nodes under ultrasound navigation using a laser. Stage 2 - intraoperative exposure to tumor tissue located directly near the dural sac and root. The general condition of patients was assessed before the operation, after it (1st day) and before discharge from the hospital (7-10th days). If patients had motor disorders, their severity was assessed on a five-point scale. The study of sensory disorders included identifying changes in superficial and deep types of sensitivity, and the nature of the disorders (segmental or conductive) was also determined. To assess the results of surgical treatment and quality of life in the pre- and postoperative period, the Frankel scale was used in both groups. Mathematical and statistical analysis of the results was performed using the standard STATISTICA 10.0 for Windows 10 software package for personal computers. Results: According to our data, movement disorders were detected in 55 of 60 patients (91.7%). On the 10th day after the surgery, regression of movement disorders occurred both in the comparison group and in the study group - in 16.7% and 26.7% of patients, respectively. The number of patients with movement disorders decreased by this time. Sensory disorders were initially detected in 58 (96.7%) of 60 patients. On the 10th day after the surgery, sensory disorders of varying degrees were detected in 22 (73.3%) patients in the study group, and in 23 (76.7%) patients in the comparison group. A month later, regression of sensory disorders was also observed: in the study group from 96.7% to 46.7%, in the comparison group - from 96.7% to 60%, which is statistically significant. Radicular pain syndrome was initially detected in 41 (68.3%) patients, and in the comparison group it was detected in 19 (63.3%) patients, and in the study group in 21 (73.3%) people. On the 10th day after the operation, radicular pain syndrome regressed in 47 (78.3%) of 60 patients and persisted in 13 (21.7%) patients. At the same time, in both groups it persisted in 6 (20%) and 7 (23.3%) patients, respectively. It was noted that in the group where LITT was used, the functional results of patient treatment were significantly better already on the 10th day after the operation in comparison with the comparison group. Thus, in the study group, a good result was obtained in 4 (13.3%) patients, satisfactory - in 16 (53.3%), unsatisfactory - in 10 (30.3%) people. In the comparison group, by this time, good results were achieved in 2 patients (6.7%), satisfactory in 8 patients (26.7%), and unsatisfactory in 20 patients (66.6%). The use of a surgical laser during operations to remove tumors of the lumbosacral region allows to reduce bleeding in the study and comparison groups, respectively (210.5 ± 20.6) and (350.0 ± 21.3) ml, (498.7 ± 75.9) and (910.5 ± 97.6) ml.

Conclusion: *The use of the LAKHT-MILON laser in comparison with exclusively traditional surgical methods reduces traction and, consequently, trauma to the spinal cord and its roots, provides lesser severity of neurological*

symptoms and a higher level of quality of life for patients in the postoperative period.

Keywords: *laser, laser interstitial thermotherapy, metastases to vertebral bodies, space-occupying lesions of the spine.*

Introduction. Spinal metastases are the third most common sites of cancer after the lungs and liver. According to autopsy data, vertebral metastases are found in more than 70% of patients with cancer. When examining the distribution of metastatic lesions in the spinal column, the thoracic and thoracolumbar regions (TLR) are affected in 70.3% of cases, the lumbar and sacral regions (LSR) in 21.6%, and the cervical region (CR) in 8.1% of patients. The largest number of cases of TLR metastasis are associated with lung cancer and breast cancer, while the lumbosacral region is most often affected by prostate cancer metastases.[1],[3] Treatment is mainly palliative, focused on neurological preservation, restoration of spinal stability, pain relief, and tumor growth control [4], [5], [6]. The practice of spinal oncology is becoming more variable with the emergence of innovations in surgical technology, immunotherapy, targeted chemotherapy, most often used in combination with radiation therapy. [2] The complexity of the selection of the treatment method is also due to the frequent presence of concomitant pathology in patients in the context of cancer progression, paraneoplastic syndrome. Accordingly, the requirements for surgical intervention in these patients should meet the requirements of minimally invasiveness, a lower risk of postoperative complications and effectiveness. The goal of surgical intervention is to ensure stabilization and decompression. [4], [39] In recent years, laser interstitial thermotherapy (LITT) has been used in neurosurgery, where it has widely demonstrated its effectiveness in relation to intracranial pathologies as a combination therapy, together with chemotherapy. [3], [10], [11], [14], [15], [33], [35], [36]. According to a systematic literature review in PubMed up to 2023 analyzing the available data on the use of laser interstitial thermotherapy (LITT) in spinal neurosurgery, patients received LITT for spinal metastases with compression fracture[9], [11]. Most lesions were thoracic (88.8%). All studies reported effective local disease control due to reduction of epidural compression after 30 days. The complication rate was 12.6%, but most were transient, and only 3.4% of patients required revision surgery. The literature on the use of LITT in spinal lesions is new, and its effectiveness is still debated.[3],[5]

We present preliminary results of the use of laser interstitial thermotherapy in the treatment of patients with metastatic spinal lesions. The clinical material is based on the results of surgical treatment of 60 patients with extramedullary tumors (EMT), operated on in NSC No. 1 in the period 2021–2024 (Table 1).

Table 1

Study group	Number of patients	Gender	Middle age	Secondary tumors	neurino-mas	neurofi-bromas
Study group	30	M-18 (60%) Ж-12 (40%)	51,4±2,31	19 (63,4 %)	7 (23,3 %)	4 (13,3 %)
Comparison group	30	M-21 (70%) Ж-9 (30%)	49,2±2,1	14 (46,6 %)	10 (33,4 %)	6 (20 %)
Total	60	M-39 (65%) Ж-21 (35%)				

Objective. To analyze the effect of laser interstitial thermotherapy in patients with space-occupying lesions of the spine on the preservation of functional activity, neurological status and quality of life.

Materials and methods. A total of 60 people took part in the study, of which two groups were formed: the study group (n = 30) and the comparison group (n = 30). Patients in the study group were operated on for EMO using the LAKHTMILON semiconductor laser, 0.97 μm wavelength, 5 W power, registration certificates No. 29/01050603/5828-03 and No. FS 022b2003/2932-06. The surgical intervention was performed in 2 stages: Stage 1 - in the preoperative period, percutaneous intracapsular exposure was performed on the tumor nodes located paravertebrally under ultrasound navigation using a laser apparatus of the surgical hyperthermic mode with a power of 5 W in pulsed mode, the duration of exposure is 1 second, the interval is 0.7 seconds; the total duration of the period is 3 minutes (periods with a change in the position of the needle in the node), (visually until the echo signal of the tumor tissue changes). Stage 2 - intraoperative exposure to tumor tissue located directly near the dural sac and root.

At the first stage, 10 patients underwent selective angiography of the tumor vessels with simultaneous partial laser vaporization of the paravertebrally located node of the space-occupying lesion.

A segmental artery and a pronounced vascular network of the tumor were visualized.

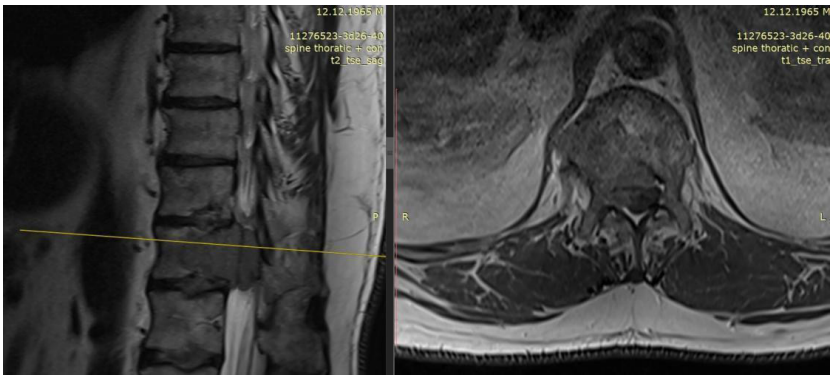

Figure 1. *MRI before the procedure*

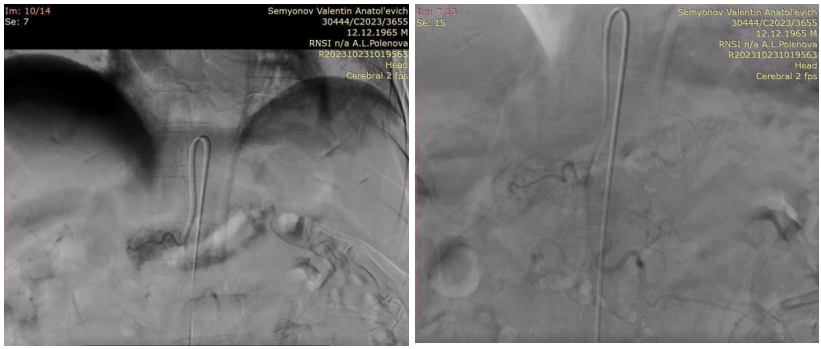

Figure 2. *Angiography before and during the procedure*

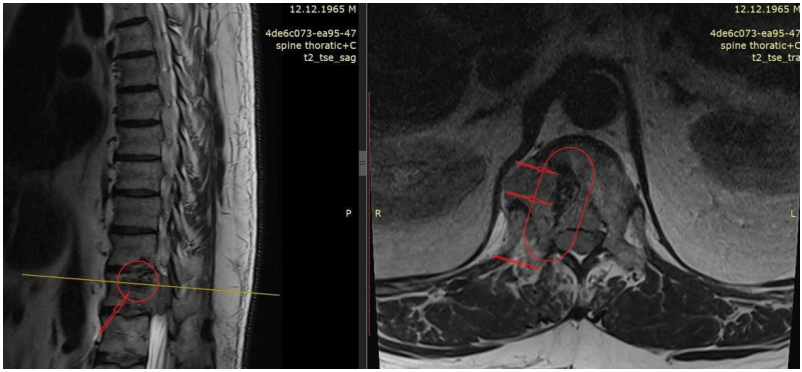

Figure 3. *MRI after the procedure*

When performing laser vaporization under selective angiography control, data on effective ablation of the tumor vascular network was obtained in all cases, which significantly reduces blood loss during subsequent open intervention. The obtained MRI data allow calculating the zone and volume of impact on the tumor tissue and the degree of node reduction.

20 patients underwent laser vaporization of the extravertebral tumor node under dynamic ultrasound control.

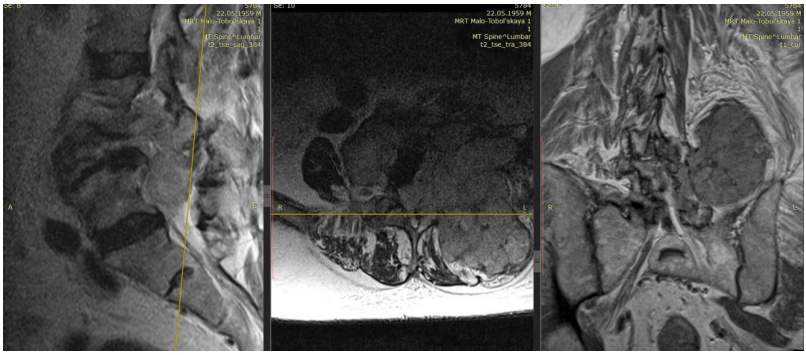

Figure 4. *MRI before the procedure*

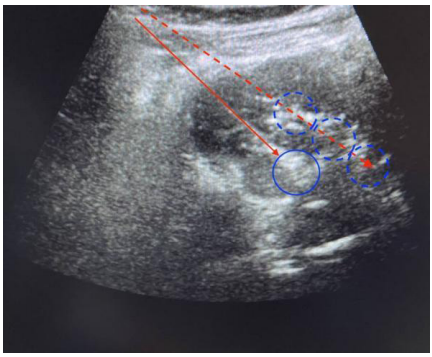

Figure 5. *Ultrasound during the procedure*

In the figure, the arrow with a dotted line is the position of the needle with the tissue vaporization zones of the space-occupying lesion, the arrow with a solid line is the vaporization zone in the area parallel to the needle positioning.

By the histological structure of neoplasms: the largest group was secondary - 19 (63.4%), neurinomas - 7 (23.3%), neurofibromas - 4 (13.3%). The comparison group consisted of 30 patients. In this group, surgical treatment was performed by

traditional methods. Of the 30 patients in the comparison group, the histological structure of tumors was as follows: secondary tumors - 14 (46.6%), neurinomas - 10 (33.4%), neurofibromas - 6 (20%). Patients of both groups were initially reliably comparable with each other by the following parameters: 1) Age; 2) age category; 3) initial level of quality of life; 4) localization of the tumor process relative to the axis of the spine, spinal canal and surface of the spinal cord; 5) prevalence of the tumor process. All patients underwent clinical and neurological examination. It was supplemented by MRI, MS CT, and spondylography data. At the first stage of surgical treatment, the study group used selective angiography and ultrasound. During the second stage, a cavitation ultrasonic surgical aspirator (CUSA) was used, combining its use with laser ablation. The general condition of patients was assessed before surgery, on the 1st day after surgery and on the 7th–10th day - immediately before discharge. If patients had motor disorders, their severity was assessed using a five-point muscle strength assessment scale [12]. The study of sensory disorders included identifying changes in superficial and deep types of sensitivity, and the nature of the disorders (segmental or conductive) was also determined. To assess the results of surgical treatment and the quality of life in the pre- and postoperative periods, the Frankel scale [4] was used in both groups. Mathematical and statistical analysis of the obtained results was performed using the standard STATISTICA 10.0 for Windows 10 software package for personal computers [12]. The following parameters were used for tumor removal: a power of 5 W in pulsed mode, an exposure duration of 1 second, an interval of 0.7 seconds inside the node, and a continuous mode with a power of 3-5 W when performing superficial ablation under visual control. The total dose was from 1000 to 3000 J per period. Laser radiation was delivered to the tumor at the first stage transcutaneously through a sterile quartz light guide with a diameter of 300 μm using a G11 Yamshidi needle, and at the second stage - a 500 μm diameter LED using a special attachment included in the device kit.

Results. According to our data, it can be concluded that movement disorders are one of the most common symptoms in patients with EMO. They were detected in 55 of 60 patients, which accounted for 91.7% of cases. In the comparison group, they occurred in 27 (90%) patients, in the study group - in 28 (93.3%) people. These indicators do not statistically significantly differ from each other. On the 10th day after the operation, regression of movement disorders was observed both in the comparison group and in the study group - in 16.7% and 26.7% of patients, respectively. The number of patients with movement disorders by this time decreased in the control group from 90 to 73.3%, in the main group - from 92.9 to 66.6%. A month later, regression of motor disorders was also observed: in the comparison group - from 90 to 56.7%, in the study group - from 92.9 to 43.3%. Moreover, where the LAKHT-MILON laser was used during the operation, their

early regression was statistically significantly observed in a larger number of patients in comparison with the patients of the comparison group, which was probably due to the possibility of minimizing the risk of bleeding and reducing traction effects during open surgery.

Sensory disorders were initially detected in 58 (96.7%) of 60 patients. Moreover, equally in the study group - in 29 (96.7%), and in the comparison group - in 29 (96.7%) people. Disorders of superficial sensitivity in the clinical picture of patients with EMO at stage I of the disease were diagnosed in 35 (58.3%) patients out of 60. In the study group, they were in 17 (56.7%) people, in the comparison group - in 18 (60%). In stages II and III of the disease, conduction-type disorders and muscular-articular proprioception disorders came to the forefront, detected in 25 (41.7%) patients out of all. In the study group, they were diagnosed in 13 (43.3%) patients, in the comparison group - in 12 (40%). All patients after the surgery showed positive dynamics of varying severity, which consisted in a decrease in sensory disorders. Moreover, in patients who underwent treatment using the LAKHT-MILON laser, statistically significant and early regression was noted. Thus, on the 10th day after the surgery, sensory disorders of varying degrees were detected in 22 (73.3%) patients in the study group, and in 23 (76.7%) patients in the comparison group. A month later, regression of sensory disorders was also observed: in the study group from 96.7% to 46.7%, in the comparison group - from 96.7% to 60%, which is statistically significant. Radicular pain syndrome was initially detected in 41 (68.3%) patients, and in the comparison group it was detected in 19 (63.3%) patients, and in the study group in 21 (73.3%) people. In all cases, the pain was unilateral and corresponded to the localization of the tumor node. On the 10th day after the operation, radicular pain syndrome regressed in 47 (78.3%) of 60 patients and persisted in 13 (21.7%) patients. At the same time, in both groups it persisted in 6 (20%) and 7 (23.3%) patients, respectively. After 3–4 weeks from the moment of tumor removal, patients still had residual pain associated with irritation of the spinal cord roots: in the comparison group, radicular pain was diagnosed in 3 (10%) patients, and in the study group in 1 (3.3%) patient.

To evaluate the results of surgical treatment, all patients were initially divided into 4 functional classes based on their quality of life. It was found that both groups were initially in equal conditions for this parameter. Surgical treatment in all patients led to regression of neurological symptoms and, thus, to an improvement in the quality of life. Moreover, it was noted that in the group where LITT was used, the functional results of patient treatment were significantly better on the 10th day after surgery compared to the comparison group. Thus, in the study group, a good result was obtained in 4 (13.3%) patients, satisfactory - in 16 (53.3%), unsatisfactory - in 10 (30.3%) people. In the comparison group, by this time, good results were observed in 2 (6.7%) patients, satisfactory - in 8 (26.7%)

and unsatisfactory - in 20 (66.6%) patients. Further evaluation of the functional results of surgical treatment (21–28 days after the operation) showed that statistically significantly higher good results of surgical treatment were also obtained in the study group. Good results were obtained in 13 (43.3%) patients, satisfactory results in 15 (50%), and unsatisfactory results in 2 (6.7%) patients. In the comparison group, after a month, good results were obtained in 6 (20%) patients, satisfactory results in 15 (50%), and unsatisfactory results in 9 (30%) people. There were no fatal outcomes among all the operated patients in any case.

Having analyzed the results of surgical treatment, obtained depending on the phases of the oncological process, we found a tendency for the number of unsatisfactory results to increase as the process of transverse SM damage progresses. In patients who were in the phase of partial and complete transverse lesion of the spinal cord, the highest number of unsatisfactory results was statistically significantly found compared to patients who were in the irritative phase of the disease. At the same time, the number of unsatisfactory treatment results was statistically significantly lower in cases where LITT was used. The results of the study show that ten days after the operation in the main group, 7 patients (23.3%) with partial compression and 2 (6.7%) with complete compression demonstrated satisfactory outcomes. In the control group, these figures were 13 (43.3%) and 5 (16.7%), respectively. A month later, the situation did not change: in the study group, the number of patients with unsatisfactory results decreased to 2 (6.7%) with partial and to 1 (3.3%) with complete compression, while in the control group there were 6 (20%) and 3 (10%). The average blood loss during EMT removal was (192.6 ± 17.3) ml in the study group and (359.5 ± 16.8) ml in the comparison group. The use of a surgical laser in operations to remove tumors in the lumbosacral spine demonstrated a statistically significant decrease in intraoperative blood loss by almost two times: (210.5 ± 20.6) ml in the study group versus (350.0 ± 21.3) ml in the control group. A clear decrease in blood loss during surgery on large tumors with high density and severe bleeding was proven, since after laser treatment the density and bleeding of the neoplasm significantly decreased, which made it possible to use an ultrasonic disintegrator.

The use of laser technology in microsurgical removal of EMT of various locations and sizes contributed to an increase in the overall level of total resections by 6.7%. According to our data, in the study groups, the percentage of complete tumor removal was 100.0% (30 patients) in the study group and 93.3% (28 patients) in the comparison group. These results are statistically significant.

Thus, the use of the LAHTA-MILON laser in the process of resection of EMOs of various sizes and locations makes it possible to achieve complete removal of tumors. It is noteworthy that even hourglass-type tumors were successfully removed in one stage without the need to expand the surgical approach. Postoperative over-

view spondylography served to verify the scope of surgical intervention and confirmed the effectiveness of the implemented laser technologies. Hemilaminectomy at two or more levels was performed in 10 (33.3%) patients; among them, 2 (6.7%) had EMO spread to two vertebrae, and 8 (26.7%) had EMO spread to three vertebrae. In cases of extensive EMO, in 2 (6.7%) patients, hemilaminectomy was performed at four levels. In situations where tumor tissue caused destruction of the arches, laminectomy at two or more levels was performed in 2 (6.7%) patients. In the control group, access was achieved only through laminectomy, while the articular processes were preserved, and the operation was performed in all patients at two to four levels.

Conclusions. Safe and effective parameters of the LAKHT-MILON laser for microsurgical resection of EMO are: 5 W power in pulsed mode, 1 second exposure duration, 0.7 second interval inside the node and continuous mode with 3-5 W power when performing superficial ablation under visual control.

The use of the LAKHT-MILON laser, in contrast to traditional surgical methods, allows to significantly reduce intraoperative traction and, as a result, minimize trauma to the spinal cord and its roots. This leads to less pronounced neurological symptoms and improved quality of life for patients in the postoperative period. Due to the pronounced coagulating properties of the LAKHT-MILON laser, intraoperative blood loss can be reduced almost twofold during operations to remove EMOs, depending on their volume, bleeding, and prevalence, and the level of total tumor removal can be increased by an average of 6.7% compared to traditional methods. The use of the developed innovative laser surgery technologies using the LAKHT-MILON laser allows for a significant reduction in the trauma of the surgical approach and the resection of EMOs through hemilaminar approaches, while preserving the articular processes of the vertebrae. Conclusion. Despite the use of this technology, known for more than several decades [12], LITT has only recently been introduced into neurosurgery, especially for the treatment of intracranial lesions [13] and epilepsy surgery [14]. The current literature has shown that LITT is an effective therapeutic option for the treatment of intracranial lesions [13]. However, there is still a research gap regarding its use in spinal lesions. LITT has been effectively used to treat intracranial lesions [10],[11], liver [23], and bone [24]. The biggest advantage of this technology is its compatibility with intraoperative MRI, which ensures the accuracy of the procedure in real time. As the heat reaches the target tissue, thermal changes in the surrounding tissue are calculated and converted into a heat map, which allows neurosurgeons to monitor in real time not only the intensity of the delivered heat but also the speed of spread, making it possible to modify the dose and target intraoperatively [24],[25].

Due to the high level of accuracy provided by MRI, this procedure is reported to be safe even for the most sensitive organs.

These clinical cases demonstrate the effectiveness of spinal laser interstitial thermotherapy as an adjunct to surgery for metastatic spinal lesions. Energy is transferred from the laser to the surrounding tissue, causing thermal damage sufficient to cause tumor cell death and coagulative necrosis [3],[38]. The extent of tissue damage is based on a thermal response model in which there is a correlation between temperature, duration of exposure, and subsequent damage, as confirmed by histological examination data – large areas of tumor tissue rarefaction have been identified. Tumor size reduction can be achieved through direct laser action.

In addition, tumors with an extensive blood supply network require less preoperative preparation due to vascular ablation. Intraoperatively, a decrease in the volume of blood loss during tumor removal is noted.

Conflict of interest. The author declares no conflict of interest.

Financing. The study was performed without external funding.

Compliance with patient rights and principles of bioethics. All patients gave written informed consent to participate in the study

References

1. Под ред. А.Д. Каприна, В.В. Старинского, А.О. Шахзадовой Состояние онкологической помощи населению России в 2022 году.− М.: МНИОИ им. П.А. Герцена − филиал ФГБУ «НМИЦ радиологии» Минздрава России, 2022. − илл. – 239 с. [A.D. Kaprin, V.V. Starinsky, A.O. Shahzadova. The state of cancer care for the Russian population in 2022.- M.: NMRC of the Ministry of Health of Russian Federation, 2022. - 239 p. (in Russ.).]

2. Patricia Zadnik Sullivan, Tianyi Niu, Jose Fernandez Abinader et al. Evolution of Surgical Treatment of Metastatic Spine Tumors., 06 January 2022, PREPRINT (Version 1) available at Research Square. https://doi.org/10.21203/rs.3.rs-1153745/v1

3. Tatsui CE, Belsuzarri TA, Oro M, Rhines LD, Li J, Ghia AJ, Amini B, Espinoza H, Brown PD, Rao G (2016) Percutaneous surgery for treatment of epidural spinal cord compression and spinal instability: technical note. Neurosurg Focus 41(4):E2. https://doi.org/10.3171/2016.8.FOCUS16175

4. Bastos DCA, Vega RA, Traylor JI, Ghia AJ, Li J, Oro M, Bishop AJ, Yeboa DN, Amini B, Kumar VA, Rao G, Rhines LD, Tatsui CE (2020) Spinal laser interstitial thermal therapy: single-center experience and outcomes in the first 120 cases. J Neurosurg Spine 1–10. https://doi.org/10.3171/2020.7.SPINE20661

5. Cardia, A., Cannizzaro, D., Stefini, R. et al. The efficacy of laser interstitial thermal therapy in the management of spinal metastases: a systematic review of the literature. Neurol Sci 44, 519–528 (2023). https://doi.org/10.1007/s10072-022-06432-x

6. Barzilai O, Fisher CG, Bilsky MH (2018) State of the art treatment of spinal metastatic disease. Neurosurgery 82(6):757–769. https://doi.org/10.1093/neuros/nyx567

7. Payer S, Mende KC, Westphal M, Eicker SO (2015) Intramedullary spinal cord metastases: an increasingly common diagnosis. Neurosurg Focus 39(2):E15. https://doi.org/10.3171/2015.5.FOCUS15149

8. Laufer I, Rubin DG, Lis E, Cox BW, Stubblefield MD, Yamada Y, Bilsky MH (2013) The NOMS framework: approach to the treatment of spinal metastatic tumors. Oncologist 18(6):744–51. https://doi.org/10.1634/theoncologist.2012-0293

9. Pennington Z, Ahmed AK, Molina CA, Ehresman J, Laufer I, Sciubba DM (2018) Minimally invasive versus conventional spine surgery for vertebral metastases: a systematic review of the evidence. Ann Transl Med 6(6):103. https://doi.org/10.21037/atm.2018.01.28

10. Tatsui CE, Stafford RJ, Li J, Sellin JN, Amini B, Rao G, Suki D, Ghia AJ, Brown P, Lee SH, Cowles CE, Weinberg JS, Rhines LD (2015) Utilization of laser interstitial thermotherapy guided by real-time thermal MRI as an alternative to separation surgery in the management of spinal metastasis. J Neurosurg Spine 23(4):400–411. https://doi.org/10.3171/2015.2.SPINE141185

11. Missios S, Bekelis K, Barnett GH (2015) Renaissance of laser interstitial thermal ablation. Neurosurg Focus 38(3):E13. https://doi.org/10.3171/2014.12.FOCUS14762

12. Bown SG (1983) Phototherapy in tumors. World J Surg 7(6):700–709. https://doi.org/10.1007/BF01655209

13. Schwarzmaier HJ, Eickmeyer F, von Tempelhoff W, Fiedler VU, Niehoff H, Ulrich SD, Yang Q, Ulrich F (2006) MR-guided laser-induced interstitial thermotherapy of recurrent glioblastoma multiforme: preliminary results in 16 patients. Eur J Radiol 59(2):208–215. https://doi.org/10.1016/j.ejrad.2006.05.010

14. Kang JY, Wu C, Tracy J, Lorenzo M, Evans J, Nei M, Skidmore C, Mintzer S, Sharan AD, Sperling MR (2016) Laser interstitial thermal therapy for medically intractable mesial temporal lobe epilepsy. Epilepsia 57(2):325–334. https://doi.org/10.1111/epi.13284

15. Silva D, Sharma M, Juthani R, Meola A, Barnett GH (2017) Magnetic resonance thermometry and laser interstitial thermal therapy for brain tumors. Neurosurg Clin N Am 28(4):525–533. https://doi.org/10.1016/j.nec.2017.05.015

16. de Almeida Bastos DC, Everson RG, de Oliveira Santos BF, Habib A, Vega RA, Oro M, Rao G, Li J, Ghia AJ, Bishop AJ, Yeboa DN, Amini B, Rhines LD, Tatsui CE (2020) A comparison of spinal laser interstitial thermotherapy with open surgery for metastatic thoracic epidural spinal cord compression. J Neurosurg Spine 1–9. https://doi.org/10.3171/2019.10.SPINE19998

17.Moses ZB, Lee TC, Huang KT, Guenette JP, Chi JH (2020) MRI-guided cryoablation for metastatic spine disease: intermediate-term clinical outcomes in 14 consecutive patients. J Neurosurg Spine 1–6. https://doi.org/10.3171/2019.11.SPINE19808

18.Tatsui CE, Nascimento CNG, Suki D, Amini B, Li J, Ghia AJ, Thomas JG, Stafford RJ, Rhines LD, Cata JP, Kumar AJ, Rao G (2017) Image guidance based on MRI for spinal interstitial laser thermotherapy: technical aspects and accuracy. J Neurosurg Spine 26(5):605–612. https://doi.org/10.3171/2016.9.SPINE16475

19.Tokuhashi Y, Uei H, Oshima M, Ajiro Y (2014) Scoring system for prediction of metastatic spine tumor prognosis. World J Orthop 5(3):262–271. https://doi.org/10.5312/wjo.v5.i3.262

20.Akeyson EW, McCutcheon IE (1996) Single-stage posterior vertebrectomy and replacement combined with posterior instrumentation for spinal metastasis. J Neurosurg 85(2):211–220. https://doi.org/10.3171/jns.1996.85.2.0211

21.Young RF, Post EM, King GA (1980) Treatment of spinal epidural metastases. Randomized prospective comparison of laminectomy and radiotherapy. J Neurosurg 53(6):741–8. https://doi.org/10.3171/jns.1980.53.6.0741

22.Molina CA, Gokaslan ZL, Sciubba DM (2012) Diagnosis and management of metastatic cervical spine tumors. Orthop Clin N Am 43(1):75–87. https://doi.org/10.1016/j.ocl.2011.08.004 (viii-ix)

23.Vogl TJ, Dommermuth A, Heinle B, Nour-Eldin NE, Lehnert T, Eichler K, Zangos S, Bechstein WO, Naguib NN (2014) Colorectal cancer liver metastases: long-term survival and progression-free survival after thermal ablation using magnetic resonance-guided laser-induced interstitial thermotherapy in 594 patients: analysis of prognostic factors. Invest Radiol 49(1):48–56. https://doi.org/10.1097/RLI.0b013e3182a6094e

24.Ahrar K, Stafford RJ (2011) Magnetic resonance imaging-guided laser ablation of bone tumors. Tech Vasc Interv Radiol 14(3):177–182. https://doi.org/10.1053/j.tvir.2011.02.010

25.McNichols RJ, Gowda A, Kangasniemi M, Bankson JA, Price RE, Hazle JD (2004) MR thermometry-based feedback control of laser interstitial thermal therapy at 980 nm. Lasers Surg Med 34(1):48–55. https://doi.org/10.1002/lsm.10243

26.Gilbert RW, Kim JH, Posner JB (1978) Epidural spinal cord compression from metastatic tumor: diagnosis and treatment. Ann Neurol 3(1):40–51. https://doi.org/10.1002/ana.410030107

27.Maranzano E, Latini P, Checcaglini F, Ricci S, Panizza BM, Aristei C, Perrucci E, Beneventi S, Corgna E, Tonato M (1991) Radiation therapy in metastatic spinal cord compression. A prospective analysis of 105

consecutive patients. Cancer 67(5):1311–1317. https://doi.org/10.1002/1097-0142(19910301)67:5<1311::aid-cncr2820670507>3.0.co;2-r

28. Yamada Y, Bilsky MH, Lovelock DM, Venkatraman ES, Toner S, Johnson J, Zatcky J, Zelefsky MJ, Fuks Z (2008) High-dose, single-fraction image-guided intensity-modulated radiotherapy for metastatic spinal lesions. Int J Radiat Oncol Biol Phys 71(2):484–490. https://doi.org/10.1016/j.ijrobp.2007.11.046

29. Sahgal A, Bilsky M, Chang EL, Ma L, Yamada Y, Rhines LD, Létourneau D, Foote M, Yu E, Larson DA, Fehlings MG (2011) Stereotactic body radiotherapy for spinal metastases: current status, with a focus on its application in the postoperative patient. J Neurosurg Spine 14(2):151–166. https://doi.org/10.3171/2010.9.SPINE091005

30. Nguyen QN, Shiu AS, Rhines LD, Wang H, Allen PK, Wang XS, Chang EL (2010) Management of spinal metastases from renal cell carcinoma using stereotactic body radiotherapy. Int J Radiat Oncol Biol Phys 76(4):1185–1192. https://doi.org/10.1016/j.ijrobp.2009.03.062

31. Clohisy DR, Perkins SL, Ramnaraine ML (2000) Review of cellular mechanisms of tumor osteolysis. Clin Orthop Relat Res 373:104–114. https://doi.org/10.1097/00003086-200004000-00013

32. Sacino M, Huang SS, Alexander H, Fayed I, Keating RF, Oluigbo CO (2020) An initial cost-effectiveness analysis of magnetic resonance-guided laser interstitial thermal therapy in pediatric epilepsy surgery. Pediatr Neurosurg 55(3):141–148. https://doi.org/10.1159/000509329

33. Hong CS, Kundishora AJ, Elsamadicy AA, Chiang VL (2020) Laser interstitial thermal therapy in neuro-oncology applications. Surg Neurol Int 8(11):231. https://doi.org/10.25259/SNI_496_2019

34. Zaed I, Bossi B, Ganau M, Tinterri B, Giordano M, Chibbaro S (2022) Current state of benefits of enhanced recovery after surgery (ERAS) in spinal surgeries: a systematic review of the literature. Neurochirurgie 68(1):61–68. https://doi.org/10.1016/j.neuchi.2021.04.007

35. Srinivasan ES, Grabowski MM, Nahed BV, Barnett GH, Fecci PE (2021) Laser interstitial thermal therapy for brain metastases. Neurooncol Adv 3(Suppl 5):v16–v25. https://doi.org/10.1093/noajnl/vdab128

36. Srinivasan ES, Sankey EW, Grabowski MM, Chongsathidkiet P, Fecci PE (2020) The intersection between immunotherapy and laser interstitial thermal therapy: a multipronged future of neuro-oncology. Int J Hyperthermia 37(2):27–34. https://doi.org/10.1080/02656736.2020.1746413

37. University of Florida (2021) Recurrent brain metastasis immune effects and response to laser interstitial thermotherapy (LITT) and pembrolizumab in combination (TORCH). clinicaltrials.gov. https://clinicaltrials.gov/ct2/show/NCT04187872. Accessed July 29, 2021

38. Чудновский В.М., Юсупов В.И., Иваненко А.В., Щедренок В.В., Себелев К.И., Могучая О.В.Анализ акустогидродинамических явлений лазерного пункционного лечения дегенеративных заболеваний межпозвонковых дисков. Журнал «Российский нейрохирургический журнал им. проф. А.Л. Поленова». – 2011. – том 3. – № 2. – С.52– 57.[Chudnovsky V.M., Yusupov V.I., Ivanenko A.V., Shedrenok V.V., Sebelev K.I., Moguchaya O.V. Analysis of acoustic and hydrodynamic phenomena of laser puncture treatment of degenerative diseases of intervertebral discs. The Russian Neurosurgical Journal named after prof. A.L. Polenov.- 2011.- Tom 3.- №2.- P. 52-57. (in Russ.).]

39. Ступак В.В., Шабанов С.В., Пендюрин И.В., Рабинович С.С. Результаты хирургического лечения пациентов с экстрамедуллярными опухолями типа песочных часов // Хирургия позвоночника. 2014. № 4. С. 65–71. [Stupak V.V., Shabanov S.V., Pendyurin I.V., Rabchinovich S.S. Results of surgical treatment of patients with hourglass-type extramedullary tumors. Spine surgery. 2014. №4. P. 65-71. (in Russ.).]

DOI 10.34660/INF.2025.49.44.139

THE ROLE OF NUTRITIONAL SUPPORT AND MICRONUTRIENTS IN RESTORING THE REPRODUCTIVE HEALTH OF WOMEN WHO HAVE SUFFERED COVID-19

Rizaeva Malikakhon Abdumanonovna
Assistant, Head of Department
Children's National Medical Center,
Tashkent, Uzbekistan

Kattakhodjaeva Makhmuda Khamdamovna
Doctor of Medical Sciences, Professor
Tashkent State Dental Institute,
Tashkent, Uzbekistan

Rizaev Jasur Alimdjanovich
Doctor of Medical Sciences, Professor, Rector
Samarkand State Medical University,
Samarkand, Uzbekistan

Annotation. *Introduction. Post-COVID syndrome in women of reproductive age is often accompanied by hormonal, vascular and metabolic disorders. Micronutrient deficiency can aggravate the restoration of reproductive function and disrupt the course of gynecological diseases.*

Objective: To assess the impact of nutritional support and micronutrient intake on reproductive health restoration in women who have had COVID-19.

Materials and methods. The study included 135 women of reproductive age. Group I (n = 80) received a complex of nutrients (vitamin D, magnesium, zinc, arginine, omega-3, etc.) along with standard therapy. Group II (n = 55) received only basic therapy. Hormonal, vascular, and ultrasound parameters, as well as psychoemotional state, were assessed. Statistical processing was performed using SPSS 23.0; $p < 0.05$ was considered significant.

Results. Women in Group I showed improvement in all key parameters: vitamin D levels increased to 32.4 ± 4.5 ng/ml versus 21.8 ± 3.9 in Group II; IL-6 decreased to 6.2 ± 1.4 pg/ml (9.1 ± 1.8 in Group II); NO levels increased to 22.1 ± 2.2 μmol/l. Endometrial thickness was 8.4 ± 1.0 mm versus 6.7 ± 1.2 mm, and AMH levels were 2.7 ± 0.6 ng/ml versus 1.9 ± 0.5, respectively. A significant decrease in anxiety and stabilization of the menstrual cycle were also recorded.

Conclusion. The use of nutritional support significantly increases the effectiveness of women's rehabilitation after COVID-19, promotes the restoration of reproductive function and improves the general condition of patients.

Keywords: *nutritional support, micronutrients, reproductive health, COVID-19, restorative therapy.*

Introduction. The post-COVID period in women of reproductive age is characterized by a complex of disorders affecting the endocrine, vascular and immune systems. An increasing number of observations indicate persistent changes in the menstrual cycle, ovarian dysfunction, as well as an increased risk of inflammatory and vascular complications, especially in patients with concomitant gynecological pathology [9, 13].

One of the significant factors contributing to the development of these conditions is micronutrient deficiency, which occurs both as a result of infection and against the background of systemic inflammatory and metabolic imbalance [1, 7]. Deficiency of vitamin D, magnesium, zinc, selenium, arginine and a number of other nutrients is associated with impaired regulation of vascular tone, immune response and hormonal homeostasis [11, 14]. These links are especially vulnerable in women who have had a coronavirus infection and often require deeper restorative intervention that goes beyond symptomatic therapy. Against this background, there is growing interest in the use of nutritional support as a pathogenetically substantiated approach that can not only replenish the deficiency of vital substances, but also promote regression of inflammatory, vascular and neuroendocrine disorders. The use of micronutrients as part of complex rehabilitation schemes can play a key role in normalizing reproductive function in women who have had COVID-19 [1, 3, 7].

The aim of the study is to determine the effectiveness of nutritional support and micronutrient intake in restoring women's reproductive health after COVID-19 infection based on the analysis of hormonal, vascular, laboratory and ultrasound parameters.

Materials and methods. The clinical study was conducted at a specialized gynecological hospital as part of an observational program for the rehabilitation of women of reproductive age who had COVID-19. The study included 135 patients aged 18 to 45 years who had a confirmed coronavirus infection at least 6 months before seeking treatment and had reproductive health problems. The clinical manifestations were predominantly menstrual disorders, signs of ovarian dysfunction, secondary infertility, chronic inflammatory diseases of the pelvic organs, endometrial hypoplasia, and manifestations of endometriosis.

To assess the effectiveness of nutritional support, the women were divided into two comparable groups. The first group (n = 80) included patients who, along with

standard therapy for the underlying gynecological disease, were prescribed targeted nutritional correction. The program included taking vitamin D3 (at a dose of 2000-4000 IU per day), magnesium in the form of citrate or orotate (300-400 mg), zinc (25-30 mg), calcium (up to 1000 mg), arginine (at a dose of 2 g / day) and omega-3 polyunsaturated fatty acids (up to 2 g / day). The duration of nutritional support was at least eight weeks. The second group (n = 55) included patients who received only standard drug therapy without additional nutritional correction.

The inclusion criteria for the study were: age 18–45 years, proven history of coronavirus infection, absence of severe somatic or oncological pathology, preserved reproductive function, and voluntary informed consent. Women with severe metabolic disorders, endocrine pathology (including diabetes mellitus), as well as those who had previously received vitamin and mineral complexes on a regular basis, were excluded from the study.

A comprehensive assessment of the effectiveness was performed before the start of therapy and after eight weeks of observation. The levels of sex hormones (FSH, LH, estradiol, progesterone, AMH), vitamin D, magnesium, zinc, folates, as well as the levels of C-reactive protein and proinflammatory cytokines (in particular, interleukin-6) were studied. The vascular component was assessed by the levels of nitric oxide and endothelin-1 in plasma. In addition, an ultrasound examination of the pelvic organs was performed to assess the condition of the endometrium, the structure and size of the ovaries, the thickness and echogenicity of the functional layer. Functional restoration of the reproductive system was analyzed by the dynamics of the menstrual cycle, complaints of premenstrual syndrome, the presence of ovulation, as well as by the subjective quality of life scale. Psychoemotional status was assessed using the Spielberger scale and the visual analogue anxiety scale.

Statistical data processing was performed using the SPSS 23.0 package. Descriptive and comparative statistics methods were used, including Student's t-test, Mann-Whitney U-test and Pearson correlation analysis. The significance level of $p < 0.05$ was considered statistically significant.

Results. The analysis showed significant differences in clinical, laboratory and functional parameters between the groups, indicating a significant effect of nutritional support on the restoration of reproductive health in women after COVID-19 infection. Against the background of complex nutritional therapy (group I), there was a significant improvement in vitamin and mineral status, a decrease in the severity of the inflammatory response, restoration of vascular tone, as well as positive dynamics of reproductive parameters. In particular, menstrual cycle parameters were normalized, the thickness and structure of the endometrium improved, and the level of anti-Müllerian hormone as a marker of ovarian reserve increased. In addition, patients in the first group showed a decrease in IL-6 levels,

accompanied by an increase in nitric oxide synthesis, which reflects the restoration of endothelial function and a decrease in systemic inflammation.

In women who did not receive nutritional support (Group II), improvements were less pronounced or were statistically insignificant. Moreover, in some cases, signs of micronutrient deficiency and dysfunction of vascular-hormonal regulation persisted. All key differences between the groups in laboratory and clinical parameters are presented in Table 1.

Table 1.

Comparative indicators between groups of patients

Indicators	Group I (with nutritional support)	Group II (without nutritional support)	p-value
Vitamin D (ng/ml)	32.4 ± 4.5	21.8 ± 3.9	<0.001
Magnesium (mmol/l)	0.83 ± 0.08	0.71 ± 0.07	<0.01
Zinc (μmol/L)	12.6 ± 1.9	9.4 ± 1.6	<0.01
IL-6 (pg/ml)	6.2 ± 1.4	9.1 ± 1.8	<0.01
NO (μmol/L)	22.1 ± 2.2	18.7 ± 2.0	<0.01
AMH (ng/ml)	2.7 ± 0.6	1.9 ± 0.5	<0.01
Endometrial thickness (mm)	8.4 ± 1.0	6.7 ± 1.2	<0.001
Menstrual cycle (duration, days)	28.5 ± 1.6	30.1 ± 2.3	<0.05
Anxiety assessment (scores, Spielberger scale)	22.4 ± 3.2	27.3 ± 3.8	<0.01

Discussion. The results of this study confirm that the use of nutritional support in women who have had COVID-19 has a significant positive effect on the restoration of reproductive function. A significant increase in the levels of vitamin D, magnesium and zinc in the first group was accompanied by normalization of hormonal levels, improvement in the morphometric characteristics of the endometrium and a decrease in markers of systemic inflammation. This is consistent with modern concepts of the importance of micronutrients in the regulation of vascular-hormonal and immune balance in women in the post-infection period [1, 7, 11]. The data obtained also confirm the role of vitamin D as a modulator of sexual function, involved in the regulation of steroid hormone synthesis, differentiation of endometrial tissue and ensuring immune tolerance in the uteroplacental link [1]. Its deficiency, widespread in the post-COVID period, is associated with menstrual irregularities, ovarian dysfunction and decreased fertility. Restoration of vitamin D levels was accompanied by an improvement in AMH levels and normalization of ovulatory cycles, which is consistent with the observations of a number of other authors [13].

An increase in nitric oxide concentration and a decrease in IL-6 in women who received nutritional therapy reflects the positive effect of amino acids and omega-3 fatty acids on vascular tone and anti-inflammatory mechanisms. This is especially important in the context of persistent endothelial dysfunction typical of the post-COVID state [14]. Restoration of microcirculation and a decrease in the pro-inflammatory cytokine background play a key role in endometrial reparation and stabilization of the menstrual cycle. Normalization of the psychoemotional state, recorded by a decrease in anxiety scores, can be due to both the direct effect of nutrients on neurotransmitter metabolism (in particular, magnesium and omega-3) and a general improvement in the somatic state. This emphasizes the need for an integrative approach to the rehabilitation of women after COVID-19, including both pharmacotherapy and nutritional support [3, 9].

The conducted study confirms the high clinical effectiveness of nutritional support as an important element of restorative medicine in women of reproductive age. The multidirectional action of vitamins, microelements and amino acids provides a holistic effect on endocrine, vascular and immune regulation, which makes this approach pathogenetically justified.

Conclusion. The study showed that the inclusion of nutritional support in the complex therapy of women who have had COVID-19 contributes to a significant improvement in the reproductive state. Against the background of taking vitamin D, magnesium, zinc, arginine and omega-3 fatty acids, there was a restoration of hormonal balance, normalization of microcirculation, a decrease in inflammatory activity and an improvement in the morphofunctional characteristics of the endometrium. In addition, the positive dynamics also affected the psychoemotional sphere, which enhanced the overall clinical improvement. The data obtained confirm the pathogenetic feasibility of prescribing nutritional components in the post-COVID rehabilitation program for women of reproductive age. This approach can increase the effectiveness of restorative therapy, reduce the time it takes to normalize the menstrual cycle and improve fertility prospects. The results of the study can serve as a basis for developing personalized nutritional correction regimens and including this strategy in standardized protocols for medical care for women in the post-COVID period.

References

1. Andreeva E.N., Absatarova Y.S. Melatonin status disorders in gynecological practice: pathogenetic aspects and therapeutic possibilities. Russian Bulletin of Obstetrician-Gynecologist. 2022;22(6):48-53. https://doi.org/10.17116/rosakush20222206148

2. Andreeva, A. A., Sharov, N. D., & Popugaylo, M. V. (2023). Features of the development of thrombocytosis and thrombocytopenia in patients with moderate and severe coronavirus infection COVID-19. Trends in the Development of Science and Education, Article 276. https://doi.org/10.18411/trnio-07-2023-276

3. Gasanova S.M., Kuzmenko G.N., Krasilnikova A.K., Popova I.G., Nazarov S.B. Features of the hemostasis system in women with abnormal uterine bleeding against the background of endometrial hyperplasia. Thrombosis, hemostasis and rheology. 2024;(3):87–96. https://doi.org/10.25555/thr.2024.3.1113

4. Gashimova, N. R. (2023). Features of the hemostasis and immunoregulation system in the mother-fetus-newborn system after COVID-19 of varying severity (Dissertation for the degree of candidate of medical sciences). Sechenov University. Moscow - 2023. https://www.sechenov.ru/upload/iblock/9d2/xe1uiwjeutwgozur3tw888aegiyoyzdn/DISSERTATSIYA-Gashimova.pdf

5. Golovchak, I. S., Boychuk, O. G., Kupchak, I. M., Matskevich, V. M., & Polishchuk, I. P. (2024). The diagnostic utility of ultrasound and morphological examination of the endometrium in patients with disabilities and a severe history of covid-19. Current nutrition in pediatrics, obstetrics and gynecology, (1), 10–15. https://doi.org/10.11603/24116-4944.2024.1.14738

6. Golovchak, I. S., Boychuk, O. G., Matskevich, V. M., Kupchak, I. M., & Polishchuk, I. P. (2024). Methodology of endometrial tissue sampling in women with infertility and a history of post-COVID syndrome. Art of Medicine, 2(30), Article 1202. https://doi.org/10.21802/artm.2024.2.30.25

7. Keshikova D. D., Olshevskaya O. K., Khidirova L. D. Endothelial dysfunction as the main component of climacteric syndrome and cardiovascular diseases // Doctor. 2023; 6 (26): 78-82. https://doi.org/10.51793/os.2023.26.6.011

8. Kozlov, V. A., & Sapozhnikov, S. P. (2021). Amyloidogenic thrombus formation in COVID-19 and neurological disorders (review of reviews, meta-analyses and special cases). COVID-19: first experience. 2020/Collective monograph. Edited by prof. PB Zotov. Tyumen: Vector-Book, 2021.–463 p., 260.

9. Litvak, O., & Petruk, O. (2022). Clinical and morphological aspects of the reproductive system of women of the reproductive age with disturbances in the menstrual cycle after COVID-19. Clinical and preventive medicine, (3), 4-10. https://doi.org/10.31612/2616-4868.3(21).2022.01

10.Makatsaria A.D. (2024) COVID-19 and systemic thrombotic syndromes. Obstetrics, Gynecology and Reproduction. 2024;18(6):908–918. https://doi.org/10.17749/2313-7347/ob.gyn.rep.2024.590

11.Romanov Y.A. SARS-CoV-2, COVID-19 and cardiovascular complications: a view from the position of vascular endothelium. Cardiological Bulletin. 2022;17(1):21-28. https://doi.org/10.17116/Cardiobulletin20221701121

12.Fedorenko V.A., Melnikov A.P. Fibrinolysis disorders in obstetric and gynecological practice. Russian Bulletin of Obstetrician-Gynecologist. 2022;22(6):18-26. https://doi.org/10.17116/rosakush20222206118

13.Khamoshina, M. B., Zhuravleva, I. S., Artemenko, Y. S., & Dmitrieva, E. M. (2021). Hormone-dependent diseases of the female reproductive system in the era of COVID-19: quo vadis?. Obstetrics and Gynecology: News. Opinions. Training, 9(Supplement 3 (33)), 35-42.

14.Bondar, M., Pilipenko, M., & Loskutov, O. (2022). The endothelium is the main target of coronavirus infection. Emergency medicine, 18(2), 13–19. https://doi.org/10.22141/2224-0586.18.2.2022.1467

DOI 10.34660/INF.2025.19.19.140
UDC 541.678.01.691.32

THE INFLUENCE OF PLASTICIZER ON THE COMPONENTS OF CONCRETE MATRIX

Kurbanbaeva A.E.
Doctor of Chemical Sciences, Chief Researcher
Academy of Sciences of the Republic of Uzbekistan,
Institute of General and Inorganic Chemistry

Latha M.S.
PhD, Associate Professor
Sri Venkateshwara College of Engineering

Jumaboev R.A.
Student
Urgench State University named after Abu Rayhan Beruni
of the Republic of Uzbekistan

Abstract. *Prerequisites for the problem. Currently, the construction industry widely uses superplasticizer C-3 to improve the technological process of concrete production and improve its quality, but its production faces the problem of naphthalene deficiency and high cost. In this regard, the development of new effective and cheap plasticizing additives is relevant.*

Objective. Study of the influence of plasticizing additives on the rheological properties of cement paste and concrete mixtures, on the structure formation of cement stone and concrete.

Methodology. To study the behavior of concrete when mixed with different percentages of surfactants, the following test methods were carried out in accordance with Indian Standards (IS codes): - slump test; -compressive strength test; - split tensile strength.

Scientific novelty. The influence of the nature of hydrophilic groups of surfactants on plasticizing activity was studied. It has been shown that SHK with hydroxyl groups has the best plasticizing properties.

Results obtained. A study of the influence of the nature of the hydrophilic groups of a surfactant on its plasticizing properties showed that, compared with sulfo groups, hydroxyl groups, due to their lower molecular weight and greater hydrophilicity, increase the plasticizing activity of the additive.

Keywords: *hydroxyl groups, concrete structure, strength, absorbency water, surfactants, workability.*

Peculiarities: *The patterns of changes in the aggregative stability and rheological properties of concrete with changes in the nature and ratio of hydrophilic groups in the surfactant have been established.*

Introduction.

Concrete is one of the most widely used materials in the construction of buildings and structures. High-strength concrete is one of the most promising structural materials for the development of the construction complex. It is distinguished by a high level of construction and technical properties, in particular, strength, waterproofness, reliability, durability, as well as simplicity of technology. The main methods for optimizing cement concrete are the introduction of chemical additives. Multifunctional chemical additives can improve the basic parameters of the workability of concrete mixtures and help improve its physical and mechanical characteristics [1-3]. When obtaining a high-strength structure, it is necessary to actively control the structure formation of concrete at all technological stages [4, 5]. The greatest influence on the main characteristics of concrete is exerted by the structure of the cement matrix, the quality of which largely depends on the parameters of its pore space, which depend on numerous technological factors [6, 7]. Based on numerous experimental results obtained by scientists during the study of the structure of the cement matrix of concrete, a number of techniques have been developed and proposed [4, 8]. The strength of cement stone decreases as its porosity increases, and to a much greater extent than the increase in the latter. Various scientists have found that the ultimate compressive strength of concrete decreases by 10-15% when its porosity increases by 2-3%.

Yambor [4] studied the dependence of the strength of cement stone of different mineralogical composition on its porosity. It has also been established that cement stone with the same pore structure can be characterized by a different crystal structure and, accordingly, have different strength. This difference is usually explained by the nature and size of the pores, so the compressive strength increases with decreasing pore size [9, 10]. In this regard, the features of the processes of hydration and structure formation of cement systems in the presence of additives have not been sufficiently studied. This makes it difficult to develop effective technologies for concrete composites for construction purposes with high technological and operational characteristics, which determines the relevance of the research being carried out.

Methods and materials. The test methods used to determine the optimum mix of concrete was: slump test -The IS code for slump test is IS 1199. The slump test procedure involves placing a slump cone mold on a tray with a smooth surface;

compressive strength test - IS 456:2000: This code covers the characteristic compressive strength of concrete. The test involves testing standard-sized concrete cubes 150 mm x 150 mm x 150 mm, under a Compression Testing Machine after 28 days of curing; split tensile strength - The IS code procedure for the split tensile test of concrete is IS-516. The test determines the splitting tensile strength of cylindrical concrete specimens. Distilled water was used to prepare surfactant solutions. The reagents were obtained at the Institute of General and Inorganic Chemistry of the Academy of Sciences of the Republic of Uzbekistan.

Results and discussion. Workability of the concrete is has significant role in proper mixing and placing of concrete in the formwork. The concrete with poor workability may result in poor workmanship and subsequent reduction in the quality of concrete with respect to strength and durability. The slump cone test was conducted to study the workability of concrete with respect to the addition of different surfactants. To determine the most effective method of adding admixture to concrete mix as per Indian Standards (IS Codes), we conducted a series of tests to produce the following compositions:

1. Composition No. 1 – control, with the introduction of an additive (A) into the concrete mixture with mixing water (W) (A+W);

2. Composition No. 2 – introduction of a surfactant into a concrete mixture already mixed with water at the end of its preparation (W, then A);

3 Composition No. 3 – two-stage mixing of the concrete mixture, in which at the 1st stage 2/3 of the mixing water is added to the mixture and mixed for 30-40 seconds, at the 2nd stage the remaining 1/3 of the water diluted in it is added adding a surfactant and mixing again until a homogeneous mass is obtained (2/3W, then 1/3W+A). (according to GOST, slump cone SK = 16-20 cm).

The test results showed that the best results in terms of process ability of the mixture obtained by two-stage introduction of the additive.

The effectiveness of two-stage mixing of a concrete mixture with water and a plasticizing additive is explained by the fact that the potential of the plasticizer is more used when it is separately introduced into the mixture at the end of its preparation, than with the traditional method of administering the supplement. Since with the traditional method, part of the plasticizer, along with the mixing water, is absorbed into the pores and capillaries of the filler, which is simply held in them in a “blocked” form due to molecular and adsorption forces. Plasticizing additives significantly affect the workability of concrete mixtures. The results of workability tests are shown below in table 1 & fig.1

Table 1

The nature of reagents and their effect on the strength of concrete

SI No.	Designation of reagents	Compressive Strength N/mm²
		N/mm2
1	UK-P-3006	37.52
2	UK-P-2906	38.01
3	K-PAV	38.90
4	KMK-PAV	36.60
5	GPA-N	38.07
6	GPA-L	37.08
7	F-2	36.06
8	JKG	35.68
9	JKG+G	38.05
10	SMF-02	37.57
11	SMF-2804	35.39
12	SHK	40.20
13	ANSN-2	37.82
14	Pol-SFM	37.00
15	3 GSM	37.52
16	2 GSF	35.75
17	Control	35.65

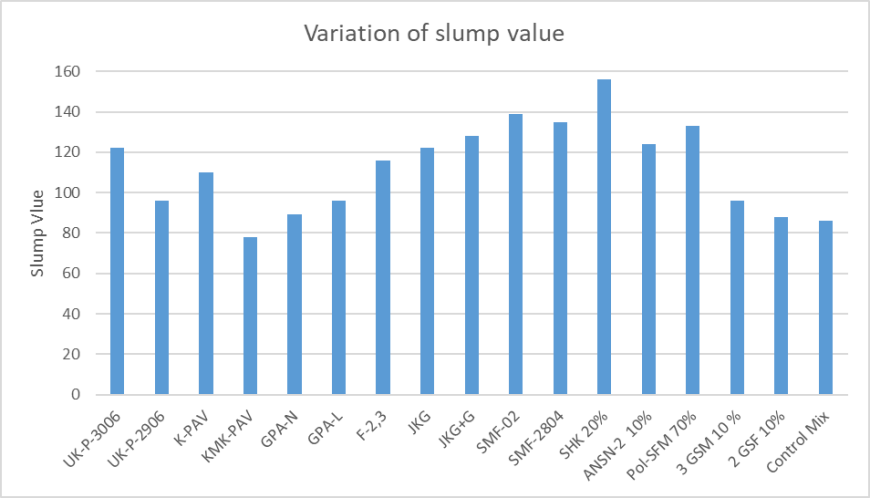

Figure 1. *Variation of slump value*

For all the concrete mixes the surfactant dosage of 0.5% by weight of cement was added and the slump cone test was performed. Referring to the variation of slump value with different surfactants under investigation the slump value of all the mixes containing the surfactants was found to be higher compared to the slump value of control concrete mix with no surfactant. The maximum value of slump value of 156 mm was achieved for the mix SHK which indicates higher workability of concrete. Unlike other SHK additives, it has good compatibility with various cements, which ensures stability of the characteristics of the concrete mixture regardless of fluctuations in the chemical composition of the cement. As the cement content of concrete increases, the effectiveness of SHK increases, both in terms of workability and water release of the concrete mixture.

Another main indicator of SHK is the increase in concrete strength. Compressive strength is the one of the important property of concrete which gives the load carrying capacity of the concrete when the concrete member is subjected to compressive forces. The following are the compressive strength results (Table 2 & fig.2) obtained for concrete mixes with different surfactants. M30 grade of concrete was chosen for the study.

Table 2

Various surfactants and their effect on compressive strength.

SI No.	Designation of reagents	Compressive Strength N/mm^2
		N/mm2
1	UK-P-3006	37.52
2	UK-P-2906	38.01
3	K-PAV	38.90
4	KMK-PAV	36.60
5	GPA-N	38.07
6	GPA-L	37.08
7	F-2,3	36.06
8	JKG	35.68
9	JKG+G	38.05
10	SMF-02	37.57
11	SMF-2804	35.39
12	SHK	40.20
13	ANSN-2	37.82
14	Pol-SFM	37.00
15	3 GSM	37.52
16	2 GSF	35.75
17	Control Mix	35.65

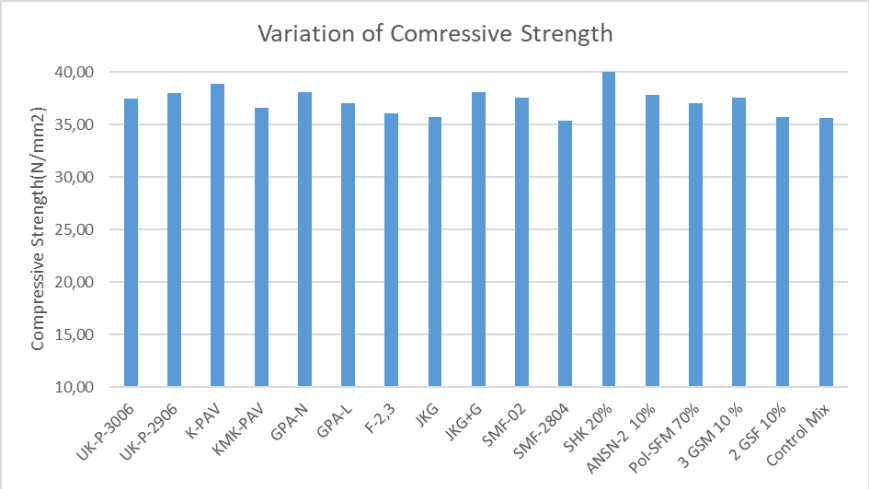

Figure 2. *Variation of Compressive Strength*

For all the concrete mixes the surfactant dosage of 0.5% by weight of cement was added and the Compressive strength test was performed. Referring to the variation of Compressive strength with different surfactants under investigation the compressive strength of all the mixes containing the surfactants was found to be higher compared to the compressive strength of control concrete mix with no surfactant. The maximum value of compressive strength obtained is 40.20 N/mm^2 for the mix SHK.

There are various practical exposures of the concrete where it is subjected to the direct or indirect tensile load. The concrete should be able to withstand these loads without undergoing any failure. The following are the split tensile strength results (Table 3 & fig.3) obtained for different mixes under investigation.

Table 3

Results of separation of tensile strength with different mixtures

SI No.	Mix Designation	Split Tensile Strength
		N/mm^2
1	UK-P-3006	3.74
2	UK-P-2906	3.89
3	K-PAV	3.71
4	KMK-PAV	3.49
5	GPA-N	3.63
6	GPA-L	3.54

7	F-2,3	3.44
8	JKG	3.41
9	JKG+G	3.63
10	SMF-02	3.59
11	SMF-2804	3.38
12	SHK	4.22
13	ANSN-2	2.97
14	Pol-SFM 7	3.53
15	3 GSM	3.58
16	2 GSF	3.41
17	Control Mix	3.19

For all the concrete mixes the surfactant dosage of 0.5% by weight of cement was added and the split tensile strength test was performed. Referring to the variation of split tensile strength with different surfactants under investigation the split tensile strength of all the mixes containing the surfactants was found to be higher compared

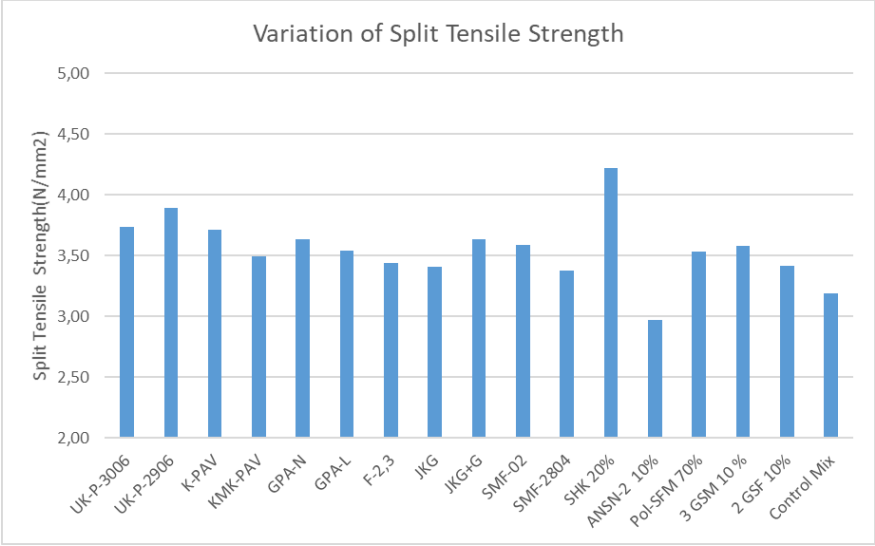

Figure 3. *Variation of Split Tensile Strength*

to the compressive strength of control concrete mix with no surfactant. The maximum value of split tensile strength obtained is 4.22 N/mm^2 for the mix SHK.

Conclusions. From the results of the study it was observed that all the mixes of concrete incorporated with surfactant has resulted in improved workability re-

sults in terms of slump value and improved compressive strength and split tensile strength results compared to the control concrete with no surfactant. The concrete mix containing SHK has resulted in higher workability results in terms of slump value, maximum compressive strength and split tensile strength of concrete.

Joint grant Uzbekistan-India: **UZB-Ind-2021-81** "Development of scientific foundations for the creation of effective high-molecular surfactants that improve the technological properties of dispersed systems"

References

1. Bui, V.K. Rapid testing method for segregation resistance of self - compacting concrete // Cement and Concrete Research 32. -2003. -PP.1489-1496.

2. Agathe Bourchy, Laury Barnes, Laetitia Bessette et. Optimization of concrete mix design to account for strength and hydration heat in massive concrete structures // Cement and Concrete Composites, 2019, 103, pp. 233-241. Ffhal-02466837.

3. Kurbanbaeva A.E., Latha M S, Halmuminova D. A Colloid-chemical properties of polycomplexes based on 1,4-dimaleatedioxyethanacrylate heptyl ether monoethanolamine salt with polyacryl acid. // Ethiopian international journal of multidisciplinary research. -India. Okt-2023. Volume: 10. Issue10. –P.6-10. eISSN: 2349-5715.

4. M. Al Shamaa, S. Lavaud, L. Divet, G. Nahas, J.M. Torrenti, Influence of relative humidity on delayed ettringite formation, Cem. Concr. Compos. 58 (2015) 14–22. 467 doi:http://dx.doi.org

5. H.Y. Ghorab, E.A. Kishar, Studies on the stability of the calcium sulfoaluminate hydrates. Part 1: Effect of temperature on the stability of ettringite in pure water, Cem. Concr. Res. 15 470 (1985) 93–99.

6. H. Minard, Etude intégrée des processus d'hydratation, de coagulation, de rigidification et de prise pour un système C3S-C3A-sulfates-alcalins, PhD Thesis, Université de Bourgogne, -2003.

7. M.M. Costoya Fernandez, Effect of particle size on the hydration kinetics and microstructural development of tricalcium silicate, Thesis, Thèse de l'Ecole Polytechnique Fédérale de Lausanne. -2008.

8. I. Joudi-Bahri, A. Lecomte, M.B. Ouezdou, T. Achour, Use of limestone sands and fillers in concrete without superplasticizer, Cem. Concr. Compos. 34 (2012) 771–780. doi:https://doi.org.

9. Y. Villagran-Zaccardi, E. Gruyaert, N. Alderete, N. De Belie, Influence of particle size distribution of slag, limestone and fly ash on early hydration of cement assessed by isothermal calorimetry, in: Int. RILEM Conf. Mater. Syst. Struct. Cem. Mater. -2016.

10. E. Berodier, Impact of the supplementary cementitious materials on the kinetics and microstructural development of cement hydration, Thesis, Thèse de l'Ecole Polytechnique Fédérale de Lausanne. -2015.

DOI 10.34660/INF.2025.20.17.141

MOLECULAR INTERACTION OF ANTIOXIDANT NARINGENIN WITH 3LFN AND 1P5F: A DOCKING STUDY

Mikita Statsi
Postgraduate, Lecturer
International Sakharov Environmental Institute of Belarussian State University

Siyamak Shahab
Doctor of Sciences in Chemistry, Professor, Head of Department
International Sakharov Environmental Institute of Belarussian State University

Abstract. *Naringenin, a flavonoid with potent antioxidant properties, has gained significant attention due to its potential neuroprotective effects. In this study, we investigate the molecular interactions between Naringenin and two target proteins, 1P5F (DJ-1) and 3LFN (cyclin-dependent kinase 2, CDK2), both of which are implicated in Parkinson's disease (PD), using computational docking analysis. DJ-1 is a multifunctional protein involved in oxidative stress response, mitochondrial function, and neuroprotection, with mutations linked to familial forms of PD. CDK2, although primarily known for its role in cell cycle regulation, has been associated with neuronal apoptosis and neurodegeneration, making it a potential target in PD pathology. Given their involvement in oxidative stress and neurodegeneration, both proteins are relevant therapeutic targets for PD.*

The three-dimensional structures of Naringenin were constructed using ChemBioOffice 2018 software and the proteins were retrieved from publicly available database (Protein Data Bank www.rcsb.org) and prepared for molecular docking analysis. Binding affinities, interaction profiles, and key residues involved in complex formation were analyzed to determine the stability and specificity of Naringenin's interactions with these proteins.

These findings suggest that Naringenin may exert neuroprotective effects by modulating oxidative stress pathways and enhancing cellular defense mechanisms, potentially offering therapeutic benefits for Parkinson's disease.

Keywords: *Naringenin, docking, DJ-1, CDK2.*

1. Introduction

1.1.1. Chemical Structure of Naringenin

Naringenin is a flavonoid belonging to the subclass of flavanones, which are characterized by a 15-carbon backbone structure with a distinct benzene ring. The molecular formula of Naringenin is $C_{15}H_{12}O_5$, and its IUPAC name is 5,7-dihydroxy-2-(4-hydroxyphenyl)-3-chromenone. The structure of Naringenin consists of a flavonoid skeleton composed of two benzene rings (A and B) connected by a three-carbon bridge (C-ring), forming a chromenone structure.

The key features of Naringenin's chemical structure include hydroxyl groups (-OH) at the 5, 7, and 4′ positions on the aromatic rings. The hydroxyl groups contribute to Naringenin's ability to scavenge free radicals and exhibit antioxidant activity. A double bond between carbons 2 and 3 in the C-ring, which is essential for its antioxidant activity (See Figure 1).

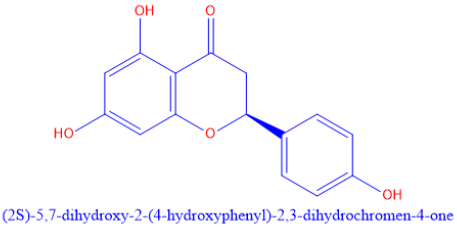

Figure 1. *Chemical structure of Naringenin*

This structure makes Naringenin a potent antioxidant by allowing it to donate electrons to neutralize free radicals and reactive oxygen species (ROS), which are damaging to cells and tissues.

1.1.2. Antioxidant Properties of Naringenin

Naringenin exhibits significant antioxidant properties, making it a promising natural compound in the prevention of oxidative stress-related diseases, including neurodegenerative disorders such as Parkinson's disease [1]. Several studies have shown that Naringenin acts through various mechanisms to exert its antioxidant effects:

1. Free Radical Scavenging:

Naringenin's chemical structure, with its hydroxyl groups, allows it to donate electrons to free radicals, thereby neutralizing them and preventing them from causing cellular damage. The antioxidant properties of Naringenin have been shown to effectively scavenge a variety of reactive oxygen species (ROS), such as superoxide anions, hydroxyl radicals, and hydrogen peroxide. Moreover, Imran et al. (2023), in a comprehensive review of polyphenolic antiox-

idants, emphasized that Naringenin modulates key oxidative stress-related signaling pathways, such as Nrf2 and MAPK, which contribute to its cytoprotective and chemopreventive effects [2].

A related mechanistic analysis by Zygmunt K., (2010) also highlighted that Naringenin's antioxidant effects involve the upregulation of endogenous antioxidant enzymes, including superoxide dismutase (SOD), catalase, and glutathione peroxidase, providing further evidence of its potential in counteracting oxidative neuronal damage [3].

Together, these findings consolidate the view that Naringenin acts not only as a direct free radical scavenger but also as a regulator of intracellular antioxidant systems, offering promising neuroprotective potential in oxidative stress-related diseases such as Parkinson's disease.

2. Reduction of Lipid Peroxidation:

Naringenin has been demonstrated to reduce lipid peroxidation, a process that results in the formation of harmful lipid peroxides and contributes to oxidative damage in cells. By inhibiting lipid peroxidation, Naringenin protects cell membranes from oxidative stress.

Cavia-Saiz et al. (2010) showed that Naringenin, compared to its glycosylated analogue naringin, offers stronger protection against lipid oxidation through radical scavenging and xanthine oxidase inhibition [4].

In a study on streptozotocin-induced hepatic oxidative stress, Rashmi et al. (2018) observed that oral administration of Naringenin significantly reduced thiobarbituric acid reactive substances (TBARS) and hydroperoxides, indicating effective suppression of lipid peroxidation in vivo [5].

Al-Amer et al. (2023) reported similar findings in renal tissues, where Naringenin in combination with coconut water and Arabic gum markedly lowered malondialdehyde (MDA) levels, a standard marker of lipid peroxidation, thereby ameliorating gentamicin-induced nephrotoxicity [6].

In a more recent in vivo rodent model, Jian Gao et al. (2024) confirmed that Naringenin administration significantly mitigated lipid peroxidation in brain tissue under oxidative stress, further substantiating its neuroprotective and membrane-stabilizing effects [7].

Collectively, these findings strongly support Naringenin's lipid peroxidation-reducing capabilities across multiple organ systems and models, validating its potential as a protective agent in oxidative stress-related pathologies.

3. Enzyme Modulation:

Naringenin has been shown to modulate a variety of enzymes, contributing to its wide-ranging therapeutic effects. In particular, Naringenin affects key enzymes involved in oxidative stress, inflammation, and metabolic pathways. For instance, a study by Calderaro et al. (2022) highlighted that Naringenin significantly inhib-

its the activity of pro-inflammatory enzymes such as cyclooxygenase (COX) and lipoxygenase (LOX), both of which are critical in the development of inflammation and associated diseases. The authors noted that this modulation helps reduce inflammatory markers and oxidative stress, reinforcing Naringenin's role as a natural anti-inflammatory agent [8].

Similarly, another study by Rabia Naz et al. (2021) demonstrated that Naringenin enhances the activity of antioxidant enzymes, such as superoxide dismutase (SOD) and catalase (CAT), while inhibiting the expression of enzymes involved in lipid peroxidation. This dual effect suggests Naringenin's potential as a powerful antioxidant, capable of protecting cellular structures from oxidative damage [9].

Additionally, Naringenin has been shown to regulate enzymes involved in drug metabolism, notably cytochrome P450 enzymes. According to a study by Wang et al. (2024), Naringenin interacts with CYP450 enzymes to influence the metabolism of various drugs, which has important implications for its pharmacokinetics and potential drug interactions [10].

These studies collectively underline the diverse enzyme-modulating properties of Naringenin, supporting its potential as a therapeutic agent in various oxidative stress-related and inflammatory diseases, as well as its relevance in pharmacological applications.

4. Regulation of the Nrf2 Pathway:

Naringenin, a flavonoid with potent antioxidant properties, has been widely studied for its role in regulating the Nrf2 (nuclear factor erythroid 2-related factor 2) signaling pathway, which plays a crucial role in the cellular defense against oxidative stress. Several studies have highlighted that Naringenin activates the Nrf2 pathway, leading to the upregulation of genes responsible for antioxidant enzyme production and detoxification processes.

In a study by Zhang et al. (2022), Naringenin was shown to significantly activate the Nrf2/ARE (antioxidant response element) signaling pathway in human hepatocellular carcinoma cells, enhancing the expression of critical antioxidant enzymes such as heme oxygenase-1 (HO-1) and NAD(P)H dehydrogenase [quinone] 1 (NQO1). The authors concluded that Naringenin's modulation of the Nrf2 pathway contributes to its protective effects against oxidative stress and cellular damage [11].

Similarly, Xu et al. (2023) demonstrated that Naringenin activates Nrf2 in human cardiomyocytes, resulting in increased levels of antioxidant enzymes, thereby reducing inflammation and protecting cells from oxidative damage. Their findings suggest that Naringenin's role in Nrf2 activation is critical for maintaining cellular homeostasis under stress conditions [12].

Furthermore, in a study conducted by Li et al. (2023), it was found that Naringenin not only activates Nrf2 but also enhances the Nrf2-mediated transcription of

genes involved in phase II detoxification, offering protection against environmental toxins. This activation is considered a vital mechanism through which Naringenin exerts its neuroprotective and anti-inflammatory effects [13].

Additionally, Naringenin's activation of Nrf2 has been linked to its immunomodulatory properties. A study by Xiong et al. (2021) confirmed that Naringenin activates Nrf2 to suppress the NF-κB pathway, leading to reduced production of pro-inflammatory cytokines. This mechanism is thought to contribute to Naringenin's effectiveness in inflammatory diseases and conditions associated with chronic oxidative stress [14].

Finally, Naringenin's regulation of the Nrf2 pathway has been shown to support its therapeutic potential in neurodegenerative diseases. In an overview by Zgorzynska et al. (2021), Naringenin was found to enhance the Nrf2 pathway in neuronal cells, promoting neuroprotection against oxidative damage and reducing neuroinflammation, which are key processes in diseases such as Alzheimer's and Parkinson's disease [15].

5. Inhibition of Oxidative Stress-Induced Apoptosis:

Naringenin has garnered attention for its ability to inhibit apoptosis induced by oxidative stress, a key mechanism involved in the pathogenesis of various diseases, including neurodegenerative and cardiovascular conditions. Numerous studies have demonstrated that Naringenin exerts protective effects by modulating apoptotic pathways triggered by oxidative damage.

In a study by Shi et al. (2024), Naringenin was shown to reduce oxidative stress and inhibit apoptosis in human hepatocytes exposed to hydrogen peroxide (H_2O_2). The authors found that Naringenin significantly upregulated the expression of anti-apoptotic proteins such as Bcl-2 while downregulating pro-apoptotic proteins like Bax, thereby suppressing the apoptotic cascade [16].

Similarly, a study by Yu et al. (2019) demonstrated that Naringenin inhibits oxidative stress-induced apoptosis in myocardial cells. The authors reported that Naringenin mitigated the activation of caspase-3 and reduced the expression of cytochrome C, both of which are critical markers of apoptosis. This suggests that Naringenin's anti-apoptotic effects extend to cardiovascular tissues as well [17].

Further research by Shin et al. (2024) supported these findings by showing that Naringenin inhibits apoptosis in neuronal cells subjected to oxidative stress. Their results demonstrated that Naringenin reduced levels of reactive oxygen species (ROS) and regulated the expression of apoptotic proteins in favor of cell survival. This suggests Naringenin's potential in preventing neurodegeneration, especially in conditions like Alzheimer's disease [18].

Additionally, a study by Zhang et al. (2017) examined the neuroprotective effects of Naringenin. They observed that Naringenin effectively decreased oxidative stress-induced apoptosis in dopaminergic neurons, which could be attributed

to its ability to activate Nrf2, a key regulator of antioxidant defenses. This further highlights the protective role of Naringenin in Parkinson's disease [19].

Moreover, Naringenin has been shown to exert its anti-apoptotic effects through multiple signaling pathways. In a study by Khajepour et al. (2024), Naringenin was found to suppress apoptosis by modulating the PI3K/Akt signaling pathway, which is crucial for cell survival and proliferation. By enhancing this pathway, Naringenin prevented cell death induced by oxidative stress in human dopaminergic cells [20,21].

Together, these studies reinforce the significant role of Naringenin in inhibiting oxidative stress-induced apoptosis, emphasizing its therapeutic potential for conditions involving excessive oxidative damage and apoptosis, such as neurodegenerative diseases, cardiovascular diseases, and renal disorders.

The mechanisms of action and Naringenin's biological relevances summarize in Table 1. This table highlights the multiple antioxidant mechanisms by which Naringenin exerts its protective effects on cells, making it a valuable compound in combating oxidative stress-related diseases.

Table 1.

Antioxidant effects of Naringenin and its biological role

Effect	Mechanism	Biological relevance
1. Free Radical Scavenging	Naringenin donates electrons to neutralize free radicals such as hydroxyl radicals and superoxide anions	Prevents cellular damage from reactive oxygen species (ROS) in various tissues, including brain and liver
2. Reduction of Lipid Peroxidation	Naringenin inhibits the oxidation of lipids, which prevents the formation of harmful lipid peroxides	Protects cell membranes from oxidative damage, which is particularly important in neurodegenerative diseases
3. Enzyme Modulation	Naringenin modulates antioxidant enzymes like superoxide dismutase (SOD), catalase, and glutathione peroxidase	Enhances the detoxification of ROS, supporting cellular defense mechanisms in oxidative stress
4. Regulation of the Nrf2 Pathway	Naringenin activates the Nrf2/ARE pathway, increasing the expression of antioxidant genes	Strengthens the cellular antioxidant response and increases the defense against oxidative damage in cells
5. Inhibition of Oxidative Stress-Induced Apoptosis	Reduces apoptosis by decreasing ROS levels and regulating signaling pathways involved in cell survival	Prevents cell death and maintains cellular integrity in various cell types such as hepatocytes and neurons.

In summary, Naringenin's chemical structure with hydroxyl groups in key positions allows it to function effectively as an antioxidant. Its ability to neutralize

free radicals, reduce lipid peroxidation, modulate antioxidant enzymes, and activate the Nrf2 pathway highlights its potential as a therapeutic agent for conditions associated with oxidative stress, including neurodegenerative diseases such PD.

1.2 Overview of Proteins 1P5F and 3LFN

1.2.1. Functions and biological relevance of target proteins

Protein with PDB ID 1P5F is DJ-1, encoded by the PARK7 gene, is a multifunctional protein critically implicated in cellular defense mechanisms against oxidative stress and in the pathogenesis of Parkinson's disease (PD). Initially identified as an oncogene product, DJ-1 was later found to be associated with autosomal recessive early-onset PD, particularly through loss-of-function mutations in the PARK7 gene encoding DJ-1 [22].

Functionally, DJ-1 operates as an oxidative stress sensor, redox-sensitive chaperone, and transcriptional regulator. It undergoes specific oxidation at cysteine residue 106 (Cys106), which is essential for its protective activity. Mutation or overoxidation at this site impairs its function and contributes to neurodegeneration [23].

Furthermore, DJ-1 modulates the activity of antioxidant response genes, partially via regulation of the Nrf2 pathway, thereby maintaining redox homeostasis [24].

Structurally, DJ-1 forms a homodimer and exhibits a characteristic α/β-fold, which is important for its enzymatic and protective roles. The crystal structure of 1P5F reveals this dimeric configuration, with the oxidized Cys106 located at a structurally significant site, supporting its redox-based activity [25].

In addition to its antioxidant properties, DJ-1 influences mitochondrial integrity and dynamics, a critical factor in the survival of dopaminergic neurons. Loss of DJ-1 function results in increased mitochondrial fragmentation, reduced membrane potential, and heightened vulnerability to apoptosis [26].

The clinical relevance of DJ-1 in PD is further supported by findings in the Norwegian medical literature, which highlights the role of PARK7 mutations among other genetic contributors to early-onset Parkinson's disease, underscoring its diagnostic and therapeutic potential [27].

Together, these findings establish DJ-1 (1P5F) as a neuroprotective protein that mitigates oxidative damage, maintains mitochondrial function, and suppresses apoptotic pathways —functions highly relevant to the pathophysiology and potential treatment strategies for Parkinson's disease.

Molecular docking studies have elucidated a range of ligands capable of binding to DJ-1 (1P5F), revealing promising avenues for therapeutic modulation of its neuroprotective function. In a flexible docking analysis, Aldakhil et al. (2025) identified three pharmacological agents — droxicam, pteroylglutamic acid, and niraparib — as potential DJ-1 ligands. These molecules exhibited strong bind-

ing affinities, particularly through interactions with key residues such as Cys106, Glu18, Asn76, and Gly75, suggesting a capacity to modulate DJ-1's function under oxidative stress conditions [28].

Complementary fragment-based screening approaches further highlighted isatin as a covalent ligand targeting the Cys106 site. Subsequent optimization led to analogs with improved DJ-1 affinity, reinforcing the therapeutic potential of small molecules targeting DJ-1's redox-sensitive region [29].

In parallel, phytochemical screening by Vijayakumar and colleagues (2021) revealed punicagluconin, a plant-derived polyphenol, as a candidate ligand exhibiting substantial docking scores with DJ-1. This natural compound displayed stabilizing interactions within the protein's active site, aligning with its documented antioxidant capacity [30].

Importantly, Kitamura et al. (2011) demonstrated that compound-23, a rationally designed synthetic ligand, not only bound to DJ-1 with high affinity but also conferred dopaminergic neuroprotection in Parkinsonian models, suggesting its utility in disease modification [31].

These findings collectively underscore the structural and functional plasticity of 1P5F (DJ-1), supporting the feasibility of ligand-based therapeutic strategies targeting 1P5F in neurodegenerative disease contexts.

Ptotein with PDB ID 3LFN, known as CDK2, is a serine/threonine kinase primarily involved in cell cycle control, particularly in driving the transition from G1 to S phase in proliferating cells. While neurons are post-mitotic and do not typically undergo cell division, some studies suggest that aberrant activation of CDK2 or other cyclin-dependent kinases (CDKs) can lead to neuronal apoptosis. Oxidative stress and mitochondrial dysfunction, both hallmarks of PD, may trigger abnormal cell cycle re-entry in neurons, leading to neurodegenerative processes [32].

F. J. Diaz-Corrales et al. (2008) indicates that exposure to dopamine can upregulate CDK2 and cyclin E in dopaminergic neurons, leading to centrosome amplification and subsequent cell death. Inhibiting CDK2 activity in these models reduced neuronal death, suggesting a direct role of CDK2 in dopaminergic neuron degeneration. Further investigation is needed to clarify its role in PD pathology [33, 34].

By targeting both 1P5F (DJ-1) and 3LFN (CDK2), Naringenin may exert neuroprotective effects by enhancing antioxidant defenses and modulating cell survival pathways. Molecular docking analysis of Naringenin with these proteins can help elucidate its potential role in neuroprotection and Parkinson's disease therapy.

1.2.2. Potential role of 3LFN and 1P5F in antioxidant-related pathways

Both 3LFN (CDK2) and 1P5F (DJ-1) have been implicated in neuronal signaling, particularly in synaptic plasticity, which is essential for memory and learning.

Oxidative stress plays a central role in neurodegenerative disorders such as Parkinson's disease (PD). The accumulation of reactive oxygen species (ROS) leads to mitochondrial dysfunction, neuronal apoptosis, and progressive neurodegeneration. DJ-1 (1P5F) is a well-established antioxidant protein, whereas CDK2 (3LFN) has an indirect role in oxidative stress responses, particularly in apoptosis regulation.

DJ-1, encoded by the PARK7 gene, is a crucial regulator of cellular redox homeostasis, mitochondrial function, and neuronal survival. It exerts its antioxidant effects through multiple mechanisms:

- Nrf2 stabilization: DJ-1 protects nuclear factor erythroid 2-related factor 2 (Nrf2) from degradation by the KEAP1-CUL3 ubiquitin ligase complex, thereby promoting the transcription of antioxidant enzymes such as superoxide dismutase (SOD), catalase, glutathione peroxidase, and heme oxygenase-1 (HO-1).
- ROS scavenging: DJ-1 undergoes oxidation at Cys106, which enhances its function as a redox sensor and contributes to direct ROS neutralization.
- Mitochondrial protection: DJ-1 helps regulate mitochondrial dynamics, reducing oxidative stress-induced mitochondrial damage and preventing neuronal apoptosis.
- Neuroprotection: DJ-1 mutations have been linked to early-onset familial Parkinson's disease, leading to a loss of antioxidant protection and increased neurodegeneration.

Given its critical role in oxidative stress defense, targeting DJ-1 with small molecules like Naringenin may enhance endogenous antioxidant mechanisms and protect dopaminergic neurons in PD.

Cyclin-dependent kinase 2 (CDK2) is primarily known for its role in cell cycle progression, particularly in the G1 to S phase transition. While it is not directly involved in antioxidant defense, some studies suggest an indirect role in oxidative stress-induced neuronal apoptosis:

- Oxidative Stress and Aberrant Cell Cycle Re-Entry: Post-mitotic neurons do not typically divide, but under oxidative stress conditions, aberrant activation of CDK2 can trigger cell cycle re-entry, leading to apoptosis instead of proliferation.
- Regulation of Apoptosis: CDK2 interacts with transcription factors such as p53 and FoxO, which are involved in oxidative stress-induced cell death pathways.
- Mitochondrial Dysfunction: Dysregulated CDK2 activity has been linked to increased mitochondrial oxidative stress, which can contribute to neurodegeneration.

Although CDK5 is more directly linked to neuronal oxidative stress and neurodegeneration, CDK2 may still contribute to oxidative damage through its involvement in apoptotic signaling and aberrant cell cycle activation in neurons.

Given these mechanisms, **Naringenin may exert neuroprotective effects by targeting DJ-1 and CDK2** in complementary ways:

Enhancing DJ-1 function could promote antioxidant gene expression and mitochondrial protection, helping reduce oxidative stress in neurons.

Modulating CDK2 activity may help regulate oxidative stress-induced apoptotic pathways, potentially preventing neuronal loss.

Molecular docking analysis of Naringenin with DJ-1 and CDK2 could provide valuable insights into its potential therapeutic role in oxidative stress regulation and Parkinson's disease.

2. Materials and Methods

2.1.1. Preparation of Naringenin Structure

The three-dimensional (3D) structure of Naringenin was constructed using ChemDraw software. After drawing the two-dimensional (2D) structure, it was converted into a 3D conformation using Chem3D. The optimized structure was then saved in Protein Data Bank (.pdb) format for further computational studies.

2.1.2. Retrieval and Preparation of Protein Structures

The 3D crystal structures of CDK2 (PDB ID: 3LFN) and DJ-1 (PDB ID: 1P5F) were retrieved from the Protein Data Bank (PDB). Each protein structure was processed and refined before molecular docking using the two steps: protein cleaning and protein optimization.

The retrieved PDB files were opened in Chimera (www.cgl.ucsf.edu/chimera), where unnecessary molecules such as water molecules, ligands, and other non-protein components were removed to ensure a clean docking environment.

To improve the accuracy of docking, each protein structure was energy-minimized using the Amber99 force field in Chimera. This step helped to remove steric clashes and optimize the structural conformation for better docking performance.

2.1.3. Molecular Docking

Molecular docking studies were performed to evaluate the interaction between Naringenin and the target proteins (3LFN and 1P5F). The docking procedure was carried out individually for each protein-ligand complex.

The prepared Naringenin (.pdb) structure was set as the ligand, while the optimized 3LFN and 1P5F structures were used as the receptor proteins. The docking was conducted using AutoDock or another suitable molecular docking tool, which calculated the binding affinity and predicted the most favorable conformations of the Naringenin-protein complexes. The docking results, including binding energy values, hydrogen bond interactions, and molecular conformations, were analyzed to determine the strength and stability of the interactions.

2.1.4. Visualization and Analysis of Docking Results

The docking results were visualized and analyzed using Biovia Discovery Studio 4.5 and Molegro Molecular Viewer 2.5. These visualization tools allowed for:

- Identification of binding sites and interaction types (hydrogen bonds, hydrophobic interactions, etc.).
- Analysis of molecular conformations, including ligand positioning within the active site of each protein.
- Comparison of docking scores and interaction profiles between Naringenin and the two target proteins (3LFN and 1P5F).

This workflow ensured that Naringenin and the selected proteins were properly prepared, optimized, and analyzed for docking interactions. The results of the docking study provided insights into the potential molecular interactions of Naringenin with crystal structures of CDK2 and DJ-1, contributing to a better understanding of its biological significance and potential antioxidant activity in cellular pathways.

2.2 Molecular Docking Approach

2.2.1. Docking software

To study the molecular interactions between Naringenin and the target proteins CDK2 (PDB ID: 3LFN) and DJ-1 (PDB ID: 1P5F), docking simulations were conducted using AutoDock Vina (MGL tools – 1.5.6). The docking procedure was carried out in the following steps:

1. Preparation of Ligand (Naringenin) for Docking

The 3D structure of Naringenin was built using ChemDraw and Chem3D, then saved in .pdb format.

The ligand structure was converted to PDB format using AutoDock Tools (ADT).

Non-polar hydrogens were merged, torsional flexibility was assigned, and the molecule was set as a flexible ligand to allow conformational adjustments during docking.

2. Preparation of Protein Structures (3LFN and 1P5F)

The 3LFN and 1P5F protein structures were obtained from the Protein Data Bank (PDB). Using Chimera, unnecessary molecules (water, ions, and non-relevant ligands) were removed. Energy minimization was performed using the Amber99 force field to refine protein structures. Proteins were converted to PDB format in AutoDock Tools

2.2.2. Parameters and grid settings used for docking

The docking grid box was set to encompass both the ligand and the entire receptor protein, ensuring that Naringenin could explore all possible binding sites rather than being restricted to a predefined active site. The grid dimensions were optimized to fully enclose the receptor, allowing AutoDock Vina to predict potential binding interactions in an unbiased manner.

Docking simulations were executed using AutoDock Vina via the command line. The software generated multiple ligand poses, ranking them based on binding energy (kcal/mol). The conformation with the lowest binding energy was selected as the most stable interaction.

2.2.3. Analysis and Visualization of Docking Results

The docking results were analyzed based on binding affinity scores (lower values indicating stronger interactions). Biovia Discovery Studio and Molegro Molecular Viewer were used to visualize key interactions, such as:

– Hydrogen bonding between Naringenin and amino acid residues.
– Hydrophobic and electrostatic interactions stabilizing the complex.
– Optimal positioning of Naringenin within the receptor.

By allowing Naringenin to explore the entire receptor surface, AutoDock Vina provided a comprehensive analysis of possible binding interactions.

3. Results and Discussion

3.1.1. Docking results

Molecular docking simulations were conducted to evaluate the interaction between Naringenin and the target proteins CDK2 (PDB ID: 3LFN) and DJ-1 (PDB ID: 1P5F). A total of five independent docking sessions were performed to ensure reproducibility and reliability of the binding results. The average docking score obtained from these sessions was -8.4 for Naringenin-3LFN complex and –6.3 for Naringenin-1P5F. This docking score represents the binding free energy of the Naringenin-protein complex, where more negative values indicate stronger and more favorable binding (*See Figure 3 and Figure 4*).

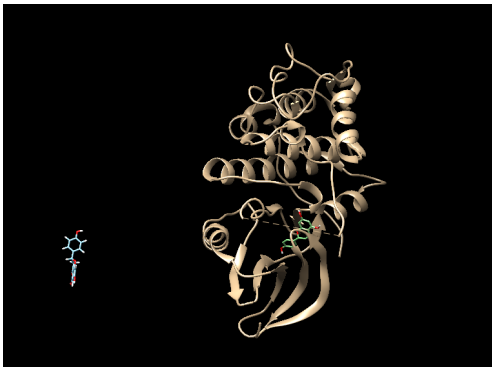

Figure 3. *Naringenin-3LFN after docking sessions. Average score (energy) value –8.4*

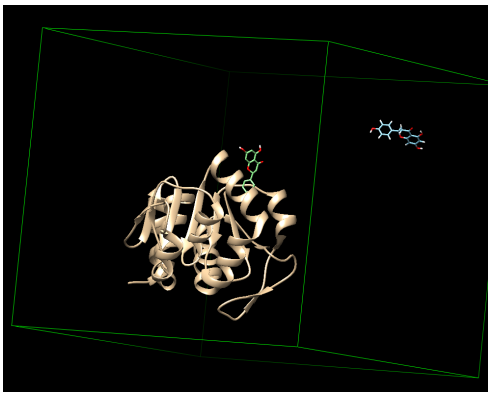

Figure 4. *Naringenin-1P5F after docking sessions. Average score (energy) value –6.3*

A score of -8.4 suggests a high-affinity interaction, indicating that Naringenin forms a stable complex with the target proteins. In molecular docking studies, a binding energy below -6.0 (kcal/mol) is generally considered to reflect moderate binding affinity, while values lower than -7.0 (kcal/mol) indicate strong and potentially biologically relevant interactions. The obtained score of -8.4 (kcal/mol) further strengthens the hypothesis that Naringenin exhibits a strong interaction with both CDK2 and DJ-1, potentially influencing their biological functions. The favorable binding energy suggests that Naringenin may effectively interact with the binding "pocket" of these proteins through various non-covalent interactions such as hydrogen bonding, hydrophobic interactions, and van der Waals forces. This strong interaction supports the hypothesis that Naringenin could modulate the activity of these proteins, which may contribute to its antioxidant and neuroprotective properties.

In the following sections, we further analyze the specific binding interactions and molecular interactions contributing to this docking result.

3.1.2. Ranking of interactions and structural visualization of docked complexes

Molecular docking analysis of the Naringenin-3LFN complex revealed multiple non-covalent interactions, including Pi-Alkyl interactions, van der Waals forces, hydrogen bonding, and an unfavorable donor-donor interaction.

1. Pi-Alkyl Interactions

Pi-Alkyl interactions are important for hydrophobic stabilization of the ligand within the binding pocket. The following residues participated in these interactions: Leu 134, Val 18, Ala 31, and Ala 144. These residues contain hydrophobic alkyl chains, which can form weak dispersion forces with the aromatic system of

Naringenin, anchoring it in the binding site. Such interactions contribute to hydrophobic stabilization but do not define binding specificity (See Figure 5).

2. Van der Waals Interactions

Several residues were involved in van der Waals interactions with Naringenin: Val 64, Phe 80, Phe 82, Ile 10, Gly 11, Gln 131, Glu 12, Gly 13, Lys 129, Asp 127, Thr 14, Asp 145 These interactions provide additional stabilization by ensuring optimal molecular packing within the binding pocket. Aromatic residues (Phe 80, Phe 82) contribute to hydrophobic contacts, while flexible residues (Gly, Gln) allow conformational adaptability. The charged residues (Lys 129, Asp 127, Glu 12) may also influence ligand binding through electrostatic effects rather than vdW interactions alone.

3. Hydrogen Bonding Interaction

A single hydrogen bond was observed between Naringenin and Glu 81. The carboxylate ($-COO^-$) group of Glu 81 likely acts as a hydrogen bond acceptor, interacting with the hydroxyl (-OH) groups of Naringenin. This interaction helps stabilize the ligand within the binding site and may contribute to binding specificity.

4. Unfavorable Donor-Donor Interaction

One unfavorable donor-donor interaction was identified at Asn 132, where two hydrogen bond donor groups are positioned too closely, leading to steric and electrostatic repulsion. This interaction may introduce minor destabilization in the complex, but its overall impact is likely mitigated by the stabilizing forces discussed above.

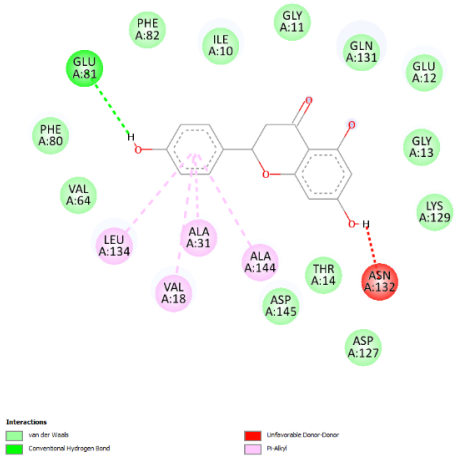

Figure 5. *Ligand map visualized by BIOVIA.*

The binding of Naringenin to 3LFN is stabilized by a combination of hydrophobic (Pi-Alkyl), van der Waals, and hydrogen bond interactions. The single donor-donor repulsion at Asn 132 suggests some structural constraints, but it does not significantly reduce the overall binding affinity. The presence of multiple stabilizing interactions supports the hypothesis that Naringenin forms a stable complex with 3LFN, potentially influencing its biological function.

To better understand the molecular interactions between Naringenin and 3LFN, the docked complex was visualized and analyzed using Biovia Discovery Studio (Figure 5). This software allows for detailed representation of binding interactions, including hydrogen bonds, van der Waals forces, hydrophobic contacts, and electrostatic interactions.

A Ligand Interaction Map (Ligand Map) was generated to illustrate all key non-covalent interactions between Naringenin and the active site of 3LFN. This diagram provides a comprehensive 2D representation of:

- Hydrophobic contacts, including Pi-Alkyl interactions at Leu 134, Val 18, Ala 31, and Ala 144.
- van der Waals interactions with residues Val 64, Phe 80, Phe 82, Ile 10, Gly 11, Gln 131, Glu 12, Gly 13, Lys 129, Asp 127, Thr 14, Asp 145.
- Hydrogen bonding between Naringenin and Glu 81, highlighting its role in ligand stabilization.
- Unfavorable donor-donor interaction at Asn 132, which may slightly reduce binding efficiency.

The visualization of the Naringenin-3LFN complex confirms the presence of multiple stabilizing interactions identified in docking analysis. The Ligand Interaction Map provides a clear overview of these interactions, demonstrating how Naringenin interacts with key residues to achieve strong binding affinity. These insights help validate the docking results and provide a structural basis for further molecular dynamics simulations.

Molecular docking analysis of the Naringenin-1P5F complex also revealed the following interactions *(See Figure 6)*:

1. Pi-Alkyl Interactions

The following residues participated in these two interactions: Ile 91, Arg 98.

2. Van der Waals Interactions

Asn 97, Gly 65, Glu 94, Lys 62, Val 70, Leu 7, Tyr 67, Gln 95, Pro 66.

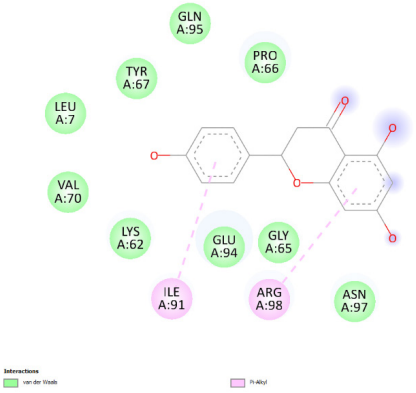

Figure 6. *Ligand map visualised by BIOVIA.*

The ligand map shows: active site of the complex and the non-covalent specificity of interactions.

3. Conclusions

This study presents evidence that naringenin exhibits promising binding activity with two proteins relevant to cellular stress response and regulatory pathways potentially implicated in Parkinson's disease: DJ-1 (PDB ID: 1P5F) and cyclin-dependent kinase 2 (PDB ID: 3LFN). Molecular docking simulations performed across five independent sessions showed that naringenin formed stable complexes with both proteins. The results indicate that Naringenin exhibits strong binding interactions with both 1P5F and 3LFN, with notable hydrogen bonding and hydrophobic interactions contributing to their stability.

Notably, naringenin displayed a stronger affinity for 3LFN, with an average docking score of –8.4, indicating robust and energetically favorable interactions. The interaction with 1P5F) was also significant, with an average docking score of –6.3, suggesting a moderate but relevant binding stability that could modulate the protein's protective role under oxidative stress.

While CDK2 is not traditionally classified among the canonical Parkinson's disease-related proteins, emerging research indicates its involvement in cell cycle regulation and neuronal apoptosis, which may indirectly intersect with neurodegenerative mechanisms. DJ-1, by contrast, is well established as a redox-sensitive chaperone involved in defending neurons against oxidative insults.

Taken together, these findings support the hypothesis that Naringenin may exert neuroprotective effects via multi-targeted mechanisms involving oxidative stress regulation and apoptosis modulation. Its consistent docking performance

highlights its potential as a candidate molecule for further investigation in the context of Parkinson's disease.

Future experimental validation in cellular and in vivo models is essential to assess the pharmacological relevance and therapeutic applicability of these interactions.

References

1. Shahab, S., Kumar, R., Sheikhi, M., Ihnatovich, Z., Siniutsich, J., Koroleva, Statsi, M., Borzehandani, M. Y. Synthesis, modeling, bioactivity, docking, binding energy analysis of new effective piperazine derivatives as effective drug candidates for treatment of Parkinson's disease. // Analytical Chemistry Letters. – 2024 – Vol. 14(5), 638–653. https://doi.org/10.1080/22297928.2024.2397798

2. Imran M., Insaf A., Hasan N., Sugandhi V.V., Shrestha D., Paudel K.R., Jha S.K., Hansbro P.M., Dua K., Devkota H.P., Mohammed Y. Exploring the Remarkable Chemotherapeutic Potential of Polyphenolic Antioxidants in Battling Various Forms of Cancer // Molecules. — 2023. — Vol. 28, № 8. — P. 3475. — DOI: 10.3390/molecules28083475.

3. Zygmunt K, Faubert B, MacNeil J, Tsiani E. Naringenin, a citrus flavonoid, increases muscle cell glucose uptake via AMPK. Biochem Biophys Res Commun. 2010 Jul 23;398(2):178-83. doi: 10.1016/j.bbrc.2010.06.048. Epub 2010 Jun 15. PMID: 20558145.

4. Cavia-Saiz M, Busto MD, Pilar-Izquierdo MC, Ortega N, Perez-Mateos M, Muñiz P. Antioxidant properties, radical scavenging activity and biomolecule protection capacity of flavonoid naringenin and its glycoside naringin: a comparative study. J Sci Food Agric. 2010 May;90(7):1238-44. doi: 10.1002/jsfa.3959. PMID: 20394007.

5. Rashmi R, Bojan Magesh S, Mohanram Ramkumar K, Suryanarayanan S, Venkata SubbaRao M. Antioxidant Potential of Naringenin Helps to Protect Liver Tissue from Streptozotocin-Induced Damage. Rep Biochem Mol Biol. 2018 Oct;7(1):76-84. PMID: 30324121; PMCID: PMC6175592.

6. Al-Amer HA, Al-Sowayan NS, Alfheeaid HA, Althwab SA, Alrobaish SA, Hamad EM, Musa KH, Mousa HM. Oral administration of naringenin and a mixture of coconut water and Arabic gum attenuate oxidative stress and lipid peroxidation in gentamicin-induced nephrotoxicity in rats. Eur Rev Med Pharmacol Sci. 2023 Nov;27(21):10427-10437. doi: 10.26355/eurrev_202311_34317. PMID: 37975366.

7. Gao J, Yuan L, Jiang H, Li G, Zhang Y, Zhou R, Xian W, Zou Y, Du Q, Zhou X. Naringenin modulates oxidative stress and lipid metabolism: Insights from network pharmacology, mendelian randomization, and molecular docking. Front

Pharmacol. 2024 Oct 15;15:1448308. doi: 10.3389/fphar.2024.1448308. PMID: 39474612; PMCID: PMC11518751.

8. Calderaro A, Patanè GT, Tellone E, Barreca D, Ficarra S, Misiti F, Laganà G. The Neuroprotective Potentiality of Flavonoids on Alzheimer's Disease. Int J Mol Sci. 2022 Nov 27;23(23):14835. doi: 10.3390/ijms232314835. PMID: 36499159; PMCID: PMC9736131

9. Naz R, Saqib F, Awadallah S, Wahid M, Latif MF, Iqbal I, Mubarak MS. Food Polyphenols and Type II Diabetes Mellitus: Pharmacology and Mechanisms. Molecules. 2023 May 10;28(10):3996. doi: 10.3390/molecules28103996. PMID: 37241737; PMCID: PMC10222362.

10.Wang D, Zhou Y, Hua L, Hu M, Zhu N, Liu Y, Zhou Y. The role of the natural compound naringenin in AMPK-mitochondria modulation and colorectal cancer inhibition. Phytomedicine. 2024 Aug;131:155786. doi: 10.1016/j.phymed.2024.155786. Epub 2024 May 28. PMID: 38875812.

11.Zhang B, Wan S, Liu H, Qiu Q, Chen H, Chen Z, Wang L, Liu X. Naringenin Alleviates Renal Ischemia Reperfusion Injury by Suppressing ER Stress-Induced Pyroptosis and Apoptosis through Activating Nrf2/HO-1 Signaling Pathway. Oxid Med Cell Longev. 2022 Oct 10;2022:5992436. doi: 10.1155/2022/5992436. PMID: 36262286; PMCID: PMC9576412.

12.Xu N, Liu S, Zhang Y, Chen Y, Zuo Y, Tan X, Liao B, Li P, Feng J. Oxidative stress signaling in the pathogenesis of diabetic cardiomyopathy and the potential therapeutic role of antioxidant naringenin. Redox Rep. 2023 Dec;28(1):2246720. doi: 10.1080/13510002.2023.2246720. Epub 2023 Sep 25. PMID: 37747066; PMCID: PMC10538464.

13.Li J, Mao B, Tang X, Zhang Q, Zhao J, Zhang H, Cui S. Protective Effects of Naringenin and Apigenin in Ameliorating Skin Damage via Mediating the Nrf2 and NF-κB Pathways in Mice. Foods. 2023 May 24;12(11):2120. doi: 10.3390/foods12112120. PMID: 37297362; PMCID: PMC10252862.

14.Xiong H, Chen Z, Lin B, Xie B, Liu X, Chen C, Li Z, Jia Y, Wu Z, Yang M, Jia Y, Wang L, Zhou J and Meng X (2022) Naringenin Regulates FKBP4/NR3C1/NRF2 Axis in Autophagy and Proliferation of Breast Cancer and Differentiation and Maturation of Dendritic Cell. Front. Immunol. 12:745111. doi: 10.3389/fimmu.2021.745111.

15.Zgorzynska E, Dziedzic B, Walczewska A. An Overview of the Nrf2/ARE Pathway and Its Role in Neurodegenerative Diseases. Int J Mol Sci. 2021 Sep 4;22(17):9592. doi: 10.3390/ijms22179592. PMID: 34502501; PMCID: PMC8431732.

16.Shi Y, Gao Z, Xu B, Mao J, Wang Y, Liu Z and Wang J (2024) Protective effect of naringenin on cadmium chloride-induced renal injury via alleviating oxidative stress, endoplasmic reticulum stress, and autophagy in chickens. Front. Pharmacol. 15:1440877. doi: 10.3389/fphar.2024.1440877.

17. Yu LM, Dong X, Zhang J, Li Z, Xue XD, Wu HJ, Yang ZL, Yang Y, Wang HS. Naringenin Attenuates Myocardial Ischemia-Reperfusion Injury via cGMP-PKGIα Signaling and In Vivo and In Vitro Studies. Oxid Med Cell Longev. 2019 Jan 8;2019:7670854. doi: 10.1155/2019/7670854. PMID: 30728891; PMCID: PMC6341255.

18. Torkzadeh-Mahani M., Barati M., Yousefi M., Safari Z., Gholizadeh-Moghaddam H., Amini-Khoei H. Naringenin modulates Nrf2 and NF-κB pathways to alleviate neuroinflammation in a mouse model of multiple sclerosis // Frontiers in Immunology. — 2021. — Vol. 12. — Article 745111.

19. Zhang Y, Liu B, Chen X, Zhang N, Li G, Zhang LH, Tan LY. Naringenin Ameliorates Behavioral Dysfunction and Neurological Deficits in a d-Galactose-Induced Aging Mouse Model Through Activation of PI3K/Akt/Nrf2 Pathway. Rejuvenation Res. 2017 Dec;20(6):462-472. doi: 10.1089/rej.2017.1960. Epub 2017 Jul 24. PMID: 28622086.

20. Khajepour, Z., Reiszadeh Jahromi, S., Dabiri, S., & Esmaeili-Mahani, S. (2024). Protective effects of naringenin against methamphetamine-induced cell death in dopaminergic SH-SY5Y cells. The American Journal of Drug and Alcohol Abuse, 50(6), 807–818. https://doi.org/10.1080/00952990.2024.2418900.

21. Long H-Z, Cheng Y, Zhou Z-W, Luo H-Y, Wen D-D and Gao L-C (2021) PI3K/AKT Signal Pathway: A Target of Natural Products in the Prevention and Treatment of Alzheimer's Disease and Parkinson's Disease. Front. Pharmacol. 12:648636. doi: 10.3389/fphar.2021.648636.

22. Bonifati V, Rizzu P, van Baren MJ, Schaap O, Breedveld GJ, Krieger E, Dekker MC, Squitieri F, Ibanez P, Joosse M, van Dongen JW, Vanacore N, van Swieten JC, Brice A, Meco G, van Duijn CM, Oostra BA, Heutink P. Mutations in the DJ-1 gene associated with autosomal recessive early-onset parkinsonism. Science. 2003 Jan 10;299(5604):256-9. doi: 10.1126/science.1077209. Epub 2002 Nov 21. PMID: 12446870.

23. Maria G. Macedo, Burcu Anar, Iraad F. Bronner, Milena Cannella, Ferdinando Squitieri, Vincenzo Bonifati, André Hoogeveen, Peter Heutink, Patrizia Rizzu, The DJ-1L166P mutant protein associated with early onset Parkinson's disease is unstable and forms higher-order protein complexes, Human Molecular Genetics, Volume 12, Issue 21, 1 November 2003, P. 2807–2816, https://doi.org/10.1093/hmg/ddg304.

24. Baulac S, LaVoie MJ, Strahle J, Schlossmacher MG, Xia W. Dimerization of Parkinson's disease-causing DJ-1 and formation of high molecular weight complexes in human brain. Mol Cell Neurosci. 2004 Nov;27(3):236-46. doi: 10.1016/j.mcn.2004.06.014. PMID: 15519239.

25. Görner K, Holtorf E, Odoy S, Nuscher B, Yamamoto A, Regula JT, Beyer K, Haass C, Kahle PJ. Differential effects of Parkinson's disease-associated

mutations on stability and folding of DJ-1. J Biol Chem. 2004 Feb 20;279(8):6943-51. doi: 10.1074/jbc.M309204200. Epub 2003 Nov 7. PMID: 14607841.

26.Junn E, Taniguchi H, Jeong BS, Zhao X, Ichijo H, Mouradian MM. Interaction of DJ-1 with Daxx inhibits apoptosis signal-regulating kinase 1 activity and cell death. Proc Natl Acad Sci U S A. 2005 Jul 5;102(27):9691-6. doi: 10.1073/pnas.0409635102. Epub 2005 Jun 27. PMID: 15983381; PMCID: PMC1172235.

27.Toft M. Genetikk ved Parkinsons sykdom // Tidsskrift for Den norske legeforening. — 2004. — Vol. 124, № 7. — P. 927–929.

28.Aldakhil, T., Altharawi, A. Drug Repurposing for the Discovery of Potential Inhibitors Targeting DJ-1 (PARK7) Against Parkinson's Disease. Crystals 2025, 15, 239. https://doi.org/10.3390/cryst15030239

29.Tashiro S, Caaveiro JMM, Nakakido M, Tanabe A, Nagatoishi S, Tamura Y, Matsuda N, Liu D, Hoang QQ, Tsumoto K. Discovery and Optimization of Inhibitors of the Parkinson's Disease Associated Protein DJ-1. ACS Chem Biol. 2018 Sep 21;13(9):2783-2793. doi: 10.1021/acschembio.8b00701. Epub 2018 Aug 15. PMID: 30063823; PMCID: PMC6370461.

30.Vijayakumar, S., Rajalakshmi, S. Exploring novel natural compound inhibitors for Parkinsonian receptor (DJ1) by homology modeling, molecular docking and MD simulations. Vegetos 34, 959–970 (2021). https://doi.org/10.1007/s42535-021-00263-5

31.Kitamura, Y., Watanabe, S., Taguchi, M. et al. Neuroprotective effect of a new DJ-1-binding compound against neurodegeneration in Parkinson's disease and stroke model rats. Mol Neurodegeneration 6, 48 (2011). https://doi.org/10.1186/1750-1326-6-48

32.Yu X, Caltagarone J, Smith MA, Bowser R. DNA damage induces cdk2 protein levels and histone H2B phosphorylation in SH-SY5Y neuroblastoma cells. J Alzheimers Dis. 2005 Sep;8(1):7-21. doi: 10.3233/jad-2005-8102. PMID: 16155345.

33.Diaz-Corrales, F.J., Asanuma, M., Miyazaki, I. et al. Dopamine induces supernumerary centrosomes and subsequent cell death through Cdk2 up-regulation in dopaminergic neuronal cells. neurotox res 14, 295–305 (2008). https://doi.org/10.1007/BF03033854

34.Statsi, M., Shahab, S. Myricetin as a perspective ligand for binding 3LFN protein of Parkinson's disease // Conference Paper. – May 2023.

DOI 10.34660/INF.2025.88.26.142

THE EFFECT OF TEMPERATURE ON THE SMOOTHNESS OF VERTICAL UPLIFTS AROUND JOINTS IN CEMENT-CONCRETE PAVED ROADS

Amirov Tursoat Jummaevich
PhD, Associate Professor
Tashkent State Transport University

Dauletov Madiyar Boranbaevich
Doctoral candidate
Tashkent State Transport University

Abstract. *This article analyzes the occurrence of slab uplift between cement-concrete road pavements during operation due to temperature effects. The main focus is on the temperature differentials that form in cement-concrete slabs under the influence of solar radiation, air temperature, and wind speed, as well as the resulting movements at compression and expansion joints.*

The following formulas were used in the work: The upper temperature T_{upper} and lower temperature T_{lower} of the cement-concrete pavement, the temperature difference ΔT, thermal expansion ΔL, angle of deflection θ, rise height δ, and International Roughness Index (IRI) were determined.

According to the analysis results, it has been determined that as the temperature difference increases, bending and lifting of the slabs are observed, which leads to an increase in the IRI indicator and a deterioration of road smoothness.

Keywords: *Smoothness, rises, joints, IRI, temperature, bending, road, deformation, expansion joint, slab.*

Introduction

The modernization of road transport infrastructure and the construction of modern, high-quality roads are among the priority areas of state policy in our republic. Specifically, the Resolution of the President of the Republic of Uzbekistan No. PP-111 dated January 25, 2022, “On Measures for Fundamental Reform of the Road Management Sector and Improvement of the Management System,” as well as Resolution No. PP-125 dated April 14, 2023, set forth tasks for creating high-quality and durable road surfaces and aligning road smoothness with international standards. In particular, the issues of widespread implementation of

cement-concrete pavements and ensuring their long-term operation are explicitly emphasized [1.2].

Cement-concrete pavement operates under complex stress conditions, subjected to repeated vehicle loads and variable temperature and moisture effects on the roadbed and pavement. Additionally, cement-concrete materials are characterized by internal stresses, which are caused by the heterogeneity of these materials' structure, as well as the continuous formation and destruction of an intersecting structure. Improving the resistance of road concrete to operational impacts is directly related to enhancing its physical-mechanical properties and structure [3,5].

Despite the high durability of cement-concrete road pavements, one of the problems encountered during their operation is vertical uplift between slabs. These uplifts are primarily associated with solar radiation, air temperature, surface temperature of the pavement, temperature of the pavement's lower layer, and the resulting temperature differential. This leads to the expansion of the slabs, causing their edges to rise upwards. This situation reduces the road's smoothness level and leads to a deterioration in the IRI (International Roughness Index) indicator [4].

This article analyzes the elevations that occur in cement concrete slabs due to temperature effects. This process is evaluated using the following mathematical models: determination of upper and lower temperatures, temperature difference, elevations at compression and expansion joints, thermal expansion, formation of inclination angle due to temperature effects, and IRI indicators.

In this scientific study, research was conducted on July 3, 2025, on the 439 km section of the A-380 "Guzar-Bukhara-Nukus-Beyneu" highway. The objective was to measure the effects of temperature-induced uplifts between cement-concrete road pavement slabs and their impact on smoothness. The temperature differences observed during the study are shown in Figure 1.

Figure 1. *Showing air temperature, surface temperature, and bottom temperature of the plate*

Research methodology

This article presents a calculation method used to assess changes in temperature-induced uplifts in cement-concrete pavement slabs. Based on the research, the temperature differences occurring on the upper and lower surfaces of the slab, thermal expansion, bending angle, and the International Roughness Index (IRI) indicator of road surface smoothness were studied using the following formulas.

Research findings

On the 439 km section of the A-380 "Guzar-Bukhara-Nukus-Beyneu" highway, we determined the temperature differences occurring on the upper and lower surfaces of the slab, thermal expansion, bending angle, compression and expansion of the slab due to temperature effects, as well as the IRI indicators of road surface smoothness (Fig. 2-12). We studied the impact of elevations at compression and expansion joints on longitudinal smoothness and presented it graphically (Fig. 9-12).

When we measure the temperature of the surface part of the cement-concrete pavement and its lower part, a temperature difference arises. We determined the expansion of the pavement due to this temperature difference using the following formula [6], as shown in Figures 2-4.

$$\boldsymbol{\Delta T} = T_{high\ temperature} - T_{low\ temperature} \qquad (1)$$

$$\Delta L = \alpha \cdot L \cdot \Delta T \qquad (2)$$

Here:

$T_{high\ temperature}$ - temperature of the surface layer of the cement concrete pavement, °C

$T_{low\ temperature}$ - temperature of the lower 25 centimeters of the cement concrete pavement, °C

α — the coefficient of thermal expansion for concrete

L — slab length, m

ΔT — temperature difference, °C

We determined the angle of bending of the slab using the following formula [7,8], which is based on the temperature difference between the surface and lower parts of the cement-concrete pavement. The results are shown in Figures 5-6.

$$\boldsymbol{\theta} \approx \frac{\boldsymbol{h \cdot \Delta T \cdot \alpha}}{\boldsymbol{2}} \qquad (3)$$

θ - angle of deflection of the cement-concrete pavement, radians

h - slab thickness, m

We determined the height of the cement concrete pavement rise due to temperature differences, and by calculating this rise height, we determined its influence on the longitudinal smoothness (IRI) at the compression joint using the following formula [7,8]. The results are presented in Figures 7-10.

$$\delta = \frac{\alpha \cdot \Delta T \cdot L^2}{8h} \qquad (4)$$

$$IRI \approx 2 \cdot \frac{\delta}{L} \cdot 1000 \qquad (5)$$

Here:

δ – height of the compression joint rise due to temperature influence, m

L – slab length, m

We determined the effect of expansion joint elevation on longitudinal smoothness (IRI) using the following formula [7,8], as shown in figures 11-12. This cal-

culation involved adding the elevation at the existing expansion joint to the elevation height of the compression joint in the cement concrete pavement (caused by temperature effects), and then subtracting this sum from the slab length.

$$IRI \approx 2 \cdot \frac{(\delta+\delta_1)}{L} \cdot 1000 \qquad (6)$$

Here:

δ_1 – rise height of the existing expansion joint, m

Here, the IRI is measured in m/km and indicates road smoothness. An increase in elevation raises the IRI value, which means that elevations at expansion joints lead to a deterioration in road smoothness.

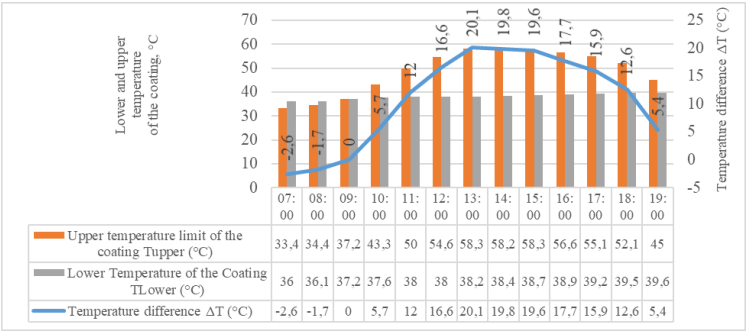

	07:00	08:00	09:00	10:00	11:00	12:00	13:00	14:00	15:00	16:00	17:00	18:00	19:00
Upper temperature limit of the coating Tupper (°C)	33,4	34,4	37,2	43,3	50	54,6	58,3	58,2	58,3	56,6	55,1	52,1	45
Lower Temperature of the Coating TLower (°C)	36	36,1	37,2	37,6	38	38	38,2	38,4	38,7	38,9	39,2	39,5	39,6
Temperature difference ΔT (°C)	-2,6	-1,7	0	5,7	12	16,6	20,1	19,8	19,6	17,7	15,9	12,6	5,4

Figure 2. *Graph for determining the daily temperature variation in cement concrete slabs*

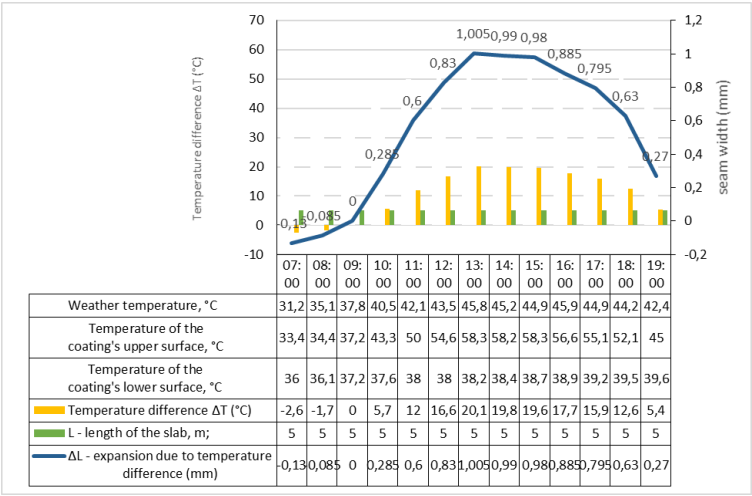

	07:00	08:00	09:00	10:00	11:00	12:00	13:00	14:00	15:00	16:00	17:00	18:00	19:00
Weather temperature, °C	31,2	35,1	37,8	40,5	42,1	43,5	45,8	45,2	44,9	45,9	44,9	44,2	42,4
Temperature of the coating's upper surface, °C	33,4	34,4	37,2	43,3	50	54,6	58,3	58,2	58,3	56,6	55,1	52,1	45
Temperature of the coating's lower surface, °C	36	36,1	37,2	37,6	38	38	38,2	38,4	38,7	38,9	39,2	39,5	39,6
Temperature difference ΔT (°C)	-2,6	-1,7	0	5,7	12	16,6	20,1	19,8	19,6	17,7	15,9	12,6	5,4
L - length of the slab, m;	5	5	5	5	5	5	5	5	5	5	5	5	5
ΔL - expansion due to temperature difference (mm)	-0,13	0,085	0	0,285	0,6	0,83	1,005	0,99	0,98	0,885	0,795	0,63	0,27

Figure 3. *Temperature-dependent expansion graph of cement-concrete pavement*

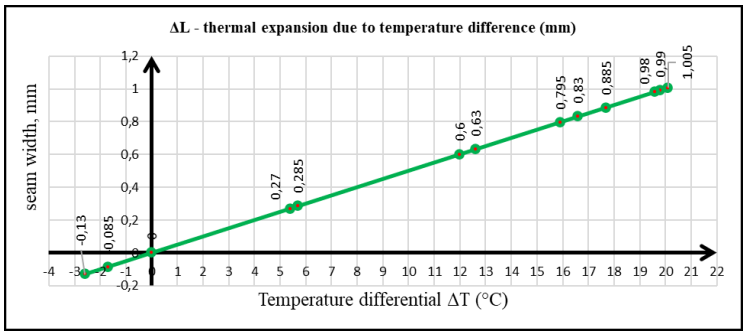

Figure 4. *Thermal expansion graph of cement-concrete pavement due to temperature differences*

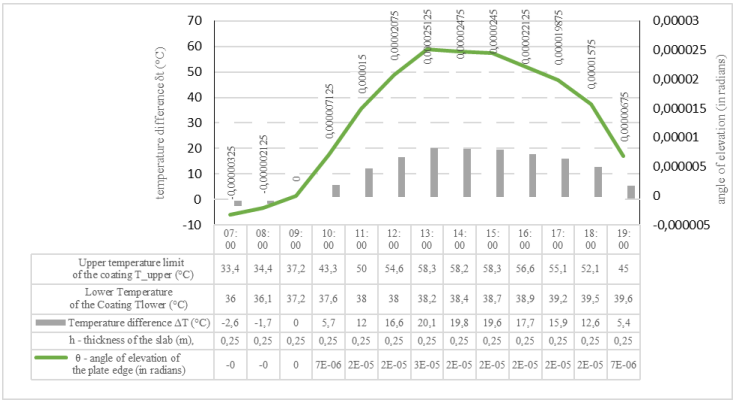

Figure 5. *Graph for determining the uplift angle of cement-concrete pavement due to temperature difference*

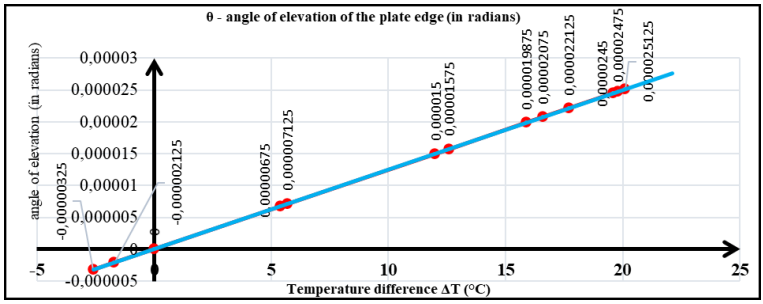

Figure 6. *Graph for determining the angle of elevation (in radians) of the slab edge depending on the temperature of the cement-concrete pavement*

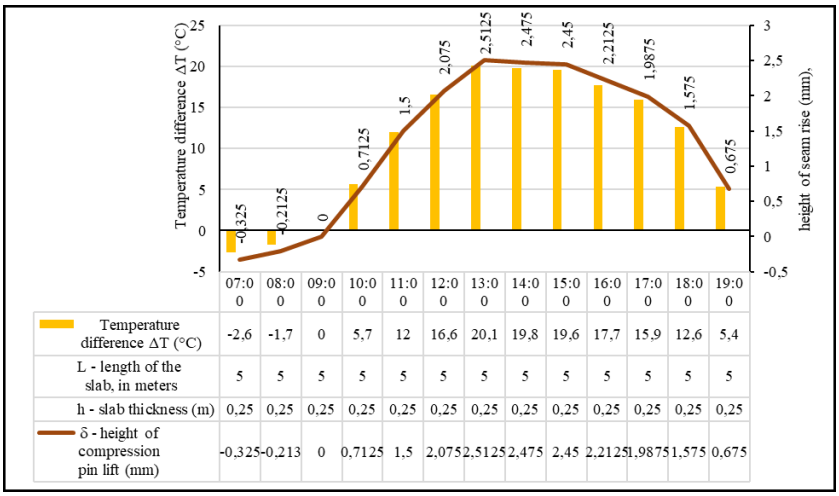

	07:00	08:00	09:00	10:00	11:00	12:00	13:00	14:00	15:00	16:00	17:00	18:00	19:00
Temperature difference ΔT (°C)	-2,6	-1,7	0	5,7	12	16,6	20,1	19,8	19,6	17,7	15,9	12,6	5,4
L - length of the slab, in meters	5	5	5	5	5	5	5	5	5	5	5	5	5
h - slab thickness (m)	0,25	0,25	0,25	0,25	0,25	0,25	0,25	0,25	0,25	0,25	0,25	0,25	0,25
δ - height of compression pin lift (mm)	-0,325	-0,213	0	0,7125	1,5	2,075	2,5125	2,475	2,45	2,2125	1,9875	1,575	0,675

Figure 7. *Graph showing the expansion of compression joints in cement-concrete pavement due to temperature effects*

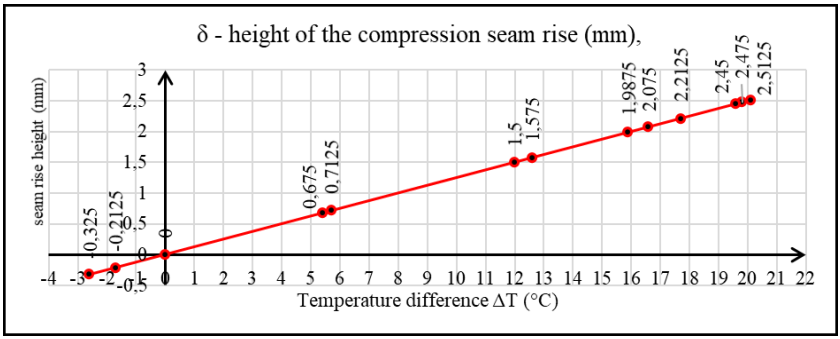

Figure 8. *Graph showing the relationship between temperature and the rise of compression joints in cement-concrete pavement*

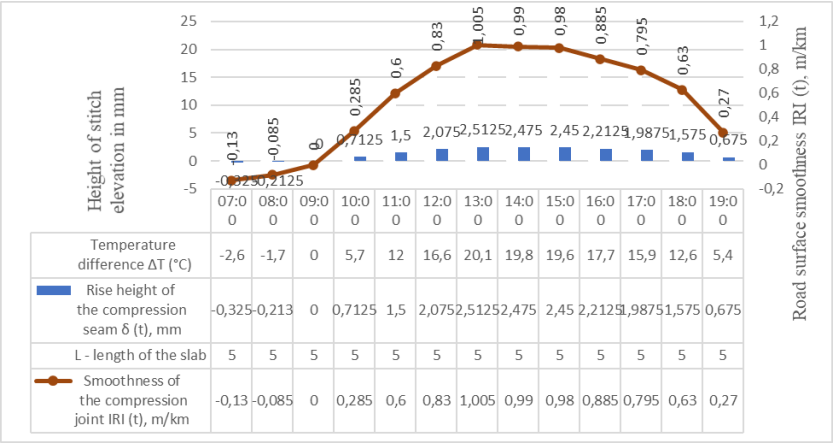

Figure 9. *Graph showing the change in smoothness (IRI) relative to the uplift height of the compression joint in cement-concrete pavement due to temperature effects*

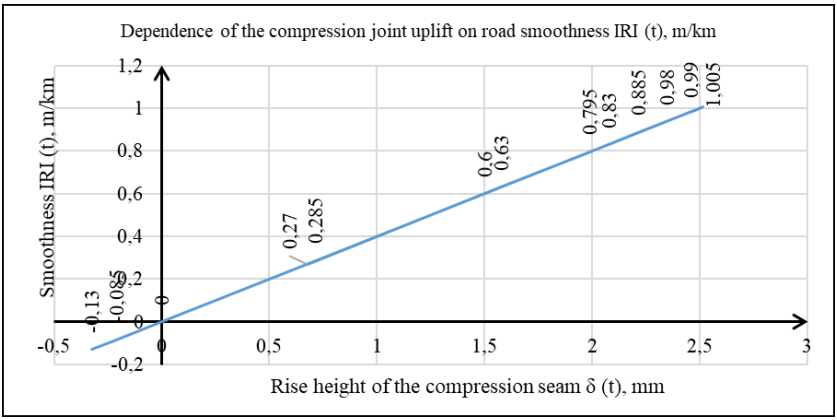

Figure 10. *Graph showing the change in compression joint height of cement-concrete pavement and road smoothness (IRI) under temperature influence*

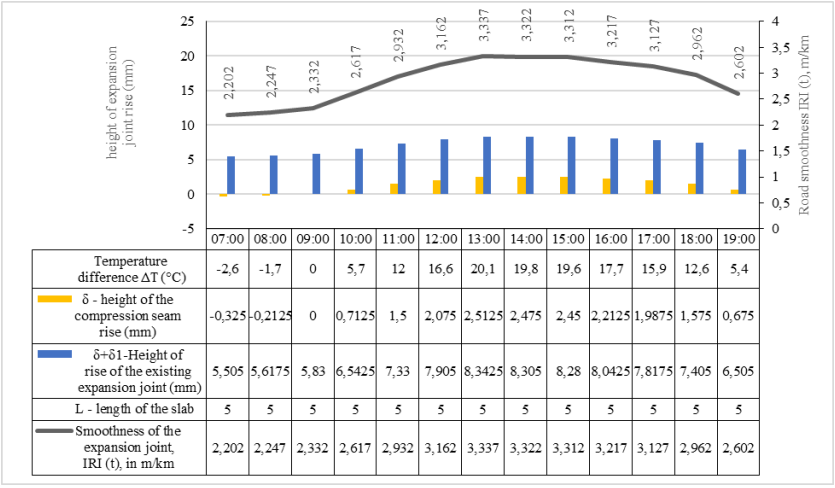

	07:00	08:00	09:00	10:00	11:00	12:00	13:00	14:00	15:00	16:00	17:00	18:00	19:00
Temperature difference ΔT (°C)	-2,6	-1,7	0	5,7	12	16,6	20,1	19,8	19,6	17,7	15,9	12,6	5,4
δ - height of the compression seam rise (mm)	-0,325	-0,2125	0	0,7125	1,5	2,075	2,5125	2,475	2,45	2,2125	1,9875	1,575	0,675
δ+δ1-Height of rise of the existing expansion joint (mm)	5,505	5,6175	5,83	6,5425	7,33	7,905	8,3425	8,305	8,28	8,0425	7,8175	7,405	6,505
L - length of the slab	5	5	5	5	5	5	5	5	5	5	5	5	5
Smoothness of the expansion joint, IRI (t), in m/km	2,202	2,247	2,332	2,617	2,932	3,162	3,337	3,322	3,312	3,217	3,127	2,962	2,602

Figure 11. *Graph showing the change in expansion joint height of cement-concrete pavement and road smoothness (IRI) under temperature influence*

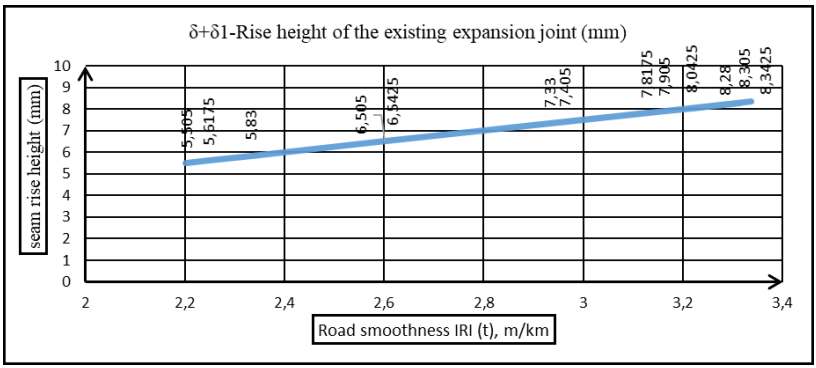

Figure 12. *Graph showing the relationship between the expansion joint height of cement-concrete pavement under temperature influence and pavement smoothness (IRI)*

Conclusion

This scientific study investigated the uplift that occurs due to temperature differences between cement-concrete road pavement slabs.

The highest temperature difference in the cement concrete slab was observed at 13:00, with the upper part at T_{upper}=58,3°C and the lower part at T_{lower}=38,2.5°C, resulting in a temperature difference of ΔT=20,1°C.

The thermal expansion of the cement concrete slab with a thickness of h=0.25 m and a length of L=5 m was $\Delta L \approx 1{,}005$ mm, with a lifting angle of $\theta \approx 0{,}000025125$ radians, which led to a lifting height of the compression joint of $\delta \approx 2{,}5125$ mm.

Additionally, the calculated IRI (International Roughness Index) smoothness indicator of the road surface at the compression joint is 1,005 m/km and at the expansion joint is 3,337 m/km, which leads to a significant deterioration in the smoothness of the concrete road surface.

Based on these results, it can be concluded that there are significant temperature differences in cement-concrete road slabs used in various climatic conditions. This leads to defects such as lifting and cracking of the slabs.

List of References

1. Decree of the President of the Republic of Uzbekistan No. PP-111, dated January 25, 2022. "On Measures for Fundamental Reform of the Road Management Sector and Improvement of the Management System."

2. Decree of the President of the Republic of Uzbekistan No. PP-125, dated April 14, 2023. "On Additional Measures for the Development of Highways and Improvement of Their Quality."

3. Amirov T.J. Construction of Cement Concrete Pavements for Highways and Airfields. Textbook - T.: "SANO STANDART." 2016, 33 pages.

4. Sodiqov I.S. Transport and Operational Indicators of Highways. Textbook. "Transport" Publishing House, Tashkent. 2021. 217 pages.

5. Amirov Tursoat Jummayevich, Dauletov Madiyar Boranbaevich. Analysis of the impact of temperature-induced deformation in compression and expansion joints between concrete pavement slabs on smoothness indicators. Proceedings of the International Conference "Scientific research of the SCO countries: synergy and integration" - Reports in English. July 2, 2025. Beijing, PRC.

6. Huang, Y. H. (2004). Pavement Analysis and Design. Pearson Prentice Hall.

7. AASHTO (1993). AASHTO Guide for Design of Pavement Structures. American Association of State Highway and Transportation Officials.

8. Zollinger, D.G., et al. (2005). Performance of Concrete Pavements Subjected to Environmental Effects. FHWA/TX-05/0-4394.

DOI 10.34660/INF.2025.20.97.143

PROPOSALS FOR THE INTERPRETATION OF THE CONCEPTS OF "MORALITY" AND "POLITENESS" IN THE FIELD OF ARTIFICIAL INTELLIGENCE

Tikhanychev OlegVasilyevich
PhD, Deputy Head of Department
Company group "Technoserv", Moscow, Russia

Abstract. *The relevance of choosing the principles of ensuring the safety of robotic systems and the object of study, which are algorithmic problems arising in terms of implementing safe interaction algorithms, as the subject of research is determined by the existing contradiction between the need for autonomous use of robotic systems and the complexity of the software implementation of this requirement, especially given that the main control of modern robots is artificial intelligence technologies. At the same time, in robotics, it is the insufficient efficiency of existing control algorithms that is the source of most safety problems. Based on an assessment of the content of the currently used concept of "trust" of artificial intelligence, possible algorithmic problems of ensuring mutual safety of interacting robotic systems are analyzed. It is concluded that the "trust" of artificial intelligence, despite the fact that existing regulatory documents equate it with "ethics", is, nevertheless, an analogue of system safety, but in reality, a more expanded approach is required, truly analogous to human ethics. Taking this into account, based on a review analysis of typical algorithms for controlling movement in space, a formulation of the scientific task of solving the problem of ensuring safety during mutually agreed and uncoordinated maneuvering has been synthesized, as an analogue of expanding "power of attorney" to "new ethics" or "politeness" of behavior of robotic systems*

Keywords: *autonomous robots, artificial intelligence, trusted artificial intelligence, robot operation safety, rules of safe behavior analogs of morality and politeness.*

1. Introduction

In recent decades, there has been active robotization of all areas of human activity: production, logistics, and transport. In all of these areas, the main trend is the development of autonomous systems, which is determined by the requirements

for the speed of their response to external changes and a reduction in the number of personnel using robotics. One of the priorities that ensures the development of autonomous robotics is the use of artificial intelligence (AI) elements in it. Currently, most robotic systems (RTS) with different levels of autonomy contain AI components.

Equipping RTS with AI components, their further autonomy using the principles of learning and self-learning, increasingly distances the principles of their behavior from previously implemented robots with external control, increasingly, at least externally, brings them closer to the reasonable, with all the pros and cons of these changes. At the same time, increasing the degree of autonomy of RTS is an objective trend based on modern and prospective requirements for the use of robotics in a variety of fields of activity.

At the same time, there are a number of unresolved problems in this area, sometimes leading to accidents and disasters in the industrial and transport spheres [1], in the sphere of armed confrontation [2,3,4]. Many accidents are determined by the unresolved problems of the subject area in terms of determining the safety of AI systems. The currently used approach based on the "power of attorney" of AI does not fully describe the problems of the safe use of RTS, it is not identical to the concept of "safety" in the comprehensive understanding of this phenomenon, and other approaches to the description of this factor are not yet proposed in regulatory documentation.

At the same time, it is the description of the subject area that serves as the basis for the development of the theory and practice of any systems. And, at the same time, the development of autonomous systems cannot be stopped, it continues, as technical progress continues, despite some restrictions reflected in official documents regulating the field of AI.

Thus, at present, the problem of clarifying the conceptual apparatus for assessing the rules of safe behavior of AI controlling RTS is extremely urgent, which makes the topic covered in this article relevant and timely.

2. Materials and Methods

A system approach was chosen as the methodological basis for the study. The use of a system approach, decomposition methods and comparative analysis made it possible to consider in a complex the problems of safety in the interaction of autonomous robots.

The source base of the study consisted of scientific articles, regulatory and legislative documents that are in the public domain.

3. Results

It is generally accepted that the basis for classifying any process is the operating conditions of the systems being described. Statistics on the prerequisites for the occurrence of disasters and accidents caused by autonomous and partially au-

tonomous RSTs show that most of the causes that gave rise to them can be divided into two large groups;

- conditionally natural, the prerequisites for the emergence of which were laid down during the development of the RTS;
- random, caused by failures or non-design operating conditions.

An example of the first group of errors is, for example, the situation with the AI's decision to kill its own operator, whom the combat RTS considered an obstacle to achieving its goal [5]. In documents regulating the development and use of AI, such errors are sometimes defined as bias.

There are significantly more examples of the second type of errors, namely dangerous accidents, both in the transport sector and in the field of robotic weapons [6,7].

Some errors are critical, often affecting human safety. Their prevention requires reliable solutions, which the scientific community is currently actively searching for.

The formalized formulation of the task of preventing errors of the first group is usually defined as the creation of a "trustworthy" artificial intelligence. Some of the results of research on the creation of safe or "trusted" artificial intelligence are reflected in the 2019 European Commission document "Ethics Guidelines for Trustworthy AI" and in the Russian state standard R 59 276-2020 "Artificial Intelligence Systems. Methods of Ensuring Trust. General Provisions". In these documents, artificial intelligence is declared trusted if it has the following properties: verifiability, controllability, stability, robustness, safety, and fault tolerance. If these requirements are met, AI is proposed to be considered "ethically verified".

However, the specified documents do not solve a number of problems in eliminating errors in the use of AI, some of which are critical.

Firstly, in which continuous and unconditional control over the behavior of artificial intelligence by a person is set as the main criterion of "trustworthiness". Within the framework of this approach, a significant part of the requirements for trusted AI, given in the documents reviewed, can be considered the implementation of a human-centric approach to its development and implementation, based on three groups of principles: transparency, reliability, human-centricity [8,9].

Secondly, it is not entirely logical to discuss AI ethics in the aspect defined by these documents. The AI trust in the content of these documents rather corresponds to the safety of their algorithms for humans, and not to a set of measures to prevent random behavioral errors, which, logically, can be attributed to the implementation of the "ethics" of behavior. For the concept of "ethics" rather corresponds to the priority consideration of the interests of interacting systems, including RTS, even if this requires sacrificing the optimality of one's own behavior.

Therefore, the "trust" of AI in the existing understanding can still be defined as an analogue of human "morality", interpreted for the rules of behavior of RTS, potentially solved by means of security control of RTS software algorithms and the formation of a system of restrictions on their behavior [10,11,12]. But, regardless of the correctness of the formulations, the problem of safe behavior is gradually being solved, although not in full and with certain terminological assumptions, the correctness of which requires additional confirmation.

To prevent errors of the second group, it is necessary to develop flexible rules for constructing control algorithms and a system of restrictions, the prototype for which, with a certain degree of assumptions, can be considered the rules not of morality, but of human politeness, interpreted for a "trusted" AI.

In the context of formalizing this problem, we can recall the famous "three laws of robotics" formulated by science fiction writer Isaac Asimov at the dawn of robotics development:

1. a robot may not, under any circumstances, harm a person;
2. the robot must carry out all human commands that do not contradict the first point;
3. A robot must take care of its own safety, unless this contradicts the first two points.

An analysis of the three laws of robotics shows that only the first and second of them relate to human safety, which covers the "trust" of AI in modern terminology. But the third rule, which should ensure the safety of the robots themselves, is not considered at all in the existing approach to organizing security.

The revealed contradictions in the applied terminology make it difficult to develop unified rules of conduct for RTS and algorithms for their implementation. This situation requires a solution that ensures the logical development of the theory and practice of AI algorithmization, including the RTS manager.

Taking into account the identified contradiction in terminology, based on the method of analogies and projecting some rules of human behavior onto the algorithms and limitations of the behavior of artificial intelligence, it is proposed to formulate the task of implementing a set of rules of "morality" and "politeness" for various aspects of the security of the use of RTS of varying degrees of autonomy, ensuring the clarification of regulatory mechanisms and codes of conduct for AI.

4. Discussion

A typical and characteristic example of a random error, the reasons for which go beyond the "trust" of AI in the current understanding, is the emergence of a risk of collision of ground-based autonomous radar systems during joint maneuvering with problems of accounting for mutual movement.

A model for the emergence of such a situation can be considered using a simple example. Let's say two autonomous vehicles, moving along trajectories converging at an acute angle or close to parallel, must make a turn by going around an obstacle. The vehicles maneuver independently, not working in a group. The software of each of these vehicles builds an optimal trajectory for itself, the turning point of which will be as close as possible to the obstacle being gone around. There is a high probability that, if certain conditions coincide, the trajectories will intersect near the turning point.

If the specified means are equipped with safe divergence systems, a collision is unlikely - these systems will detect the danger and the RTS software will form an emergency divergence maneuver or an emergency change in speed. But the problem is that the divergence will be emergency, it will be necessary to form divergence options, change the speed or trajectory in a very short period of time, there will be no talk of the optimality of the route. In such conditions, the probability of successful divergence will not be 100%. This is a typical case of uncoordinated interaction of moving agents.

In such a situation, if the AI in the software of the maneuvering RTS had calculated the situation in advance, the emergency divergence could have been avoided by specifying the movement parameters in advance, taking into account the presence of a potential problem. By slightly deviating from the optimal trajectory at the early stage of planning, it would have been possible to avoid significant losses in optimality or the risk of a collision during the divergence.

In the described problem of emergency divergence, two components can be distinguished:

- logical apparatus that determines the rules for making a divergence;
- the mathematical apparatus necessary for calculating the parameters of the discrepancy.

From the point of view of the mathematical support of AI, the algorithm of "politeness" or "ethics" in the above-described situation can be implemented as calculations for typical variants of divergence, carried out relative to the RTS, correcting the trajectory [13].

In the problem under consideration, several options can be used to determine the maneuver parameters, calculated using well-known mathematical apparatus:

- change in the speed of one of the participants, for example, a decrease by $\Delta V = Vin - Vreq$, from the initial to the required value, ensuring a divergence of distance ΔS. In this case, the value of the speed decrease is easily determined from the equation of motion of a material point, taking its motion as rectilinear and uniformly accelerated and using the known initial speed of motion Vin and the distance to the turning point (divergence) S as initial data:

$$V_{req} = V_{in}\left(1 - \frac{\Delta S}{S}\right);$$

- change in the trajectory of movement, ensuring a shift in the turning point and a divergence at the minimum safe distance Lmin, determined by the formula:

$$L_{min} = L_M \frac{\sin(q_{T0} - Q)}{sinQ},$$

Where Q– critical course angle, the maximum at which divergence can be achieved;

qTO – initial course angle of the RTS that does not change the direction of movement ("target");

L.M.– the distance from the maneuvering aircraft to the "target";

The value of Q is calculated, as a rule, based on the ratio of the speed vectors of the maneuvering aircraft and the "target":

$$Q = \frac{V_M}{V_T}.$$

A simple example shows that there is already a fairly wide choice of mathematical apparatus that allows for the implementation of "polite" divergence in different situations.

But the logic of forming the rules of "polite" behavior, namely who should perform an evasive maneuver, is a much more problematic issue. This is a highly complex problem, and its solution must be sought on the border of mathematics and formal logic.

One can, of course, object that similar tasks are already formally solved in practice by developing and applying sets of rules and regulations implemented in specialized documents: traffic regulations, air and water codes. But this assumption is not entirely correct. Firstly, movement and maneuvering are particular cases of using RTS, in reality the range of their application is much wider. Secondly, the cases described in the listed documents are particular, they are implemented under conditions of significant restrictions determined, in particular, by the boundaries of the road surface, markings, pre-set routes and echelons, a simple set of behavioral rules for various typical situations.

Much more complex and less formalized situations arise in cases typical for the functioning of RTS of varying degrees of autonomy. Moreover, these situations are usually complicated by the limited time for its adoption. They require the development and implementation of dynamic algorithms for solving problems of discrepancy with weakly formalized initial data.

Based on this, when developing algorithms for RTS software, a non-trivial scientific task arises - the development of rules of mutual behavior, an analogue of human etiquette. At the same time, software "etiquette", like the usual one, will probably be divided into situational and professional, and the latter will be subdivided into areas of application with corresponding variations of actions. Within the framework of these provisions, behavior during maneuvering, in the previously described maneuvering task, is part of professional, namely transport, "etiquette". And everything that is associated with the obviously dangerous use of RTS for others should be resolved within the framework of a system of restrictions and prohibitions similar to human morality.

When implementing the proposed approach, the restrictions and, accordingly, the clarified content of the concept of "trusted" AI will be based on two sets of rules: analogues of "etiquette" and "morality", with the choice of the type of professional etiquette suitable for each situation under consideration within the framework of the implementation of the control algorithm:

1) assessment of the situation;

2) calculations for the formation of control actions that ensure the achievement of the goal;

3) forecast of the development of the situation during the execution of the task, taking into account the possible ranges of behavior of interacting and third-party agents;

4) assessment of the safety of the implementation of control actions in relation to the first law of robotics;

5) assessment of one's own safety in relation to the third law of robotics;

6) correction, if necessary, of the calculated values of control actions;

7) forecasting the development of the situation taking into account the adjustment of control parameters;

8) completing the task with cyclical clarification of data according to points 3-7.

The use of the clarifications proposed in the article based on the analogies of "morality" and "politeness" of the AI controlling the RTS, as one of the conditions for the execution of this algorithm, will allow solving a number of important problems of the safety of the behavior of autonomous robots, especially in weakly formalized conditions of interaction.

5. Conclusions

The analysis conducted in the article showed that one of the conditions for implementing the specified algorithm of safe interaction is: clarification of the conceptual apparatus and development of a mechanism for the formation, clarification and supplementation of decision rules, the logic of their application. The solution to this problem does not concern direct copying of human concepts of

"morality" and "politeness", but clarification of the concept of "trusted" AI in one of two ways:

- leaving the concept of "trusted" AI as a synonym for AI with guaranteed safe behavior algorithms, add an additional definition of "polite" AI that ensures safe behavior in group settings based on the use of "polite" algorithms;
- expand the concept of "trusted" AI by adding the property of "politeness" of behavior, which consists of predicting the results of proposed actions and verifying them based on a set of special rules.

When implementing the above options, it is necessary to take into account that it is impossible to train AI in advance to act in specialized situations typical for autonomous systems, the state space is too large. Therefore, when working with the AI RTS manager, we should not talk about training, but about some analogue of "education", the formation of basic principles of behavior, analogues of "morality" for the implementation of the first two laws of robotics and "politeness" - for the third. The task is non-trivial, but humanity once solved it for itself, and probably a solution will be found for artificial intelligence.

References

1. *Chirov D. and Novak K. (2018) Promising areas for the development of special-purpose robotic systems, Security Issues 2: 50-59 https://doi.org/10.25136/2409-7543.2018.2.22737.*
2. *Khripunov S., Blagodaryashchev I. and Chirov D. (2015) Military robotics: modern trends and development vectors, Trends and Management 4: 410-422. URL: https://nbpublish.com/library_read_article.php?id=67141.*
3. *Pflimlin É (2017) Drones et robots: La guerre des futurs. (France: Levallois-Perret).*
4. *Roosevelt, Ann. Army Directs Cuts, Adjustments, To FCS. Defense Daily. (2017).*
5. *Hamilton T. (2023) How AI will Alter Multi-Domain Warfare. Future Combat Air & Space Capabilities Summit, 4 URL: https://www.aerosociety.com/events-calendar/raes-future-combat-air-and-space-capabilities-summit.*
6. *Tikhanychev O. (2022) Influence of the Problem of Safety Control of Heuristic Algorithms on the Development of Robotics. In: Shamtsyan, M., Pasetti, M., Beskopylny, A. (eds) Robotics, Machinery and Engineering Technology for Precision Agriculture. Smart Innovation, Systemsand Technologies 247 (Singapore: Springer) https://doi.org/10.1007/978-981-16-3844-2_31.*
7. *Beard J. (2014) Autonomous weapons and human responsibilities, Georgetown Journal of International Law 45: 617–681.*

8. Schuller A. (2017) At the Crossroads of Control: The Intersection of Artificial Intelligence in Autonomous Weapon Systems with International Humanitarian Law, Harvard National Security Journal 8: 379–425.

9. Ukhobotov V. and Izmestyev I. (2016) On a pursuit problem under resistance of a medium. Bulletin of the South Ural State University series "Mathematics. Mechanics. Physics" 8(2): 62-66 https://doi.org/10.14529/mmph160208.

10. Tikhanychev O. (2023) Self-Check System of Heuristic Algorithms as a "New Moral" of Intelligent Systems AIP Conference Proceedings. 2700, 040028 https://doi.org/10.1063/5.0124956.

11. Ćwiąkała, P. (2019) Testing Procedure of Unmanned Aerial Vehicles (UAVs) Trajectory in Automatic Missions. Appl. Sci. 9: 3488. https://doi.org/10.3390/app9173488.

12. Johnson D. (2016) Computer Systems: Moral entities but not moral agents. In: Ethics and Information Technology 8: 195-204 https://doi.org/10.1007/s10676-006-9111.

13. Dubanov A. (2021) Simulation of the trajectory of the pursuer in space with the method of parallel approach. Program systems and computational methods 2: 1-10. https://doi.org/ 10.7256/2454-0714.2021.2.36014.

DOI 10.34660/INF.2025.78.22.144

BUILDING A LINEAR REGRESSION MODEL AND FORECASTING USING A NEURAL NETWORK

Klimau Yury Valerevich
Candidate of Technical Sciences, Associate Professor
Belarusian National Technical University

Abstract. *the advantages of using a linear regression model are considered, the main stages of creating a neural network and constructing a linear regression model are presented, a forecast is made using a neural network, and a comparative analysis of forecasting methods is carried out.*

Keywords: *neural network, regression model, regression analysis, least squares method, comparative analysis, prediction, forecasting, data normalization.*

In scientific research, a set of statistical methods are used to conduct regression analysis. Currently, methods using neural networks are being developed that can successfully solve the problem.

Linear regression is a regression model that characterizes the dependence of one (explained, dependent) variable on one or more other variables (factors, regressors, independent variables) with a linear dependence function. The graph of a linear function is a straight line.

The linear function has the following form:

$$y = k * x + b \quad (1)$$

where y is the dependent variable;

k– an angular coefficient that determines the steepness of the slope of a straight line;

x– independent variable;

b– a free term that determines the point of intersection of the graph with the OY axis.

The advantages of linear regression include:

ease of understanding and interpretation;

fast modeling with small amounts of data;

obtaining a sufficiently high-quality estimate of the model parameters (unbiasedness, consistency and efficiency of the estimate) when implementing classical assumptions using the least squares method;

widely used in various fields of science and in business decision-making (for example, for constructing a trend line).

The main disadvantages are:

difficulty of designing when using nonlinear data;

inefficiency with complex structure and large volumes of data.

Suppose that a set of a certain number of points is given. The goal of linear regression is to find the line that best fits these points. Thus, the solution to linear regression is to determine the values of the coefficients to approximate f(x) as closely as possible to the dependent variable y.

First, let's create a simple linear regression model in the Python algorithmic language. To implement the code provided in the article, you will need to import the libraries listed below and set specific initial values for the random number generator included in NumPy. Then, you need to create a synthetic dataset containing 100 values, as shown in Figure 1.

Since this is a linear regression y = k * X + b, we will set the coefficient values k = 0.5 and b = 1.4. We will also add normally distributed random noise. To reproduce the same input data and compare subsequent experimental results, it is necessary to save them in an array (insert into the program code).

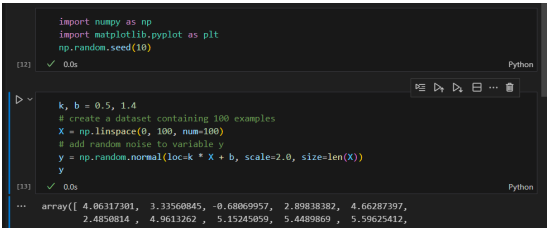

Figure 1. *Creating a synthetic dataset*

A neural network can also be used to estimate unknown parameters of regression models from sample data.

The main stages of creating a neural network and constructing a linear regression model when working with the Tensorflow 2.x library are:

importing necessary libraries;

data preprocessing (data preparation and normalization);

defining the model architecture;

model compilation;

model training;

model evaluation (if necessary);
model prediction.
Importing the required libraries

To create a neural network and implement the code given in the article in Python, you will need to import the specified libraries (Figure 2) and set specific initial values for the random number generators included in NumPy and TensorFlow ((This example uses the Keras API).

```
import tensorflow as tf
import numpy as np
import matplotlib.pyplot as plt

np.random.seed(10)
tf.random.set_seed(10)
```

Figure 2. *Importing the required libraries*

Data preprocessing (data preparation and normalization)

The result of the work primarily depends on the preparation of data for the model. Missing data should be removed (rows should be cleared) if there are few such records. To do this, you can write your own functions in Python or use the sklearn.preprocessing library. TensorFlow itself also has tools for preprocessing in the tf.keras.preprocessing module.

In machine learning, normalization is a method of preprocessing numerical features in a training dataset to bring them to a common scale without losing information about the difference in ranges. Normalization is necessary because different features of the training dataset can be represented at different scales and vary in different ranges. The ranges of change of individual features differ by hundreds and thousands of times. During calculations, the data is multiplied by the model weights. Thus, the scale of the output data and the scale of the gradients depend on the scale of the input data. As a result, the trained model may produce incorrect results. The model can converge without normalizing the features, but normalization makes training more stable.

There are several basic methods of normalization.

With minimax normalization, the problem can be solved by applying the following formula:

$$X' = \frac{(X_i - X_{min})}{X_{max} - X_{min}} \quad (2)$$

where is the minimum value in the training data; X_{min}
X_{max} – the maximum value in the training data.

The most commonly used range casts are [0,1] and [-1,1].

The disadvantage of minimax normalization is the presence of anomalous data values that “stretch” the range, which leads to the normalized values again being

concentrated in some narrow range near zero. To avoid this, the range should be defined not by the maximum and minimum values, but by the mean and standard deviation using mean normalization (Z-normalization):

$$X' = \frac{(x_i - \bar{x})}{\sigma_x} \quad (3)$$

where is the average value (mathematical expectation); $\bar{X}$

σ_x – standard deviation.

The values obtained by this formula are called Z-scores in mathematical statistics. Their absolute value is an estimate of the distance between x and its average value in the general population.$\bar{X}$

When using the ratio method, each value of the original data is divided by a user-specified number or by the value of a statistical indicator calculated from the data set (mean value, standard deviation, variation range, etc.).

A simple way to add feature normalization to a neural network model is to create a normalization layer and fitting the state of the pre-processing layer to the data shown in Figure 3.

```
# creating a normalization layer
normalizer = tf.keras.layers.Normalization(input_shape=[1,], axis=None)
# fit the state of the preprocessing layer to the data
normalizer.adapt(y)

normalizer
```

✓ 1.2s Python

```
<keras.src.layers.preprocessing.normalization.Normalization at 0x7f6eeb19d790>
```

Figure 3. *Creating a normalization layer*

When the layer is called, the input data is returned, with each value being normalized independently (Figure 4).

```
first = np.array(y)

with np.printoptions(precision=2, suppress=True):
  print('First example:', first)
  print()
  print('Normalized:', normalizer(first).numpy())
```

Python

```
First example: [ 4.06  3.34 -0.68  2.9   4.66  2.49  4.96  5.15  5.45  5.6   7.32  9.36
  5.53 10.02  8.93  9.87  7.21 10.26 13.46  8.84  7.55  8.52 13.04 17.79
 15.77 17.37 14.73 17.83 15.   17.27 16.02 15.96 17.83 17.11 21.19 19.47
 20.38 19.41 23.1  19.63 22.92 21.41 20.73 22.14 22.01 23.7  23.95 25.76
 26.77 25.85 26.6  27.74 26.58 29.58 30.36 29.58 34.47 32.02 30.47 30.47
 31.24 31.2  34.97 31.82 33.56 33.17 36.83 32.4  35.02 36.   37.39 38.18
 37.33 40.25 39.4  44.21 36.77 41.53 38.7  39.7  45.77 45.8  39.1  42.87
 43.69 40.07 44.74 46.13 46.28 42.36 49.07 47.85 47.74 46.86 50.3  51.22
 48.92 50.57 52.55 47.49]

Normalized: [-1.55 -1.6  -1.87 -1.63 -1.5  -1.65 -1.48 -1.47 -1.45 -1.44 -1.32 -1.18
 -1.44 -1.14 -1.21 -1.15 -1.33 -1.12 -0.9  -1.22 -1.31 -1.24 -0.93 -0.6
 -0.74 -0.63 -0.81 -0.6  -0.79 -0.64 -0.72 -0.73 -0.6  -0.65 -0.37 -0.49
 -0.42 -0.49 -0.24 -0.48 -0.25 -0.35 -0.4  -0.3  -0.31 -0.2  -0.18 -0.05
  0.01 -0.05  0.    0.08  0.    0.21  0.26  0.21  0.54  0.38  0.27  0.27
  0.32  0.32  0.58  0.36  0.48  0.45  0.71  0.4   0.58  0.65  0.74  0.8
  0.74  0.94  0.88  1.21  0.7   1.03  0.83  0.9   1.32  1.32  0.86  1.12
  1.18  0.93  1.25  1.34  1.35  1.09  1.55  1.46  1.46  1.39  1.63  1.69
  1.54  1.65  1.79  1.44]
```

Figure 4. *Data normalization*

Defining the model architecture

The model architecture is defined using the tf.keras.Sequential class, which accepts a list of layers (Figure 5). To view the contents of the model, call the summary() method.

```
norma_model = tf.keras.Sequential([
    normalizer,
    tf.keras.layers.Dense(units=1)
])

norma_model.summary()
```

Python

```
Model: "sequential_3"
_________________________________________________________________
 Layer (type)                Output Shape              Param #
=================================================================
 normalization_2 (Normaliza  (None, 1)                 3
 tion)

 dense_3 (Dense)             (None, 1)                 2

=================================================================
Total params: 5 (24.00 Byte)
Trainable params: 2 (8.00 Byte)
Non-trainable params: 3 (16.00 Byte)
_________________________________________________________________
```

Figure 5. *Defining the model architecture*

Compiling the model

To compile the model, there is a compile() method. When compiling, two important parameters should be defined: the optimization algorithm and the loss function, on which the training result and further optimization of the model depend (Figure 6).

A well-chosen optimizer and choice of learning rate parameter will allow the model to be trained faster and, if possible, local minima to be avoided.

The loss function is a measure of the amount of error that our linear regression makes on the data set. The loss functions used generally calculate the distance between the predicted value f(x) and its actual value. For example, the error distance between the actual and predicted values is extracted. The most common loss functions used for regression problems are the Mean Squared Error (MSE) and the Mean Absolute Error (MAE). To calculate the MSE, all error values are used, their lengths are squared, and then averaged. In this way, an attempt is made to determine the lowest value, i.e., to minimize the MSE. The Mean Squared Error (MSE) loss function is more sensitive to outliers compared to the Mean Absolute Error (MAE) function. The use of a specific loss function is determined by the problem being solved.

```
norma_model.compile(
    optimizer=tf.optimizers.Adam(learning_rate=0.1),
    loss='mean_absolute_error')
```

Python

Figure 6. *Compiling the model*

Model training

The fit() method is used to perform model training. It takes input data, the maximum number of episodes, and other configurable parameters.

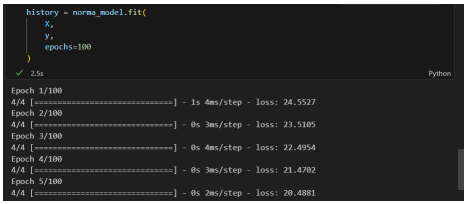

Figure 7. *Compiling the model*

The output shows the result of each epoch (Figure 7). The epoch number, the time spent on the epoch, and the calculated loss function are displayed.

The progress of the model training is visualized using the plot_loss() function using the object statistics (Figure 8).

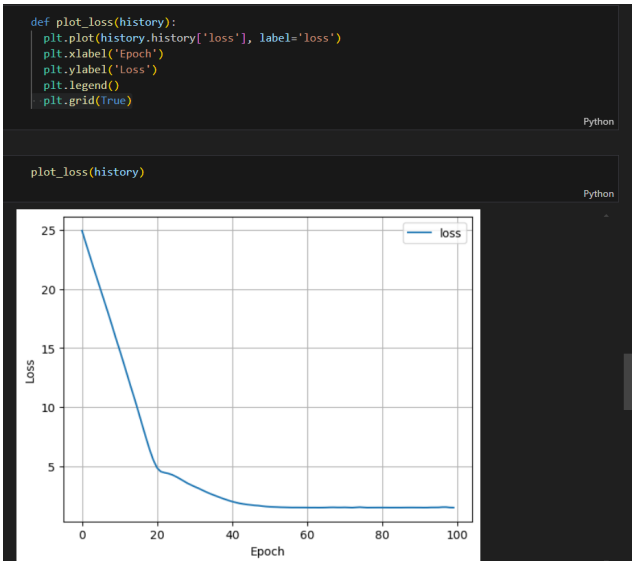

Figure 8. *Calculated loss function*

Model prediction

To get the predicted values, the predict() method is used.

```
# get predicted values
y_predict = norma_model.predict(X)
```
Python
```
4/4 [==============================] - 0s 2ms/step
```

Figure 9. *Method for model prediction*

```
plot_predict(X, y, y_predict)
```
Python

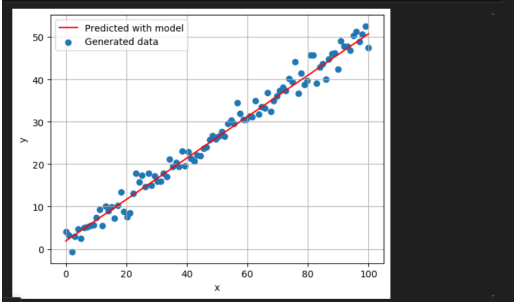

Figure 10. *Model prediction using neural network*

```
# Neural network prediction for x=100
y_predict_100 = norma_model.predict(X[99:])

y_predict_100
```
Python
```
1/1 [==============================] - 0s 21ms/step

array([[50.751755]], dtype=float32)
```

Figure 11. *Model prediction for x=100*

A forecast was made on the trained neural network for the value x=100, the result was y=50.751755 (Figure 11).

The author of the article set a scientific task to analyze the impact of data normalization with fixed experimental results (learning rate=0.1). At the same time two options were considered: a model architecture with and without a normalization layer.

As a result of the scientific experiment, the forecast deviation was 0.9% downward for the model architecture with the normalization layer, which indicates its effectiveness.

When comparing the forecast value of the linear regression model using the least squares method and the model architecture with a normalization layer, the forecast deviation was 0.1% downwards.

When comparing the forecast of a linear regression model using the least squares method and the model architecture without normalization, the forecast

deviation was 0.8% upwards, which indicates some difference in the calculation methods used and the need for further optimization.

Thus, the study of linear regression calculation methods allowed us to draw the following conclusions:

To conduct regression analysis, it is necessary to collect a large amount of input data to eliminate the influence of random factors;

Calculations using linear regression models are characterized by ease of understanding, rapid modeling and wide application in various fields of science;

creating a neural network requires knowledge of a programming language, building a model architecture and optimizing it;

normalization of features makes neural network training more stable and improves its convergence;

A comparative analysis of the forecast of the linear regression model using the least squares method and a neural network with a normalization layer shows the adequacy and complete comparability of the results.

DOI 10.34660/INF.2025.42.77.145

THE COORDINATED WORK OF AN AUTONOMOUS SYSTEM IN MONITORING MOBILE OBJECTS OVER A LARGE AREA IS BUILDING DRONES

Ulanov Sergey Ivanovich
Research Assistant
Institute for Artificial Intelligence Problems, Donetsk, Russia

Ivanova Svetlana Borisovna
Director
Institute for Artificial Intelligence Problems, Donetsk, Russia

Nikitina Angela Anatolyevna
Research Assistant
Institute for Artificial Intelligence Problems, Donetsk, Russia

Butov Oleg Anatolyevich
Research Assistant
Institute for Artificial Intelligence Problems, Donetsk, Russia

Abstract. *This study corresponds to the priority areas of scientific and technological development of the Russian Federation and is carried out within the framework of the research work "Theoretical foundations of detection and assessment of objects on the ground by intelligent robotic systems in a rapidly changing environment" (State order FREN-2023-0004) Development of a methodological approach to preliminary data processing and software for an automated system for continuous monitoring of the situation on a given area of the terrain. The solution to this problem determines the transition to innovative digital and intelligent production technologies, work with robotic complexes, modern design methods, the development of big data analysis systems, machine learning and artificial intelligence.*

Keywords: *unmanned aerial vehicle (UAV), formation, swarm, network control systems, wireless networks, intra-network computing.*

The aim of the work is to develop a theoretical basis for a traffic management system (UAV) by monitoring using optical sensors operating in a multi-position mode. The coordination of the system elements will allow for accurate assessment of the parameters for safe, fast and reliable UAV control and minimization of potentially

dangerous situations in order to achieve common goals. UAVs are autonomous or remotely controlled aircraft that are widely used due to their versatility, affordable price and ease of implementation. The areas of application cover both military and civilian spheres. In the military field, UAVs are used to prevent personnel losses and identify objects. In the civilian sphere, drones are used to collect data on the earth's surface, provide wireless communication, deliver cargo and control traffic. The limitations of individual UAVs complicate the performance of long-term tasks, such as covering large areas and providing information promptly [1]. Control of a drone formation by integrating network and computing resources, forming a multi-agent system, where each drone acts as an individual agent. Distribution of tasks between drones allows solving complex problems, as indicated in the study [2]. This will entail increased flexibility in task execution and improved reliability due to resource reservation, providing a high degree of automation and adaptability. The developed UAV formation control systems can be built in a decentralized manner or with a single control center. Since wireless communication channels are used in most cases, it is necessary to solve technical problems related to ensuring security, data transmission and computing performance of agents [3]. In addition, much effort is directed at overcoming the limitations associated with the scalability of the agent system due to changes in the quality of wireless communication channels, as well as collision avoidance and formation management, which potentially affect the success of the mission.

The self-organizing behavior of a drone swarm requires the integration of network and computing systems with a controller for updating the system status. Consolidation provides synergy: the network system selects data transmission channels based on the computational system's assessments of the channel quality. Drones are modeled as a network control system (NCS), where control is implemented through a radio communication network. NCS consists of a computing system (data collection, decision making, command execution) and an information exchange network (communication modules with protocols). Integration into the network increases the efficiency of each drone.

Drone deployment uses non-cooperative and cooperative strategies. The zero-touch strategy assumes that each drone is directly connected to the ground control station (monitoring, decision-making, sending commands). This is a simple network where each drone can create a closed control loop. In the zero-touch strategy, the communication between drones and the command post is bidirectional. Recommended for small coverage areas and simple scenarios. Limitation: the ground control station is a single point of failure with possible transmission delays. The strategy is based on the air-to-ground channel model.

The main algorithms for implementing the strategy under consideration are as follows: drones collect their own information and the environment; the drone communicates with the ground control station to process the collected data; the ground station

transmits the result of the computing system back to the drones or the processed result further via another communication channel to the customer of this information; local actuators of the drone process the corresponding control commands from the ground station.

Cellular technologies such as LTE (Long-Term Evolution) are suitable for implementing the algorithm, providing improved system capacity, coverage, high data rates and reduced deployment latency [4]. This deployment strategy can be based simply on accurate mobility models or path planning functions based on intelligent algorithms such as particle swarm optimization [5].

System components. Let us consider the properties of two main elements of the drone system: the network system and the computing system, each of which solves specific problems, meets certain requirements and has a number of issues. The network system of the drone system builds a communication graph for the exchange of data between unmanned aerial vehicles, as well as between drones and the ground infrastructure. It must guarantee a closed loop of data flow control between the implementation of the monitoring task, decision making and the implementation of these decisions. One solution to this problem is to redistribute these functions among several drones, while maintaining the joint execution of the assigned mission. For example, an unmanned aerial vehicle may detect a new obstacle that does not interfere with its own movement, but may affect the flight of other members of the flock. This information is provided to another unmanned aerial vehicle, which is able to calculate the action that can be performed by a set of other drones located in the path of such an obstacle. In a swarm, communication is not only necessary for disseminating observations, tasks, and control information, but can also help coordinate UAVs more efficiently and safely. Communication requirements vary significantly across applications. However, providing a reliable network is particularly challenging due to the limited power supply of UAVs and external factors such as wireless shadowing and intermittent availability of communication channels.

Network requirements. The data traffic associated with the operation of the system can be divided into two main types [1]: control traffic, intended for tracking and modifying the behavior of UAVs by the ground control point, as well as monitoring information messages about the state of the UAV; coordination traffic, including information related to the interaction of UAVs and preventing their collisions.

Additionally, data is exchanged between UAVs about the payload and services implemented on board. For air-to-ground links, the International Telecommunication Union, within the framework of the 3rd Generation Partnership Project (3GPP) [6], has classified command and control communications as well as payload communications for safe operations of unmanned aerial vehicles in terms of throughput, reliability and latency. Table 1. The listed performance requirements are aimed at ensuring timely communications, high-quality data processing and the implementation of

coordinated movement in real time. The 3GPP information applies to air-to-ground links in a non-interacting deployment strategy.

Table 1

Air-to-ground communication requirements defined by 3GPP [6]

Communication	Data Type	Bandwidth	Reliability	Delay
DL (ground station - UAV)	Control Commands and Directives	60-100 Kbps	Packet Error Rate 10-3	50 ms
UL (UAV - ground station)	Control Commands and Directives	60-100 Kbps	Packet Error Rate 10-3	-
UL (UAV - ground station)	Application Data	Up to 50 Kbps	-	Similar to ground use

It is assumed that air-to-air communications are of primary importance for drone mission execution, as UAVs require information exchange among themselves to be able to make local decisions; UAV formations require reliable wireless communications for distributed coordination and real-time processing to achieve system-wide objectives [1]. Therefore, to provide broadband communications that support coordinated and distributed real-time data processing, the network system must have network performance characteristics that include reliability, high throughput, and low latency. From a reliability perspective, UAV flight is challenging due to the intermittent nature of the wireless links used, which may result in reduced network transmission performance. Synchronous maneuvering of neighboring UAVs may be affected by the Doppler effect or antennas. Ensuring the mobility of UAVs can be solved by increasing the data transmission capacity and expanding the communication channel by implementing store, carry and forward functions (SCF) [7]. Unmanned aerial vehicles are subject to actuator failures and system uncertainties, which affect the system performance. Uncertainties also exist in the UAV system itself due to parametric changes in mass and inertia, speed, altitude and position dynamics, elevation angles and random noise from another aircraft during flight. The UAV can also be exposed to external weather influences and system changes [8]. The main cause of attenuation in the transmission of air-to-air and air-to-ground signals are atmospheric conditions such as rain and gas pollution. In addition, shadowing effects can be caused by the UAV body itself and by the misalignment of the forging die pair due to the angular position of the antennas on the UAV. The main limitation of shadowing effects in air-to-ground communications of unmanned aerial vehicles is largely due to the limitations of the acceptable operating altitudes of the UAV, which restrict its operation to lower altitudes and hence are prone to shadowing by obstacles from tall build-

ings and ground objects in the air-to-ground data path. Ground links cause signal dispersion, which affects the communication efficiency.

The computing system of drones is based on a similar concept to NCS, in which simple data can lead to complex decisions. Therefore, the development of a suitable computing system is based on the study of the best decision-making strategies depending on the deployment strategy and reconnaissance algorithms used. Implementation of the method of formation in flights. Standard software tools for UAV control assume a flight over specified areas at established coordinate points along a certain route sequentially in time. Here, loss of information is possible, the movement of an object is missed, with possible mechanical loss of the aircraft itself. Therefore, it is necessary to develop a method that allows constructing an optimal flight trajectory with the ability to protect against damaging factors and possible control of the territory in online mode, preventing the passage of an intruder.

Implementation in the method of monitoring moving objects in the controlled territory of UAVs that fly at a certain speed in a vertical closed trajectory. At the upper flight level with a sufficient altitude protected from a certain defeat from the ground, photography is carried out at the coordinate points of adjacent sections of the protected area, performing the task of detecting and recognizing the intruder and monitoring the presence of UAVs located at the lower flight level, also performing photography and determining the direction of the mobile object and also its classification.

Unmanned aerial vehicles are capable of moving autonomously and helping to perform those tasks that were previously carried out by people. One of the important areas of use of UAVs is scanning objects on the territory, which allows you to monitor the presence and condition of objects in this area. This is relevant in monitoring extended border areas or contact zones in military operations.

At the upper flight level with a sufficient altitude protected from a certain defeat from the ground, photography is carried out at the coordinate points of adjacent sections of the protected area, performing the task of detecting, recognizing the intruder and monitoring the presence of UAVs located at the lower flight level. The lower UAV also takes photographs, determines the direction of the intruder's movement, and classifies it. It is assumed that the set of coordinate points is known in advance and is set from the outside, displayed on the map.

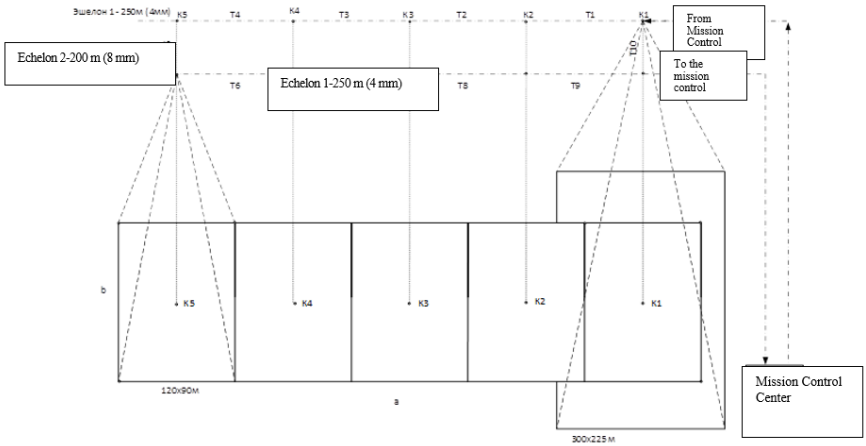

Figure 1. *Flight task calculation scheme*

To solve the problem, it is necessary to create a flight task – generate a UAV flight trajectory and calculate intermediate coordinate points for photographing along the trajectory based on the technical capabilities of the available UAV. In the context of the problem, the trajectory is a sequence of coordinate points and flight altitude in a format suitable for launching into the flight control program. It is assumed that the UAV moves from point to point along the shortest path, adjusted for the dynamic capabilities of the device.

UAV flight along a closed vertical trajectory improves the quality of the task being solved and control over the damaging factor of its UAVs, located at the lower flight level, operating as part of a group. This method involves a UAV group flying over a controlled area of terrain, like a column formation, where each one in turn photographs the area at the current time at the current coordinate points sequentially along the entire flight trajectory. Analysis of the characteristics of the lens and camera:

- the focal length of the lens is 4 mm, the camera with a 1K matrix, the distance to the object is 250 m makes it possible to control an area of 300 × 225 m, and the minimum size of the detected object will be 29 × 22 cm, - the focal length is 8 mm and the distance to the object is 200 m, the characteristics are somewhat improved, which reduces the risk of not identifying the detected object, which fully satisfies the requirements for detection and recognition.

To form a flight task, it is necessary to enter the coordinate points (K1, K5) of the controlled territory on the electronic map by dividing the line into equal sections, obtaining intermediate coordinate points (K2, K3, K4). Thus, the coordinate points for photographing are determined (Fig. 1).

Flight time to K1:

$$T_0 = S / V_{П_1},$$

where $V_{П_1}$ — maximum takeoff speed,

S – path from the flight control center (FCC) to K1.

To determine the flight time for the cycle, it is necessary to take into account the flight speed at two flight levels and the time of movement from one flight level to another Fig. 1.

$$Tc = \Sigma Tn + T_5 + T_{10}.$$

$$Tn = k / V_{П_2}$$

where, $V_{П_2}$ – maximum speed above sea level without wind,

k — distance between adjacent coordinate points.

The number of unmanned vehicles involved should be selected taking into account the target's speed and the flight time per cycle and rounded up to the maximum integer value:

$$N = Tc / T_б$$

Time of target movement through the controlled area:

$$T_б = b / V_б,$$

where b is the width of the controlled area, $V_б$ is the target speed.

The result of processing the presented data is a MATLAB software file with information about the points located in the sequence for performing the flight task, which allows importing data into the UAV program to work with the modified flight task. In this method, an array of points on the map that are interconnected is processed. A method has been developed and software has been implemented. Based on the proposed method for monitoring moving objects through a controlled area using a UAV, a predetermined set of coordinates is received, along which it is necessary to fly in the proposed way. Application. The system device and method can be used: for UAV flights on the state border for control and protection, for monitoring the line of contact between the parties in the theater of military operations.

Conclusion

The implementation of the proposed method of UAV formation as an NCS will increase the productivity of the entire system in solving operational and environmental problems. The division of drones into network and computing systems creates an effectively functioning self-organizing system. At the same time, it seems important when creating a network system not to rely on the identification of hosts, but rather on their computing functions, which can be deployed in any drone. The developed control system provides monitoring in the control of "their" UAVs in flight, transmission and correction of data to the Mission Control Center. Not to be detected and hit from the ground and in the air Integration of the network system The software in the UAV calculates the flight time of a new drone for its

introduction into the formation, the target's course transmits data on the target to the Mission Control Center. It implements a solution for each drone from the named data and functions in a transparent way, allows realizing the property of self-organization of the formation. Further developments are underway within the framework of scientific research work.

References

1. Dovgal V.A., Dovgal D.V. Analysis of communication interaction systems of drones performing a search mission as part of a group // Bulletin of Adyghe State University. Series: Natural, Mathematical and Technical Sciences. 2020. Issue 4 (271). P. 87–94. URL: http://vestnik.adygnet.ru.

2. A survey of using swarm intelligence algorithms in IoT / W. Sun, M. Tang, L. Zhang, Z. Huo, L. Shu // Sensors. 2020. Vol. 20. P. 1420.

3. Dovgal V.A., Dovgal D.V. Analysis of problems of ensuring information security of wireless sensor networks and methods of ensuring security of the Internet of Things // Bulletin of Adyghe State University. Series: Natural, Mathematical and Technical Sciences. 2021. Issue 1 (276). P. 75–83. URL: http://vestnik.adygnet.ru.

4. New radio (NR) and its evolution toward 5G-advanced / Y. Kim, J. Oh, H. Ji [et al.] // IEEE Wireless Communication. 2019. Vol. 26. P. 2–7.

5. Dovgal V.A. Making decisions about the placement of unmanned aerial vehicles based on the implementation of an artificial immune system in relation to information processing // Proceedings – 2021: International Conference on Industrial Engineering, Applications and Manufacturing. ICIEAM 2021. P. 828–833.

6. DoD command, control, and communications (C3) modernization strategy. URL: https:// dodcio.defense.gov/Portals/0/Documents/DoD-C3-Strategy.pdf (дата обращения: 08.02.2022).

7. Din C.Z. Development of methods for the construction and operation of a rapidly deployable flying network for emergency services: specialty 05.12.13 "Telecommunication systems, networks and devices": author's abstract. diss. candidate of technical sciences. St. Petersburg, 2020. 22 p.

8. Karlov A.M., Volkhonskaya E.V., Goza N.S. Model studies of the bit error rate in a communication channel with small-scale Rayleigh fading // Radio Engineering. 2019. No. 2. pp. 52–55. DOI: 10.18127/j00338486-201902-10.

DOI 10.34660/INF.2025.17.84.146
UDC 536.2

CALCULATION OF A NON-STATIONARY TEMPERATURE FIELD IN A POLAR-ORTHOTROPIC ANNULAR PLATE OF A POWER-LAW PROFILE WITH THERMALLY INSULATED BASES USING THE DUHAMEL METHOD

Karalevich Uladzimir Vasil'evich
Professor
International Center for Modern Education (ICME),
Prague, Czech Republic

Abstract. *The article provides a solution to the non-stationary thermal conductivity problem for a polar-orthotropic annular plate of a power-law profile with thermally insulated bases. To find the temperature distribution in such a plate, the Duhamel method is used, according to which the temperature function is represented as the sum of two terms: the stationary temperature and some coordinate- and time-dependent function describing the temperature deviation in the plate from the stationary regime. Expressions are given for the temperature function in an anisotropic annular plate of a power profile with thermally insulated bases in the general case and for an annular plate of constant thickness as a special case.*

Keywords: *unsteady and stationary modes, polar-orthotropic annular plate, power-law profile, equation of unsteady thermal conductivity, Bessel and Neumann functions, temperature function.*

Introduction

Annular plates made of composite materials are widely used in modern energy equipment, machine-building and aerospace structures, and devices in the food, chemical and pharmaceutical industries. They can often be located in time-varying thermal fields. In this paper, we will study the distribution of unsteady temperature in polar-orthotropic annular plates of variable thickness with thermally insulated bases.

Formulation of the problem and the basic equation of unsteady thermal conductivity for a polar-orthotropic annular plate of variable thickness with thermally insulated bases

Consider an annular plate, the thickness $h(r)$ of which varies along the radius r according to a given law. The plate has cylindrical orthotropy, and the axis of anisotropy coincides with the geometric axis of the plate, and at each point of the plate there are three mutually orthogonal planes of elastic symmetry.

We introduce a cylindrical coordinate system *r,θ,z* by placing the origin at the intersection point of the anisotropy axis with the median plane of the plate. Let's point the z-axis vertically upwards.

Let a constant temperature T_1^* be maintained on the inner contour (at $r = r_0$) of the plate , and on the outer contour (at $r = R$) the time variable *t* is temperature $\tilde{T}(r,t)$. The bases of the annular plate $z = \pm\frac{h(r)}{2}$ are thermally insulated. There are no internal heat sources in the plate. Consequently, the thermal field in such a polar-orthotropic plate will be nonstationary and axisymmetric.the field.

We will assume that the thermophysical characteristics of the plate material - radial λ_r, tangential λ_θ coefficients of thermal conductivity and specific heat capacity *c* - do not depend on the temperature $T(r,\theta,t)$ of the anisotropic body. Then the equation of nonstationary thermal conductivity for a polar orthotropic plate of variable thickness with thermally insulated bases will be written as [1]:

$$\lambda_r \cdot \frac{\partial^2 T(r,\theta,t)}{\partial r^2} + \left(\frac{h'(r)}{h(r)} + \frac{1}{r}\right) \cdot \lambda_r \frac{\partial T(r,\theta,t)}{\partial r} + \frac{\lambda_\theta}{r^2} \frac{\partial^2 T(r,\theta,t)}{\partial \theta^2} = c\rho \frac{\partial T(r,\theta,t)}{\partial t}, \quad (1)$$

where *p* is the density of the composite material.

If the nonstationary thermal field is axisymmetric, then the temperature *T* will not depend on the angular coordinate *θ* and the third term on the left side of equation (1) can be eliminated. As a result, we have the following equation:

$$\frac{\partial^2 T(r,t)}{\partial r^2} + \left(\frac{h'(r)}{h(r)} + \frac{1}{r}\right) \cdot \frac{\partial T(r,t)}{\partial r} = \frac{c\rho}{\lambda_r} \frac{\partial T(r,t)}{\partial t}. \quad (2)$$

Let's assume that on the outer contour of the annular plate, the temperature $\tilde{T}(r,t)$ changes over time *t* according to the law:

$$\tilde{T}(r_1,t) = \left[T_2^* + A\sin^2\left(\pi\frac{t}{Z}\right)\right], \quad (3)$$

where T_2^* is the constant temperature on the external circuit; *A, Z* are the amplitude and period of the temperature field change, respectively. The law of temperature $\tilde{T}(r,t)$ change can be set by any other function, it does not affect the course of solving the non-stationary problem of thermal conductivity.

Thus, when an $t \le 0$ anisotropic annular plate is in a stationary thermal field, when constant temperatures $T_i^*\left(i = \overline{1,2}\right)$ are maintained on its contours, and the bases of the plate are thermally insulated. In the case of an $t > 0$ external circuit, the temperature is already changing in time *t* according to the law established

by formula (3), and therefore the temperature field in the plate will already be non-stationary.

Solution of the equation of unsteady thermal conductivity for a polar-orthotropic ring plate of a power profile with thermally insulated bases by the Duhamel method

Let us solve the unsteady thermal conductivity problem for a polar-orthotropic annular plate with thermally insulated bases by the Duhamel method using the example of a power-law annular plate. The thickness $h(r)$ of the annular plate of a power profile is given by the expression:

$$h(r) = h_0 \left(\frac{r_0}{r} \right)^{\alpha}, \tag{4}$$

where h_0 is the thickness of the plate on the inner contour of the radius r_0; r is the current radius $(r_0 \le r \le R)$; exponent $\alpha \in \square$.

Let us first solve the axisymmetric stationary thermal conductivity problem for the polar-orthotropic annular plate under consideration.

The differential equation (2) will take the form:

$$\frac{d^2 T_{st.}(r)}{dr^2} + \left(\frac{h'(r)}{h(r)} + \frac{1}{r} \right) \cdot \frac{dT_{st.}(r)}{dr} = 0, \tag{5}$$

where $T_{st.}(r)$ is the temperature of the stationary thermal field in the plate.

Given expression (4) for the thickness $h(r)$ of the plate, we obtain from equation (5) the following differential equation:

$$\frac{d^2 T_{st.}(r)}{dr^2} + \left(\frac{1-\alpha}{r} \right) \cdot \frac{dT_{st.}(r)}{dr} = 0 \tag{6}$$

with boundary conditions: $T_{st.}(r_0) = T_1^*$, $T_{st.}(R) = T_2^*$; $T_1^* < T_2^* < T_m$, T_m - melting point of the composite material of the annular anisotropic plate.

For the exponent $\alpha \neq 0$, the solution of equation (6) under the given boundary conditions is:

$$T_{st.}^{(\alpha)}(r) = \left[\frac{\left(R^{\alpha} - r^{\alpha} \right)}{\left(R^{\alpha} - r_0^{\alpha} \right)} T_1^* + \frac{\left(r^{\alpha} - r_0^{\alpha} \right)}{\left(R^{\alpha} - r_0^{\alpha} \right)} T_2^* \right]. \tag{7}$$

In the case of an exponent $\alpha = 0$ (an annular plate of constant thickness h_0), the solution of equation (6) under given boundary conditions has the form:

$$T_{st.}^{(0)}(r) = \left[\frac{\ln\left(\frac{r}{R} \right)}{\ln\left(\frac{r_0}{R} \right)} T_1^* + \frac{\ln\left(\frac{r_0}{r} \right)}{\ln\left(\frac{r_0}{R} \right)} T_2^* \right]. \tag{8}$$

Let us now proceed to solving the non-stationary thermal conductivity problem for a polar-orthotropic annular plate of a power profile with thermally insulated bases by the Duhamel method. To do this, we represent the temperature

function $T(r,t)$ as the sum of two terms of the stationary temperature $T_{st.}(r)$ and some function $U(r,t)$ describing the deviation from the stationary regime:

$$T(r,t)=T_{st.}(r)+U(r,t). \tag{9}$$

Substituting expression (9) into differential equation (2), we obtain:

$$\left(\frac{d^2T_{st.}}{dr^2}+\frac{(1-\alpha)}{r}\frac{dT_{st.}}{dr}\right)+\left(\frac{\partial^2U}{\partial r^2}+\frac{(1-\alpha)}{r}\frac{\partial U}{\partial r}\right)=\frac{c\rho}{\lambda_r}\frac{\partial U}{\partial t}. \tag{10}$$

By virtue of equality (6), the first term on the left side of equation (10) is zero, we obtain a partial differential equation for the function $U(r,t)$:

$$\frac{\partial^2U}{\partial r^2}+\frac{(1-\alpha)}{r}\frac{\partial U}{\partial r}=\frac{c\rho}{\lambda_r}\frac{\partial U}{\partial t}. \tag{11}$$

Let's add the initial and boundary conditions to equation (11):

the initial condition: $U(r,0)=0;$ (12)

boundary conditions: $U(r_0,t)=0$ and $U(R,t)=Q(t)=A\sin^2\left(\pi\frac{t}{Z}\right).$ (13)

The solution of the boundary value problem (11) – (13) is [2]:

$$U(r,t)=\int_0^t Q(\tau)\frac{\partial}{\partial t}R(r,t-\tau)\,d\tau, \tag{14}$$

where $R(r,t)$ is the auxiliary function determined from the solution of boundary value problem (11) – (13) for $Q(t)\equiv 1$.

Let's represent the function $R(r,t)$ as the sum of two terms:

$$R(r,t)=V(r)+P(r,t). \tag{15}$$

Here, the function $V(r)$ describes the stationary regime, and the function $P(r,t)$ describes the deviation from it.

For the function $V(r)$, the boundary value problem is posed as follows:

$$\frac{d^2V}{dr^2}+\frac{(1-\alpha)}{r}\frac{dV}{dr}=0, \tag{16}$$

$$V(r_0)=0,\quad V(R)=1. \tag{17}$$

For the exponent $\alpha\neq 0$, the solution of equation (16) under the given boundary conditions (17) is:

$$V^{(\alpha)}(r)=\frac{\left(r^\alpha-r_0^\alpha\right)}{\left(R^\alpha-r_0^\alpha\right)}. \tag{18}$$

In the case of the exponent $\alpha=0$ (an annular plate of constant thickness h_0), the solution of equation (16) under the given boundary conditions (17) has the form:

$$V^{(0)}(r)=\frac{\ln\left(\frac{r_0}{r}\right)}{\ln\left(\frac{r_0}{R}\right)}. \tag{19}$$

For the function $P(r,t)$, the boundary value problem is posed as follows:

$$\begin{cases} \dfrac{\partial^2 P}{\partial r^2}+\dfrac{(1-\alpha)}{r}\dfrac{\partial P}{\partial r}=\dfrac{c\rho}{\lambda_r}\dfrac{\partial P}{\partial t}; & (20) \\ P(r,0)=-V(r) \text{ – the initial condition;} & (21) \\ P(r_0,t)=0 \text{ и } U(R,t)=0 \text{ – boundary conditions.} & (22) \end{cases}$$

Let's solve the boundary value problem (20) – (22) by the method of separation of variables [2]. Let's represent the function $P(r,t)$ as a product of two functions:

$$P(r,t)=\Phi(r)\cdot\Psi(t). \quad (23)$$

Substituting function (23) into equation (20) and dividing by $\frac{c\rho}{\lambda_r}\Phi(r)\Psi(t)$, we obtain:

$$\frac{\Phi''(r)+\dfrac{(1-\alpha)}{r}\Phi'(r)}{\dfrac{c\rho}{\lambda_r}\Phi(r)}=\frac{\Psi'(t)}{\Psi(t)}=-\lambda. \quad (24)$$

In order for this equality to be fulfilled identically, it is necessary and sufficient that the left and right sides of equation (24) are equal to the same constant $(-\lambda)$. As a result, we have two identities:

$$\Phi''(r)+\frac{(1-\alpha)}{r}\Phi'(r)+\lambda\frac{c\rho}{\lambda_r}\Phi(r)\equiv 0, \quad (25)$$

$$\Psi'(t)+\lambda\Psi(t)\equiv 0. \quad (26)$$

Let's find the solution to equation (25). Multiplying it by r^2, we get:

$$r^2\Phi''(r)+(1-\alpha)\cdot r\Phi'(r)+\lambda\left(\frac{c\rho}{\lambda_r}\right)\cdot r^2\Phi(r)\equiv 0. \quad (27)$$

In equation (27), we introduce a new variable:

$$\xi=\sqrt{\lambda\left(\frac{\tilde{n}\rho}{\lambda_r}\right)}\cdot r \quad (28)$$

and we'll make a replacement:

$$\Phi(r)=r^{\frac{\alpha}{2}}\cdot y(\xi). \quad (29)$$

Substituting expressions (28) – (29) into equation (27) leads it to the Bessel differential equation for the function $y(\xi)$:

$$\xi^2 y''(\xi)+\xi y'(\xi)+\left[\xi^2-\left(\frac{\alpha}{2}\right)^2\right]y(\xi)=0. \quad (30)$$

The solution of equation (30) for non-integers $\nu=\frac{\alpha}{2}$ is:

$$y^{(\nu)}(\xi)=C_1^{(\nu)}\cdot J_\nu(\xi)+C_2^{(\nu)}\cdot J_{-\nu}(\xi),$$

where $J_\nu(\xi)$ is the Bessel function of the 1st kind of the ν-th order; $C_1^{(\nu)}, C_2^{(\nu)}$ - arbitrary constants.

For integers $\nu = \frac{\alpha}{2} = m$ $(m = 0,1,2,3....)$, the solution of equation (30) will be:

$$y^{(m)}(\xi) = C_1^{(m)} \cdot J_m(\xi) + C_2^{(m)} \cdot Y_m(\xi),$$

where $Y_m(\xi)$ is the Bessel function of the 2nd kind of the m-th order or the Neumann function of the m-th order; $C_1^{(m)}, C_2^{(m)}$ - arbitrary constants.

Thus, the solution of the differential equation (27) for non-integers *v* is:

$$\Phi^{(\nu)}(r) = r^\nu \left[C_1^{(\nu)} \cdot J_\nu \left(\sqrt{\lambda \left(\frac{\tilde{n}\rho}{\lambda_r} \right)} \cdot r \right) + C_2^{(\nu)} \cdot J_{-\nu} \left(\sqrt{\lambda \left(\frac{\tilde{n}\rho}{\lambda_r} \right)} \cdot r \right) \right]. \quad (31)$$

For integers $\nu = m$, the solution of equation (27) will be:

$$\Phi^{(m)}(r) = r^m \left[C_1^{(m)} \cdot J_m \left(\sqrt{\lambda \left(\frac{\tilde{n}\rho}{\lambda_r} \right)} \cdot r \right) + C_2^{(m)} \cdot Y_m \left(\sqrt{\lambda \left(\frac{\tilde{n}\rho}{\lambda_r} \right)} \cdot r \right) \right]. \quad (32)$$

The boundary conditions for the function Φ (*r*) are homogeneous:

$$\Phi(r_0) = 0, \quad \Phi(R) = 0. \quad (33)$$

Let us satisfy solution (31) to the first of the boundary conditions (33):

$$\Phi^{(\nu)}(r_0) = r_0^\nu \left[C_1^{(\nu)} \cdot J_\nu \left(\sqrt{\lambda \left(\frac{c\rho}{\lambda_r} \right)} \cdot r_0 \right) + C_2^{(\nu)} \cdot J_{-\nu} \left(\sqrt{\lambda \left(\frac{c\rho}{\lambda_r} \right)} \cdot r_0 \right) \right] = 0,$$

from here

$$C_2^{(\nu)} = -C_1^{(\nu)} \frac{J_\nu \left(\sqrt{\lambda \left(\frac{c\rho}{\lambda_r} \right)} \cdot r_0 \right)}{J_{-\nu} \left(\sqrt{\lambda \left(\frac{c\rho}{\lambda_r} \right)} \cdot r_0 \right)}.$$

The solution (31) can be written as:

$$\Phi^{(\nu)}(r) = C_1^{(\nu)} r^\nu \left[\frac{J_\nu \left(\sqrt{\lambda \left(\frac{c\rho}{\lambda_r} \right)} \cdot r \right) \cdot J_{-\nu} \left(\sqrt{\lambda \left(\frac{c\rho}{\lambda_r} \right)} \cdot r_0 \right) - J_\nu \left(\sqrt{\lambda \left(\frac{c\rho}{\lambda_r} \right)} \cdot r_0 \right) J_{-\nu} \left(\sqrt{\lambda \left(\frac{c\rho}{\lambda_r} \right)} \cdot r \right)}{J_{-\nu} \left(\sqrt{\lambda \left(\frac{c\rho}{\lambda_r} \right)} \cdot r_0 \right)} \right]. \quad (34)$$

Let's substitute solution (34) into the second boundary condition (33):

$$\Phi^{(\nu)}(R)=C_1^{(\nu)}R^{\nu}\left[\frac{J_{\nu}\left(\sqrt{\lambda\left(\frac{c\rho}{\lambda_r}\right)}\cdot R\right)\cdot J_{-\nu}\left(\sqrt{\lambda\left(\frac{c\rho}{\lambda_r}\right)}\cdot r_0\right)-J_{\nu}\left(\sqrt{\lambda\left(\frac{c\rho}{\lambda_r}\right)}\cdot r_0\right)J_{-\nu}\left(\sqrt{\lambda\left(\frac{c\rho}{\lambda_r}\right)}\cdot R\right)}{J_{-\nu}\left(\sqrt{\lambda\left(\frac{c\rho}{\lambda_r}\right)}\cdot r_0\right)}\right]=0.$$

From here we get the equation for determining the eigenvalues:

$$\left[J_{\nu}\left(\sqrt{\lambda\left(\frac{c\rho}{\lambda_r}\right)}\cdot R\right)\cdot J_{-\nu}\left(\sqrt{\lambda\left(\frac{c\rho}{\lambda_r}\right)}\cdot r_0\right)-J_{\nu}\left(\sqrt{\lambda\left(\frac{c\rho}{\lambda_r}\right)}\cdot r_0\right)J_{-\nu}\left(\sqrt{\lambda\left(\frac{c\rho}{\lambda_r}\right)}\cdot R\right)\right]=0. \quad (35)$$

Let 's denote $\mu=\sqrt{\lambda\left(\frac{c\rho}{\lambda_r}\right)}\cdot R,\ \ \delta=\frac{r_0}{R}<1$. Then equation (35) will be written as:

$$\left[J_{\nu}(\mu)\cdot J_{-\nu}(\mu\cdot\delta)-J_{\nu}(\mu\cdot\delta)\cdot J_{-\nu}(\mu)\right]=0. \quad (36)$$

Let be $\mu_1,\mu_2,\mu_3,.....,\mu_n,...$ the positive roots of the transcendental equation (36). Then the eigenvalues will be numbers $\lambda_n=\left(\frac{\lambda_r}{c\rho}\right)\frac{\mu_n^2}{R^2}$.

The eigenfunctions have the form:

$$\Phi_n^{(\nu)}(r)=r^{\nu}\left[J_{\nu}\left(\mu_n\cdot\frac{r}{R}\right)\cdot J_{-\nu}(\mu_n\cdot\delta)-J_{\nu}(\mu_n\cdot\delta)\cdot J_{-\nu}\left(\mu_n\cdot\frac{r}{R}\right)\right].$$

For integers $\nu=m$, the equation for determining the eigenvalues is:

$$\left[J_m(\mu)\cdot Y_m(\mu\cdot\delta)-J_m(\mu\cdot\delta)\cdot Y_m(\mu)\right]=0, \quad (37)$$

and the eigenfunctions are equal:

$$\Phi_n^{(m)}(r)=r^{m}\left[J_m\left(\mu_n\cdot\frac{r}{R}\right)\cdot Y_m(\mu_n\cdot\delta)-J_m(\mu_n\cdot\delta)\cdot Y_m\left(\mu_n\cdot\frac{r}{R}\right)\right].$$

Let us now consider equation (26). His general solution at $\lambda=\lambda_n$ is:

$$\Psi_n(t)=C_n\cdot e^{-\lambda_n t}$$

Then for non-integers $\nu=\frac{\alpha}{2}$

$$P^{(\nu)}(r,t)=\sum_{n=1}^{\infty}C_n^{(\nu)}e^{-\lambda_n t}\Phi_n^{(\nu)}(r)=\sum_{n=1}^{\infty}C_n^{(\nu)}e^{-\lambda_n t}\cdot r^{\nu}\left[J_{\nu}\left(\mu_n\cdot\frac{r}{R}\right)\cdot J_{-\nu}(\mu_n\cdot\delta)-J_{\nu}(\mu_n\cdot\delta)J_{-\nu}\left(\mu_n\cdot\frac{r}{R}\right)\right].$$

We will find the coefficients $C_n^{(\nu)}$ from the initial condition, using the orthonality condition of the eigenfunctions $\Phi_n^{(\nu)}(r)$:

$$C_n^{(\nu)}=-\frac{1}{\left\|\Phi_n^{(\nu)}\right\|^2}\int_{r_0}^{R}\frac{\left(r^{2\nu}-r_0^{2\nu}\right)}{\left(R^{2\nu}-r_0^{2\nu}\right)}\cdot r^{\nu}\left[J_{\nu}\left(\mu_n\cdot\frac{r}{R}\right)\cdot J_{-\nu}(\mu_n\cdot\delta)-J_{\nu}(\mu_n\cdot\delta)\cdot J_{-\nu}\left(\mu_n\cdot\frac{r}{R}\right)\right]\cdot rdr,$$

where $\left\|\Phi_n^{(\nu)}(r)\right\|^2=\int_{r_0}^{R}r^{2\nu}\left[J_{\nu}\left(\mu_n\cdot\frac{r}{R}\right)\cdot J_{-\nu}(\mu_n\cdot\delta)-J_{\nu}(\mu_n\cdot\delta)\cdot J_{-\nu}\left(\mu_n\cdot\frac{r}{R}\right)\right]^2\cdot rdr.$

For non-integers v, the function $R^{(v)}(r,t)$ is:

$$R^{(v)}(r,t)=\frac{\left(r^{2v}-r_0^{2v}\right)}{\left(R^{2v}-r_0^{2v}\right)}+\sum_{n=1}^{\infty}C_n^{(v)}e^{-\lambda_n t}\cdot r^{v}\left[J_v\left(\mu_n\cdot\frac{r}{R}\right)\cdot J_{-v}\left(\mu_n\cdot\delta\right)-J_v\left(\mu_n\cdot\delta\right)\cdot J_{-v}\left(\mu_n\cdot\frac{r}{R}\right)\right].$$

The solution of the boundary value problem (11) – (13) is:

$$U^{(v)}(r,t)=\int_0^t Q(\tau)\frac{\partial}{\partial t}\left[R^{(v)}(r,t-\tau)\cdot\eta(t-\tau)\right]d\tau=\int_0^t Q(\tau)\frac{\partial}{\partial t}R^{(v)}(r,t-\tau)\,d\tau+Q(t)R^{(v)}(r,0)=$$

$$=-A\sum_{n=1}^{\infty}\int_0^t e^{\lambda_n\tau}\sin^2\left(\pi\frac{\tau}{Z}\right)d\tau\cdot\lambda_n C_n^{(v)}e^{-\lambda_n t}r^{v}\left[J_v\left(\mu_n\cdot\frac{r}{R}\right)\cdot J_{-v}\left(\mu_n\cdot\delta\right)-J_v\left(\mu_n\cdot\delta\right)\cdot J_{-v}\left(\mu_n\cdot\frac{r}{R}\right)\right]+$$

$$+A\sin^2\left(\pi\frac{t}{Z}\right)\cdot R^{(v)}(r,0).$$

For non-integers $v=\frac{\alpha}{2}$, the temperature $T(r,t)$ distribution in a polar-orthotropic ring plate of a power profile with thermally insulated bases is:

$$T^{(\alpha)}(r,t)=\left[\frac{\left(R^{\alpha}-r^{\alpha}\right)}{\left(R^{\alpha}-r_0^{\alpha}\right)}T_1^{*}+\frac{\left(r^{\alpha}-r_0^{\alpha}\right)}{\left(R^{\alpha}-r_0^{\alpha}\right)}T_2^{*}\right]+U^{\left(\frac{\alpha}{2}\right)}(r,t). \tag{38}$$

For integers $v=\frac{\alpha}{2}=m$, the function $P^{(m)}(r,t)$ is:

$$P^{(m)}(r,t)=\sum_{n=1}^{\infty}C_n^{(m)}e^{-\lambda_n t}\Phi_n^{(m)}(r)=\sum_{n=1}^{\infty}C_n^{(m)}e^{-\lambda_n t}\cdot r^{m}\left[J_m\left(\mu_n\cdot\frac{r}{R}\right)\cdot Y_m\left(\mu_n\cdot\delta\right)-J_m\left(\mu_n\cdot\delta\right)\cdot Y_m\left(\mu_n\cdot\frac{r}{R}\right)\right].$$

We will find the coefficients $C_n^{(v)}$ from the initial condition, using the orthogonality condition of the eigenfunctions $\Phi_n^{(m)}(r)$:

$$C_n^{(m)}=-\frac{1}{\left\|\Phi_n^{(m)}\right\|^2}\int_{r_0}^{R}\frac{\left(r^{2m}-r_0^{2m}\right)}{\left(R^{2m}-r_0^{2m}\right)}\cdot r^{m}\left[J_m\left(\mu_n\cdot\frac{r}{R}\right)\cdot Y_m\left(\mu_n\cdot\delta\right)-J_m\left(\mu_n\cdot\delta\right)\cdot Y_m\left(\mu_n\cdot\frac{r}{R}\right)\right]\cdot rdr,$$

where

$$\left\|\Phi_n^{(m)}(r)\right\|^2=\int_{r_0}^{R}r^{2m}\left[J_m\left(\mu_n\cdot\frac{r}{R}\right)\cdot Y_m\left(\mu_n\cdot\delta\right)-J_m\left(\mu_n\cdot\delta\right)\cdot Y_m\left(\mu_n\cdot\frac{r}{R}\right)\right]^2\cdot rdr.$$

For integers $v=m$, the function $R^{(m)}(r,t)$ is:

$$R^{(m)}(r,t)=\frac{\left(r^{2m}-r_0^{2m}\right)}{\left(R^{2m}-r_0^{2m}\right)}+\sum_{n=1}^{\infty}C_n^{(m)}e^{-\lambda_n t}\cdot r^{m}\left[J_m\left(\mu_n\cdot\frac{r}{R}\right)\cdot Y_m\left(\mu_n\cdot\delta\right)-J_m\left(\mu_n\cdot\delta\right)\cdot Y_m\left(\mu_n\cdot\frac{r}{R}\right)\right].$$

The solution of the boundary value problem (11) – (13) for integers $v=m$ is:

$$U^{(m)}(r,t)=\int_0^t Q(\tau)\frac{\partial}{\partial t}\left[R^{(m)}(r,t-\tau)\cdot\eta(t-\tau)\right]d\tau=\int_0^t Q(\tau)\frac{\partial}{\partial t}R^{(m)}(r,t-\tau)\,d\tau+Q(t)R^{(m)}(r,0)=$$

$$=-A\sum_{n=1}^{\infty}\int_0^t e^{\lambda_n\tau}\sin^2\left(\pi\frac{\tau}{Z}\right)d\tau\cdot\lambda_n C_n^{(m)}e^{-\lambda_n t}r^m\left[J_m\left(\mu_n\cdot\frac{r}{R}\right)\cdot Y_m(\mu_n\cdot\delta)-J_m(\mu_n\cdot\delta)\cdot Y_m\left(\mu_n\cdot\frac{r}{R}\right)\right]+$$

$$+A\sin^2\left(\pi\frac{t}{Z}\right)\cdot R^{(m)}(r,0).$$

For integers $\nu=\frac{\alpha}{2}=m$, the temperature distribution in a polar-orthotropic ring plate of a power profile with thermally insulated bases is:

$$T^{(\alpha)}(r,t)=\left[\frac{\left(R^{2m}-r^{2m}\right)}{\left(R^{2m}-r_0^{2m}\right)}T_1^*+\frac{\left(r^{2m}-r_0^{2m}\right)}{\left(R^{2m}-r^{2m}\right)}T_2^*\right]+U^{(m)}(r,t). \tag{39}$$

In the special case, for an annular plate of constant thickness, the exponent $m=0$ and temperature distribution in the plate will be:

$$T^{(0)}(r,t)=\left[\frac{\ln\left(\frac{r}{R}\right)}{\ln\left(\frac{r_0}{R}\right)}T_1^*+\frac{\ln\left(\frac{r_0}{r}\right)}{\ln\left(\frac{r_0}{R}\right)}T_2^*\right]+U^{(0)}(r,t), \tag{40}$$

where

$$U^{(0)}(r,t)=\int_0^t Q(\tau)\frac{\partial}{\partial t}\left[R^{(0)}(r,t-\tau)\cdot\eta(t-\tau)\right]d\tau=\int_0^t Q(\tau)\frac{\partial}{\partial t}R^{(0)}(r,t-\tau)\,d\tau+Q(t)R^{(0)}(r,0)=$$

$$=-A\sum_{n=1}^{\infty}\int_0^t e^{\lambda_n\tau}\sin^2\left(\pi\frac{\tau}{Z}\right)d\tau\cdot\lambda_n C_n^{(0)}e^{-\lambda_n t}\left[J_0\left(\mu_n\cdot\frac{r}{R}\right)\cdot Y_0(\mu_n\cdot\delta)-J_0(\mu_n\cdot\delta)\cdot Y_0\left(\mu_n\cdot\frac{r}{R}\right)\right]+$$

$$+A\sin^2\left(\pi\frac{t}{Z}\right)\cdot R^{(0)}(r,0),$$

$$R^{(0)}(r,t)=\frac{\ln\left(\frac{r_0}{r}\right)}{\ln\left(\frac{r_0}{R}\right)}+\sum_{n=1}^{\infty}C_n^{(0)}e^{-\lambda_n t}\cdot\left[J_0\left(\mu_n\cdot\frac{r}{R}\right)\cdot Y_0(\mu_n\cdot\delta)-J_0(\mu_n\cdot\delta)\cdot Y_0\left(\mu_n\cdot\frac{r}{R}\right)\right].$$

$$C_n^{(0)}=-\frac{1}{\left\|\Phi_n^{(0)}\right\|^2}\int_{r_0}^{R}\frac{\ln\left(\frac{r_0}{r}\right)}{\ln\left(\frac{r_0}{R}\right)}\cdot\left[J_0\left(\mu_n\cdot\frac{r}{R}\right)\cdot Y_0(\mu_n\cdot\delta)-J_0(\mu_n\cdot\delta)\cdot Y_0\left(\mu_n\cdot\frac{r}{R}\right)\right]\cdot r\,dr,$$

$$\int_0^t e^{\lambda_n\tau}\sin^2\left(\pi\frac{\tau}{Z}\right)d\tau=\frac{1}{\lambda_n}\frac{1}{\left(\mu_n^2+4\right)}\left\{\left(\left[\mu_n\sin\left(\pi\frac{t}{Z}\right)-\cos\left(\pi\frac{t}{Z}\right)\right]^2+\left[1+\sin^2\left(\pi\frac{t}{Z}\right)\right]\right)e^{\lambda_n t}-2\right\}.$$

Conclusion

Formulas (38), (39), (40) describe the temperature distribution in a polar-orthotropic annular disk of a power profile with thermally insulated bases for various cases of the exponent α. They can be used in the calculation of thermoelastic stresses in anisotropic annular plates of various designs operating in alternating thermal fields.

Bibliographic references

1. Prusov I.A. Thermoelastic anisotropic plates. Minsk. Publishing house of BSU. 1978. 200 p. (in Russian).

2. Arsenin V.Ya. Methods of mathematical physics and special functions. Moscow: Nauka. 1984. 384 p. (in Russian).

Proceedings of International Science Conference

EDUCATION AND PRACTICE IN THE CONTEXT OF MODERN SCIENCE

Delhi, India

July 16, 2025

Signed in print 16.07.2025 60x84/16.
Ed. No. 1. Circulation of 500 copies. India, 2025.
Infinity publishing, 2025